JYVÄSKYLÄ STUDIES IN BIOLOGICAL AND ENVIRONMENTAL SCIENCE
203

Kirsi Pakkanen

From Endosomes Onwards

Membranes, Lysosomes and Viral Capsid Interactions

JYVÄSKYLÄN YLIOPISTO

JYVÄSKYLÄ STUDIES IN BIOLOGICAL AND ENVIRONMENTAL SCIENCE 203

Kirsi Pakkanen

From Endosomes Onwards

Membranes, Lysosomes and Viral Capsid Interactions

Esitetään Jyväskylän yliopiston matemaattis-luonnontieteellisen tiedekunnan suostumuksella
julkisesti tarkastettavaksi yliopiston Agora-rakennuksessa (Ag Aud. 2)
syyskuun 11. päivänä 2009 kello 12.

Academic dissertation to be publicly discussed, by permission of
the Faculty of Mathematics and Science of the University of Jyväskylä,
in the Building Agora, Ag Aud. 2, on September 11, 2009 at 12 o'clock noon.

UNIVERSITY OF JYVÄSKYLÄ

JYVÄSKYLÄ 2009

From Endosomes Onwards

Membranes, Lysosomes and Viral Capsid Interactions

JYVÄSKYLÄ STUDIES IN BIOLOGICAL AND ENVIRONMENTAL SCIENCE 203

Kirsi Pakkanen

From Endosomes Onwards

Membranes, Lysosomes and Viral Capsid Interactions

UNIVERSITY OF JYVÄSKYLÄ

JYVÄSKYLÄ 2009

Editors
Varpu Marjomäki
Department of Biological and Environmental Science, University of Jyväskylä
Pekka Olsbo, Marja-Leena Tynkkynen
Publishing Unit, University Library of Jyväskylä

Jyväskylä Studies in Biological and Environmental Science

URN:ISBN:978-951-39-3663-1
ISBN 978-951-39-3663-1 (PDF)

ISBN 978-951-39-3640-2 (nid.)
ISSN 1456-9701

Jyväskylä University Printing House, Jyväskylä 2009

I must go down to the seas again,
to the vagrant gypsy life,
To the gull's way and the whale's way,
where the wind's like a whetted knife;
And all I ask is a merry yarn
from a laughing fellow-rover,
And quiet sleep and a sweet dream
when the long trick's over.

John Masefield

ABSTRACT

Pakkanen, Kirsi
From endosomes onwards. Membranes, lysosomes and viral capsid interactions.
Jyväskylä: University of Jyväskylä, 2009, 118p.
(Jyväskylä Studies in Biological and Environmental Science
ISSN 1456-9701; 203)
ISBN 978-951-39-3663-1 (PDF), 978-951-39-3640-2 (nid.)
Yhteenveto: Endosomeista eteenpäin. Lipidikalvoja, lysosomeja ja viruskapsidin vuorovaikutuksia.

To understand cellular functions one must learn how biological membranes behave. Lipid bilayers are the first line of defence against parasites invading cells -- and consequently, crossing the lipid bilayer is one of the rate limiting steps of a successful infection. In this thesis membrane interactions important for the entry of canine parvovirus (CPV) were elucidated. The virus was found to interact with sphingomyelin causing conformational changes in the capsid. Moreover, cholesterol was found to be important for CPV entry. Cholesterol together with low pH triggered the virus to fluidise model membranes and this fluidisation occurred also during infection. Without normal cholesterol content, and presumably without proper cholesterol-facilitated organisation of intracellular membranes, CPV trafficking was impaired and the infection inhibited. Desipramine, a tricyclic antidepressant, was with atomistic molecular dynamics simulations found to have an disordering effect on cholesterol-rich membranes. The drug also inhibited CPV entry, which makes it an interesting candidate for an antiviral agent.

The properties of lysosomal membranes have remained uncharacterised despite the biomedical interest to understand the organelle function. The effect of triolein on phospholipid membrane properties were investigated in a model membrane system to provide information on the possible role of triglycerides in lysosomal membranes. At the saturation limit triolein induced complex macroscopic phase behaviour in fluid phospholipid membrane. In one of the two phases triolein significantly reduced water penetration to the upper part of the membrane as well as fluidised the membrane. This is proposed to contribute to the barrier properties of lysosomes.

The last part of the thesis describes long tubulin-containing protrusions in CPV-infected cells at late stage of infection. These protrusions are suggested to be related to egress of the virus.

Keywords: Virus-membrane interactions; cholesterol; desipramine; triglyceride; membrane properties; virus egress

Kirsi Pakkanen, University of Jyväskylä, Nanoscience Center, Department of Biological and Environmental Science, P.O. Box 35, FI-40014 University of Jyväskylä, Finland

Author's address Kirsi Pakkanen
Nanoscience Center
Department of Biological and Environmental Science
P.O. Box 35
FI-40014 University of Jyväskylä
Finland
kirsi.i.pakkanen@jyu.fi

Supervisors Professor Matti Vuento, Ph.D.
Nanoscience Center
Department of Biological and Environmental Science
P.O. Box 35
FI-40014 University of Jyväskylä
Finland

Professor Henrik Kunttu, Ph.D.
Nanoscience Center
Department of Chemistry
P.O. Box 35
FI-40014 University of Jyväskylä
Finland

Reviewers Docent Eeva-Liisa Eskelinen, Ph.D.
Department of Biological and Environmental Sciences
Division of Biochemistry
University of Helsinki,
Finland

Professor J. Peter Slotte, Ph.D.
Department of Biochemistry and Pharmacy
Åbo Akademi University,
Finland

Opponent Docent Pentti Somerharju, Ph.D.
Institute of Biomedicine
University of Helsinki,
Finland

CONTENTS

LIST OF ORIGINAL PUBLICATIONS

The thesis is based on the following original papers, which will be referred to in the text by their Roman numerals.

I Pakkanen, K., Karttunen, J., Virtanen, S. & Vuento, M. 2008. Sphingomyelin induces structural alteration in canine parvovirus capsid. Virus Research 132: 187–191

II Pakkanen K., Kirjavainen S., Mäkelä A. R., Rintanen N., Oker-Blom C., Jalonen T. O. & Vuento M. 2009. Parvovirus capsid disorders cholesterol-rich membranes. Biochemical and Biophysical Research Communications. 379: 562–566.

III Pakkanen K., Salonen, E., Mäkelä A. R., Oker-Blom, C., Vattulainen, I. & Vuento, M. Desipramine induces disorder in cholesterol-rich membranes: implications for viral trafficking. Submitted manuscript.

IV Pakkanen K., Duelund L., Vuento M. & Ipsen J. H. Phase coexistence in a triolein-phosphatidylcholine system. Implications for lysosomal membrane properties. Submitted manuscript.

V Pakkanen K., Nykky J. & Vuento M. 2008. Late steps of parvoviral infection induce changes in cell morphology. Virus Research 137: 271–274.

RESPONSIBILITIES OF KIRSI PAKKANEN IN THE THESIS ARTICLES

Article I: I planned the article together with Matti Vuento. I was responsible for the circular dichroism and tryptophan fluorescence measurements. I performed most of the fluorescence spectroscopy and supervised the measurements performed by Jenni Karttunen and Salla Virtanen. I was responsible for all the data analysis. I wrote the article.

Article II: I planned the article together with Matti Vuento with the help of Tuula Jalonen. I performed the *in vitro* spectroscopical measurements and analysed both *in vitro* and cellular data. I wrote the article. All authors participated in finalising it.

Article III: I planned the cellular studies together with Matti Vuento. I was responsible for the cell experiments and for the most part of microscopy. Emppu Salonen and Ilpo Vattulainen were responsible for the molecular dynamics simulations of the study. I analysed the data from cell experiments. I wrote the article together with Emppu Salonen with the help of Ilpo Vattulainen and Matti Vuento. All authors participated in finalising it.

Article IV: John Ipsen, Lars Duelund and I planned the article together. I performed the Laurdan emission measurements and most of the Laurdan GP measurements as well as sample preparation. Lars Duelund and I performed the TLC studies and DPH anisotropy measurements as well as the DSC measurements. I analysed the TLC, GP and anisotropy data. I wrote the article together with Lars Duelund and John Ipsen.

Article V: I planned the article. I was responsible for all the experiments and imaging with NLFK cell line. Jonna Nykky prepared and imaged the samples made with A72 cell line. I performed all data analysis and wrote the article.

ABBREVIATIONS

a_0	optimal area for lipid
A72	canine fibroma cell line
Ac-His-VP2	recombinant VP2 protein (CPV) with a His-tag
Arf6	ADP-ribosylation factor 6
ARV	avian reovirus
ATP	adenosine triphosphate
BDV	borna disease virus
BMP	bis(monoacylglycero)phosphate
CAR	coxsackie B virus and adenovirus receptor
CCP	clathrin-coated pit
CCV	clathrin-coated vesicle
CD	circular dichroism
Cd-MPR	cation-dependent mannose 6-phosphate receptor
CD4	cluster of differentiation 4
Cdc42	cell division cycle 42 protein (GTPase)
Ci-MPR	cation-independent mannose 6-phosphate receptor
CM	chylomicron
CPV	canine parvovirus
DAF	decay accelerating factor (CD55)
DHA	docosahexaenoic acid
DIC	differential interference contrast
DMI	desipramine
DMPC	dimyristoyl phosphatidylcholine
DMSO	dimethyl sulfoxide
DOPC	dioleoyl phosphatidylcholine
DPH	1,6-diphenyl-1,3,5-hexatriene
DPPC	dipalmitoyl phosphatidylcholine
DRM	detergent resistant membrane
DSC	differential scanning calorimetry
DSPC	distearoyl phosphatidylcholine
EE	early endosome
EEA1	early-endosomal autoantigen
EGFR	epidermal growth factor receptor
EPR	electron paramagnetic resonance
ER	endoplasmic reticulum
ERp29	endoplasmic reticulum protein 29
ESCRT	endosomal sorting complex required for transport
EV1	echovirus 1
GM1	monosialotetrahexosylganglioside
GP	general polarisation
GPI	glycosylphosphatidylinositol
GTP	guanosine triphosphate

HA	hemagglutinin
HBV	hepatitis B virus
HCV	hepatitis C virus
HHV6	human herpes virus 6
HIV	human immunodeficiency virus
HPV-31	human papillomavirus type 31
HRV2	human rhinovirus 2
HSV1	herpes simplex virus 1
ISVP	infectious subvirion particle
K	area compressability modulus
K_a	area expansion modulus
κ	bending rigidity modulus
L_α	fluid phase
LAMP	lysosome-associated membrane protein
$L_{\beta'}$	gel phase
LBD	light buoyant density
LBPA	lysobisphosphatidic acid
l_c	critical chain length
ld	liquid disordered phase
LDL	low density lipoprotein
LDLR	low-density lipoprotein receptor
LE	late endosome
LIMP	lysosomal integral membrane protein
lo	liquid ordered phase
LUV	large unilamellar vesicle
LY	lysosome
MβCD	methyl-β-cyclodextrin
MD	molecular dynamics
MLV	multilamellar vesicle
MP	monopalmitin
MTOC	microtubule organising center
MVB	multivesicular body
MVM	minute virus of mice
μ_N	chemical potential (of a molecule)
μ_N^0	standard free energy (per molecule)
N	aggregation number
NA	neuraminidase
NET	norepinephrine transporter
NLFK	Norden laboratory feline kidney cell line
NMR	nuclear magnetic resonance
NPC1	Niemann-Pick C protein 1
NBV	Nelson Bay Virus
PC	phosphatidylcholine
PDI	protein disulfide isomerase

PI(3)K	phosphatidyl inositol-3 kinase
PI(4,5)P	phosphatidylinositol-4,5-biphosphate
PI3P	phosphatidylinositol-3-phosphate
PIKFyve	FYVE domain-containing PtdIns(3)P5-kinase
PLA_2	phospholipase A_2
POPC	palmitoyloleoyl phosphatidylcholine
Rab	Ras-like proteins from rat brain (GTPase)
Rac1	Ras-related C3 botulinum toxin substrate 1 (GTPase)
RE	recycling endosome
RhoA	Ras homolog gene family member A (GTPase)
RSV	respiratory syncytial virus
SARS	severe acute respiratory syndrome
S_{CD}	deuterium order parameter
SDS-PAGE	sodium dodecyl sulfate polyacrylamide gel electrophoresis
SE	sorting endosome
S*f*9	Spodoptera *frugiperda* insect cell line
SFV	Semliki Forest virus
so	solid ordered phase
SPC	single point charge
SUV	small unilamellar vesicle
SV40	Simian virus 40
TfR	transferrin receptor
TGN	*trans*-Golgi network
TLC	thin-layer chromatography
TM	transmembrane
TO	triolein
v	volume
VLDL	very low density lipoprotein
VLP	virus-like particles
X_N	molar fraction of aggregates of size N

1 INTRODUCTION

The limiting membrane, the plasma membrane, generates the concept of a cell: it creates a separate entity by forming a border between the inside and the outside. Similarly are formed also the inner compartments within eukaryotic cells. The interior of a cell is not a homogeneous mass but a mosaic of different organelles, each lined with their unique membranes. Having this membranous barrier is important for the cell not only in a semantic sense but also in practice: a membrane forms a border which contributes to forming a barrier for maintenance of gradients. Moreover, it functions as the first line of defence against pathogens.

Pathogens entering the cell must pass the plasma membrane to be able to infect the cell. Many of them have evolved to use endocytosis, a natural and important function of the cell, as means of entry into the cell. The membranous border line is there to provide protection for the cell and renders an obstacle for the pathogens to overcome. To be able to penetrate deeper into the cell a pathogen entering by endocytosis must penetrate the endosomal membrane at some point of the complex delivery pathway. Both understanding membranes, their composition and role in facilitating cellular functions, and elucidating the interactions between proteins and membranes are crucial in effort to rationalise the numerous events which take place when a mammalian cell is invaded by a pathogen.

In this thesis, virus-membrane interactions as well as biological membranes, and endosomal membranes in particular were studied with a multidisciplinary focus. In addition, the late steps in the life of the model virus in question, were investigated. The information gained on the membrane-interactions of the non-enveloped model virus helps us to understand how crucial the intracellular membranes are also for non-enveloped viruses and how the virus capsid can directly be influenced by lipid bilayers. This thesis, covering viewpoints from cellular biochemistry to biophysical chemistry, gives new insights into the intracellular membranes and the challenges and opportunities they provide for viral journey from endosomes onwards.

2 REVIEW OF LITERATURE

2.1 Structure and organization of biological membranes

Biological membranes have a crucial role in the survival of all living things. Equally as imperative for an unicellular organism and for a human being, membranes create cells, the smallest units of life by forming a barrier between the inside and the outside. This barrier has intrigued scientists since the days of Robert Hooke, who was the first to introduce the word "cell" in 1665 (Tien & Ottowa 2001). The first evidence of the biological membrane, the plasma membrane, to be a lipid bilayer was provided centuries later, in 1920s. After that numerous models to interpret the complexity of biological membranes have been posed (Tien & Ottowa 2001; Singer 2004). In 1972 the Singer-Nicolson model presented the membrane as a two-dimensional fluid. Molecules were supposed to be randomly distributed in the plane of the membrane based on their unrestricted freedom of mobility (Singer & Nicolson 1972). Despite of the evident superiority of the Singer-Nicolson model compared to those preceding it, it contained many inaccuracies. The later years have attempted to rectify these with the help of substantial development in biochemical and biophysical methodology (Vereb et al. 2003; Engelman 2005). One of the key issues of the present understanding of biological membranes is lateral heterogeneity of the membrane structure. Thermodynamical principles drive lipids to seek the company of those alike or those posing complementary properties. Particularly strongly this tendency is seen with cholesterol, which mixed with phospholipids forms ordered domains at a large range of concentration and temperature (Ipsen et al. 1987; Vist et al. 1990). In cellular studies the more ordered domains in the cell membranes, called in that context lipid rafts, connect biological function to the lateral structure of membranes (Simons & Ikonen 1997). Although the concept of lipid rafts has gained widespread acknowledgment, the details of their existence are still in some respect controversial (Munro 2003). In many cases seeing is believing and so far the rafts, being most likely minute in size, have not been imaged directly on the plasma membrane. However, indirect

evidence has accumulated on plasma membrane hotspots of particular lipid and protein composition. Distinct areas rich in cholesterol, saturated phospholipids, sphingomyelin and characteristic proteins, such as GPI-anchored proteins, have been found to be part of many crucial cellular functions including signalling, endocytosis and cargo delivery (Schroeder et al. 1994; Brown & London 1998; Simons & Toomre 2000; Rajendran & Simons 2005). It seems that rafts are not restricted to plasma membrane. Evidence is accumulating on rafts present on endosomal membranes and on their role on regulating endosome organisation and dynamics (Sobo et al. 2007; Nada et al. 2009).

2.1.1 Lipids

In general terms, lipids are small carbon-based amphipathic or hydrophobic molecules which are formed by ketoacyl or isoprene groups. Based on the chemical structure of their backbone lipids can be divided into polyketides, acylglycerols, sphingolipids, prenols and saccharolipids, but typically a more generalised classification is used (Table 1). Typically glycerophospholipids and sterol lipids are considered separate from other glycerolipids and prenols based mainly on historical reasons (Fahy et al. 2005).

TABLE 1 General classification of some common lipids.
Adapted from (Hauser & Poupart 2005).

Substituted hydrocarbons	Long-chain alcohols
	Long-chain fatty acids
	Steroids
Simple esters	Acylglycerols
	Cholesteryl esters
	Waxes
Complex lipids	Glycerophospholipids
	Sphingolipids
Glycolipids	Glycoglycerolipids
	Glycosphingolipids
	Cerebrocides
	Gangliosides
	Lipopolysaccharides

All biological membranes are composed of lipids, but not all molecules considered to be lipids are ideal for forming membranes. Large diversity of lipid species

in biological membranes provides the basis for fine-tuning the physical properties of the membrane (Cullis et al. 1986).

Glycerophospholipids (see Figure 1) are the most common lipids in biological membranes of eukaryotes. They are formed by a glycerol backbone which has one of its hydroxyls linked to a phosphate-containing group and two others to hydrophobic chains. For most glycerophospholipids the hydrophobic fatty acid chains are attached to 1-*sn* and 2-*sn* positions. The phosphate group, residing in *sn*-3 position, is further linked to an additional group, eg. choline, *myo*-inositol, serine or ethanolamine, which contribute strongly to the packing properties of the lipid as well as determine the more detailed nomenclature of glycerophospholipids, yielding phosphatidylcholine, phosphatidylinositol, phosphatidylserine and phosphatidylethanolamine, respectively (Gennis 1989). Further nomenclature of phospholipids is determined by their fatty acid structure. Combining different fatty acid species under one headgroup gives numerous possibilities for forming differently behaving phospholipid molecules. Table 2 lists some common fatty acids found in membrane lipids of eukaryotes.

TABLE 2 Some common fatty acids.

Fatty acid common name	chain length and unsaturation
Arachidic	20:0
Arachidonic	20:4
Lauric	12:0
Linoleic	18:2
α-Linoleic	18:3 (9-*cis*, 12-*cis*, 15-*cis*)
γ-Linoleic	18:3 (6-*cis*, 9-*cis*, 12-*cis*)
Linolenic	18:6
Myristic	14:0
Oleic	18:1
Palmitic	16:0
Palmitoleic	16:1
Stearic	18:0

Sterols are ubiquitous hydrophobic molecules found throughout taxonomic ranks. Sterols comprise of a steroid ring structure, nonpolar hydrocarbon tail and a hydroxyl group forming a polar head for the molecule. The steroid ring is formed by four fused rings and shared by all sterol lipids. Sterols vary in structure both in having different functional groups attached to their nonpolar tail and by the oxidation state of their ring structure.

Cholesterol (see Figure 1) is the most common sterol and is present in cellular membranes of higher eukaryotes. In phospholipid membranes cholesterol is positioned upright, parallel to the membrane normal with it's hydroxyl head at the level of glyceryl-fatty acid ester bonds (Franks 1976;

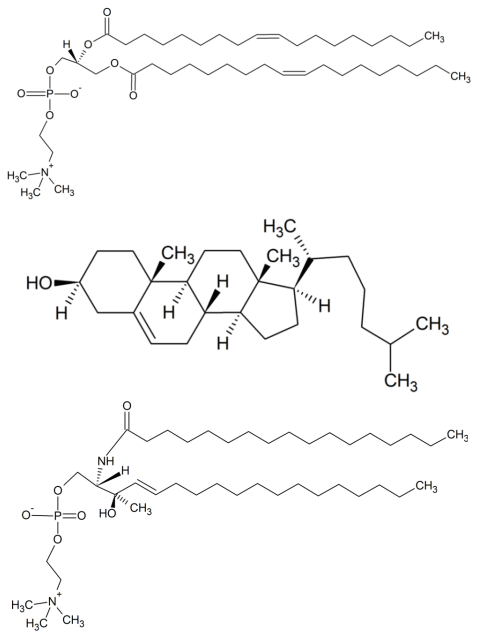

FIGURE 1 Structures of a glycerophospholipid (dioleyl glycerophosphocholine; top), cholesterol (middle) and a sphingolipid (sphingomyelin, bottom).

Worcester & Franks 1976; Dufourc et al. 1984). Effects of cholesterol on phospho- and sphingolipid bilayers have been studied widely. Particularly pronounced the interactions are with phospho- and sphingolipids possessing saturated fatty acid chains (Sankaram & Thompson 1990; Wang & Silvius 2003; Silvius 2003; Ohvo-Rekilä et al. 2002). In cellular membranes cholesterol has been found present in lipid rafts (Simons & Ikonen 1997).

Plant sterols are commonly called phytosterols and include numerous different molecular species. The major phytosterol in plants is sitosterol. In addition, stigmasterol, campesterol, brassicasterol, and avenasterol are found (Piironen et al. 2000). Ergosterol, another structural variant of the sterol family, is present in lower eukaryotes, such as fungi and yeast. Lanosterol, the biosynthetic precursor of both cholesterol and ergosterol is found in prokaryotic membranes. Different sterols have shown to have similar effects on the material properties of phospholipid membranes. Sterols in general stiffen the membrane, which is seen for example as increased elastic moduli (Endress et al. 2002; Henriksen et al. 2004; Henriksen et al. 2006).

Sphigolipids (see Figure 1) are a heterogenous group of lipids having a long sphingoid base, typically sphingosine or sphinganine, as a backbone onto which fatty acids are attached via amide bonds. The simplest of sphingolipids are ceramides, which have only two hydroxyl groups as the hydrophilic regions. More complex sphingolipids such as sphingomyelin and glycosphingolipids

have larger headgroups, phosphorylcholine and sugar residues, respectively. Sphingolipids have been found to be connected to important cellular signalling functions controlling eg. proliferation and apoptosis in cells (Goeztl et al. 1999; Maceyka et al. 2002; Futerman & Hannun 2004). In addition, particular interest for sphingolipids, and especially for sphingomyelin, has been raised in the context of domain formation and lipid rafts. Saturated sphingolipids prefer to partition into ordered domains in membranes (Wang & Silvius 2003) and show particularly strong interactions with cholesterol (Leventis & Silvius 2001; Ramsted & Slotte 2006). In plasma membranes sphingomyelin is found in areas considered as lipid rafts (Simons & Ikonen 1997).

2.1.2 Self-assembly of lipids

Lipids have several functions in biological systems ranging from signalling to serving as precursors on metabolic routes. Their fundamental role, however, is to form membranes, which on their part create barriers and compartments, form a matrix for membrane-embedded proteins and even control the influx of material into the cell. In aqueous solutions amphiphilic molecules, such as lipids, self-associate into different types of aggregates. One type of these aggregates is a bilayer, which is the basis of most biological membranes.

Lipid aggregates, such as micelles and bilayers, are formed by non-covalent interactions between lipid molecules. The non-polar hydrocarbons in the lipids contribute to the hydrophobic effect in aggregate formation. The hydrocarbon chains cannot break the water structure by forming hydrogen bonds and are therefore energetically and entropically unfit to reside in aqueous environment. When mixing oil and water this leads to phase separation, in the case of amphiphilic molecules, such as lipids which have a hydrophobic tail and a hydrophillic head, aggregates are formed. The precise form of te aggregate depends on the molecular details of the lipids in question. Packing of lipids into different types of aggregates, micellelles and bilayers, is governed by a number of factors. Interfacial tension attracts the lipids closer together by reducing the cross-sectional areas of the lipid tail and head regions. Repellant contribution to the matter is on the other hand given by steric and electrostatic interactions. Balancing these opposing forces determines the molecular details of aggregate formation. Formation of lipid bilayer, for example, requires the tail and the head cross-sectional areas of the participating lipids to be similar (Israelachvili 1992; Gennis 1989).

Self-assembly of amphiphiles, such as lipids, is governed by fundamental principles of equilibrium thermodynamics stating that in all aggregates formed in a solution each individual molecule should have equal chemical potential. Israelachvili (Israelachvili 1992) writes the same following the simple approach of Tanford (Tanford 1980) as follows:

$$\mu = \mu_1^0 + kT \log X_1 = \mu_2^0 + \frac{1}{2}kT \log \frac{1}{2}X_2 = \mu_3^0 + \frac{1}{3}kT \log \frac{1}{3}X_3 = ... \qquad (1)$$

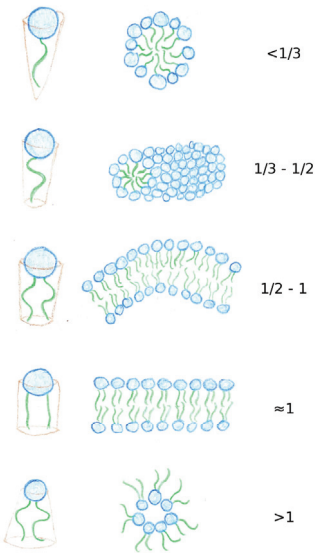

FIGURE 2 Packing shapes of lipids and the formed structures. Structures from the top: micelle, tubular micelle, flexible bilayer or vesicle, planar bilayer and inverted micelle. Critical packing parameters ($v/a_0 l_c$) for each type of lipids are presented on the right. Modified from (Israelachvili 1992)

or in a more simplified manner:

$$\mu = \mu_N = \mu_N^0 + \frac{kT}{N} \log(\frac{X_N}{N}) = \text{constant, N = 1, 2, 3...} \quad (2)$$

where in an aggregate of size N, μ_N is the chemical potential of a molecule, μ_N^0 the standard free energy per molecule and X_N the molar fraction of aggregates of size N. μ_N^0, the standard free energy, represents all the free energy resulting from the opposing forces forming the aggregate whereas $\frac{kT}{N} \log(\frac{X_N}{N})$ is the entropy for moving the aggregate in the solution (translational entropy). $N = 1$ corresponds to individual lipids (monomers) in solution.

Equation 2 is the thermodynamic equilibrium condition. The standard chemical potential (μ_N^0) of the aggregate components, that is to say the individual lipid molecules, has a mininimum at some size N^* corresponding to the micelle size, or stays constant for increasing and large N, which is the case for a lipid bilayer. Put in simpler terms, for lipids (and in general for all amphiphiles) micellarisation, the formation of aggregates of certain finite size, is favoured by free energy. In contrast, alkenes, as for example oil, form infinite aggregates which leads to phase separation in stead of micellarisation (Israelachvili 1992).

Lipids are able to assemble themselves into different kinds of structures, micelles, inverted micelles or bilayers which can seal themselves into vesicles. The type of the forming structure is dictated by principles of molecular packing which, based on the geometry of the participating molecules, favour the

formation of distinct types of structures for distinct types of lipids. The dimensionless packing parameter, v/a_0l_c, for lipids of certain optimal headgroup area a_0, certain molecular volume v and critical chain length l_c, that is to say the maximum chain length for the lipid, describes the types of structures they form. Spherical micelles are formed mainly by single chain lipids with v/a_0l_c below $\frac{1}{3}$. They have relatively large optimal headgroup areas, typically caused by charged headgroups. Lipids with smaller optimal headgroup areas compared to their tail region, v/a_0l_c from $\frac{1}{3}$ to $\frac{1}{2}$, are prone to form cylindrical micelles. When the headgroup area of the lipids is roughly equal to the area occupied by the tail region, corresponding to v/a_0l_c of 1, the lipids favour packing into bilayers. Typically, the situation arises with lipids having two fatty acid chains. A planar bilayer is energetically challenged as the rim the hydrophobic core of the bilayer is exposed to water. Therefore, if the lipids can keep their optimal headgroup area also in a curved environment, sealing the planar bilayer into a spherical vesicle is favoured. In these cases the shape of the lipid resembles a truncated cone and v/a_0l_c lies in the order of $\frac{1}{2}$ - 1. If lipid has a very small optimal headgroup area, as typically seen with phosphatidylethanolamine, or voluminous tail region, which can occur typically with polyunsaturated tail chains, the v/a_0l_c can exceed 1. In these cases inverted micelles are formed - or the lipids simply precipitate (Israelachvili et al. 1976; Israelachvili 1992). Figure 2 summarises lipid shapes and the formed structures.

2.1.3 Thermotropic phase behaviour of phospholipid bilayers

The main phase transition of a lipid bilayer is a co-operative process where the membrane shifts from gel to fluid phase. In the process the molecular motion of the fatty acid hydrocarbon chains is increased as they transfer from *all*-trans into gauche conformations (Figure 3). The temperature at which the transition occurs is characteristic for each lipid and depends, in addition to the lipid headgroup, on saturation and length of the fatty acid chains (Koynova et al. 1998). For example, distearyl phosphatidylcholine (DSPC) has it's melting temperature at 55.3°C (Lewis et al. 1987) whereas the main transition for dioleoyl phosphatidylcholine (DOPC), having the same chain length but with a *cis* bond in the 9-positions of the chains, is as low as -17.3°C (Lewis et al. 1988). On the other hand, dipalmitoyl phosphatidylcholine (DPPC), with tail chains two carbons shorter than those of DSPC, has its transition temperature at a markedly lower temperature, at 41.4°C (Lewis et al. 1987).

For each lipid the temperature for the melting transition is determined by thermodynamical balance between different contributing factors. The rigid gel phase favours the attractive forces between lipids arising from van der Waals interactions, whereas the disordered tail chains in gauche conformations present in fluid phase are entropically favoured in comparison to the rigid *all*-trans configurations of the gel state. In addition to these aspects also interactions between the headgroups, whether attractive or repulsive, affect the situation (Gennis 1989).

When the membrane undergoes the main phase transition, several

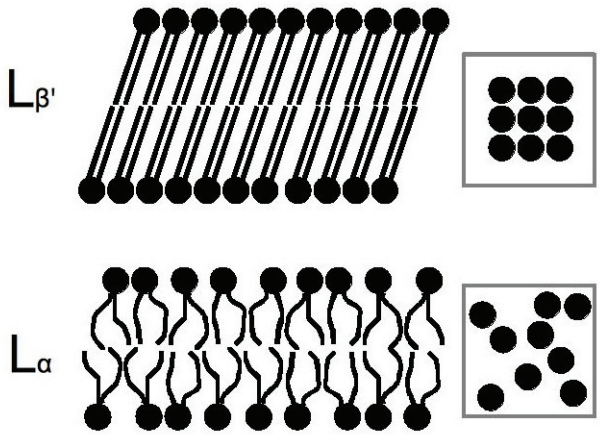

FIGURE 3 Organisation and packing of lipid bilayers in gel ($L_{\beta'}$) and fluid (L_{α}) phase. Drawings on the left represent the ordering of the acyl chains and in the boxes on the right the packing of lipids in the plane of the membrane is illustrated. Modified from (Hauser & Poupart 2005)

properties of the bilayer are altered. The area and thickness of the bilayer change, which results in a membrane volume change (Heimburg 1998). For DPPC, the change in the membrane area has been noted to be about 17% (Janiak et al. 1976). Similarly, the bilayer thickness appears to decrease approximately 18% (calculated from (Nagle et al. 1996)). However, the change in the volume of the membrane during transition has been reported to be merely in the range of 4% (Nagle & Wilkinson 1978). In addition to these, close to the main transition the bilayer softens. The area compressibility of the membrane increases and, consequently, the bending elastic modulus decreases, indicating the membrane to become more elastic and more easily deformable. A striking example for the distinct difference in the area compressibility modulus (K) of the membrane on either side of the main transition is seen with dimyristoyl phosphatidylcholine (DMPC). At 8.3°C , when the membrane is in gel ($L_{\beta'}$) phase, K measured with micropipette aspiration, was 855 mN/m, whereas in the fluid (L_{α}) phase the value was as low as 145 mN/m (Needham & Evans 1988).

The transition from gel to fluid phase is not in all cases a simple melting process. Even in one-component phospholipid membranes the density distribution of the bilayer may exhibit pronounced lateral variability during transition leading to dynamic heterogeneity in the membrane (Ruggiero & Hudson 1989; Ipsen et al. 1990a). In addition, the transition may include pretransitions and formation of ripples in the membrane (Janiak et al. 1976; Rand et al. 1975; Heimburg 2000). Mixing of phospholipids with different kinds of chains is

nonideal and, consequently, the complex nature of the main phase transition of phospholipids is seen pronouncedly in lipid mixtures, where coexisting regions containing both gel and fluid areas are found (Sankaram et al. 1992; Inoue et al. 1999).

2.1.4 Cholesterol-phospholipid interactions

Cholesterol associates particularly strongly with saturated choline phospholipids, sphingomyelin being the most preferred species (Ohvo-Rekilä et al. 2002). This association is enhanced by the preferential partitioning of cholesterol into membranes with sphingomyelin or saturated phospholipids (Niu & Litman 2002). The rigid steroid ring structure of cholesterol intercalates more favourably in a bilayer with saturated acyl chains (Lund-Katz et al. 1988). Interactions of cholesterol with saturated phosphatidyl choline and sphingomyelin bilayers are characterized by more pronounced van der Waals attractions (Lund-Katz et al. 1988) and association of cholesterol with the carbonyl groups of phospholipid hydrocarbon chains (Sankaram & Thompson 1990). Hydrogen bonding between the amide linkage of sphingomyelins and the hydroxyl group of cholesterol has been proposed to render interactions with sphingomyelin especially preferred (Sankaram & Thompson 1990). In natural membranes preference of cholesterol for sphingomyelins is enforced by the fact that sphingomyelin species abundant in nature have long and saturated acyl chains, whereas phosphatidyl cholines are typically shorter and contain unsaturated chains (Ohvo-Rekilä et al. 2002). Multiple unsaturations in acyl chains counteract the condensing effect of cholesterol on bilayers (Needham & Nunn 1990; Smaby et al. 1997).

Interactions between saturated phospholipids and cholesterol result in very particular phase behaviour of the mixtures (Ipsen et al. 1987; Vist et al. 1990; Sankaram & Thompson 1990). Similar behaviour has also been shown for sphingomyelin-cholesterol mixtures (Sankaram & Thompson 1990; Chachaty et al. 2005). Cholesterol has been shown to induce an increase in the acyl chain order of the phospholipid in egg lecithin (Stockton & Smith 1976) and DPPC (Vist et al. 1990; Ipsen et al. 1990b; Hofsa et al. 2003) bilayers. The underlying reason for cholesterol-induced ordering is, based on a theoretical model, proposed to be the specific short-range interactions between cholesterol and the nearby phospholipids (Ipsen et al. 1987). Effects of cholesterol are not limited to rigidifying the fluid phase. In the solid phase cholesterol breaks the lattice-structure of the membrane by decreasing translational order by decoupling the ordering of the phospholipids from that of the solid phase. At high cholesterol concentrations this occurs even at temperatures below the main phase transition of the bilayer (Ipsen et al. 1987; Vist et al. 1990).

The main phase transition temperature of phosphatidyl choline bilayers is depressed by increasing concentrations of cholesterol (Genz et al. 1986; McMullen et al. 1997; Ipsen et al. 1990b). The complex phase behaviour of PC-cholesterol systems gives raise to a very special form for the phase diagram.

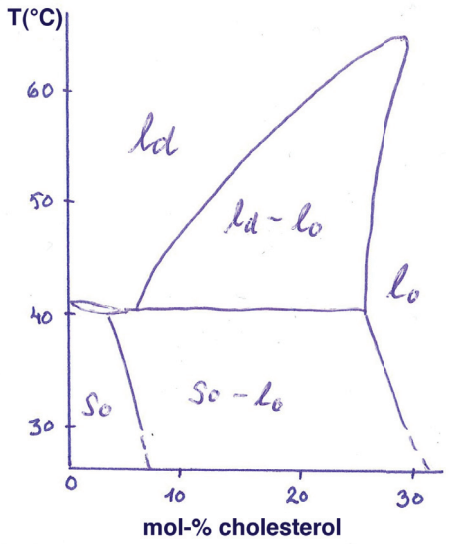

FIGURE 4 Phase diagram of DPPC-cholesterol system (modified from (Ipsen et al. 1987)). Notations for different phases: so, solid ordered; ld, liquid disordered; lo, liquid ordered. The small region at the beginning of the triple line corresponds to so/ld coexistence.

The full phase diagram for PC-cholesterol system was first calculated for DPPC (Ipsen et al. 1987) followed by confirmation by an experimental study (Vist et al. 1990). Later, the general form for the phase diagram was shown to apply for a number of PC-cholesterol binary systems (Thewalt & Bloom 1992). In the phase diagram (Figure 4), in temperatures below the main phase transition and with low cholesterol concentration, the bilayer is in gel, or solid ordered (so) phase. The truly fluid liquid-disordered (ld) phase in higher temperatures and low cholesterol concentration is transformed by increasing amount of cholesterol into the liquid-disordered (lo) phase. This unique phase is characterised by attributes of both ordered and disordered, each originating from the interactions between cholesterol and acyl chains of the lipids. The liquid-ordered phase presents both high degree of acyl chain ordering, or conformational order, seen in the solid phase and translational disorder typical for the liquid-disordered phase (Ipsen et al. 1987). Originally, cholesterol was deciphered not to influence the lateral diffusion of phospholipids in fluid bilayers based on measurements with egg yolk lecithin, DPPC and DOPC membranes (Lindblom et al. 1981), but later criticism for this interpretation was raised based on NMR measurements with DMPC bilayers (Oradd et al. 2003). The two liquid phases, ld and lo, coexist at a wide temperature and concentration range (Ipsen et al. 1987; Vist et al. 1990; Sankaram & Thompson 1990; Sankaram & Thompson 1991). In addition, the solid ordered phase with it's crystal packing perturbed by cholesterol exhibits coexistence of solid ordered and liquid-ordered phases (Ipsen et al. 1987).

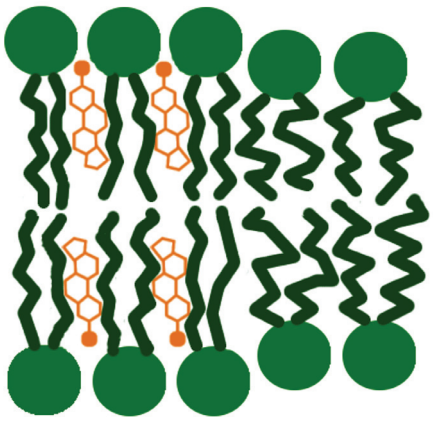

FIGURE 5 Position of cholesterol in phospholipid bilayer. Cholesterol molecules (orange) are aligned to the membrane normal with their polar hydroxyl heads at the level of the glycerol groups of phospholipids (green) (Franks 1976; Worcester & Franks 1976; Dufourc et al. 1984). Cholesterol increases conformational order of the lipid tail chains (left in figure), which is characteristic for the liquid-ordered phase (Ipsen et al. 1987).

The phase behaviour of cholesterol-phospholipid mixtures is seen clearly as differences in the physical properties of the bilayers. The area expansion modulus (K_a) (Needham & Nunn 1990; Needham et al. 1988; Endress et al. 2002; Henriksen et al. 2004) and the bending rigidity modulus (κ) (Duwe et al. 1990; Meleard et al. 1998; Henriksen et al. 2004) both increase with cholesterol. In the case of POPC vesicles the increase in bending rigidity measured with vesicle fluctuation analysis has been reported to be nearly proportional to the concentration of cholesterol in the bilayer (Henriksen et al. 2004). With increasing cholesterol concentration the membrane area decreases and the bilayer gains thickness (Ipsen et al. 1990b; Hofsa et al. 2003; de Meyer & Smit 2009). In fact, the thickness mismatch of cholesterol-rich areas and rest of the lipid bilayer is proposed to contribute to immiscibility seen in cholesterol-phospholipid systems (Kučerka et al. 2008).

2.1.5 From phase separation to lipid rafts

Different phases have different physical properties - and very often also different molecular composition. Although in physiological conditions most biological membranes are in fluid phase (Cullis et al. 1986), the complex phase behaviour of cholesterol containing systems (see: section 2.1.4) brings about peculiarities in the properties of the membrane. At the same time, the lateral heterogeneity of cellular membranes enhanced by cholesterol provides opportunities for controlled functions. Lipid rafts, as mentioned already in the

beginning of this literature review, are areas of cellular membranes rich in cholesterol, saturated phospholipids and sphingomyelin (Simons & Ikonen 1997). In addition to lipids, rafts contain proteins which preferentially partition into the ordered regions. These include e.g. proteins with GPI-anchors (Varma & Mayor 1998; Chatterjee & Mayor 2001), palmitoylated and myristoylated proteins (Rajendran et al. 2003) as well as cholesterol-binding proteins such as caveolin, which is present in caveolae structures (Song et al. 1996; Simons & Ehehalt 2002).

Unlike in model membranes, where classical raft lipid mixtures present pronounced ld/lo phase separation (Dietrich et al. 2001; Veatch & Keller 2003; Lindblom et al. 2006), the situation in the plasma membrane is complicated by constant addition and removal of lipids in the membrane (Simons & Vaz 2004). Furthermore, long- and short term ordering in different time scales can produce ordered domains of variable sizes. This is further aided by the contribution of membrane proteins and the cell cytoskeleton (Jacobson et al. 2007). Correspondingly, the lateral heterogeneity of biological membranes has been proposed include also non-raft domains in addition to rigid membrane areas. Origin of these alternate domains has been suggested to be in eg. dynamic fluctuations of membrane density (Ruggiero & Hudson 1989; Ipsen et al. 1990a) and presence of polyunsaturated fatty acids such as DHA (Wassall & Stillwell 2008).

Rafts, however, are not just any domains found on the plasma membrane. Originally rafts were defined by detergent resistance, stemming from evidence on insolubility of ordered, sphingolipid-rich areas of plasma membrane in cold non-ionic detergents, and by characteristic buoyancy of the recovered membrane fragments on density gradients (Brown & Rose 1992; Brown 1994). Concern has been raised on the fact that the detergent itself can create aggregation of lipids generating thus inherent artefacts in the detergent isolation method (Heerklotz 2002), but also an opposite view has been presented (Staneva et al. 2005). The raft theory has evoked a rather elaborate scientific debate during which opposing convictions and indications have been argued (see e.g. (Powell & Leslie 2006; Lichtenberg et al. 2005; Munro 2003; Hancock 2006; London & Brown 2000). The discussion has refined the view on rafts and shifted the notion from ambiguous detergent-isolated clusters into distinct type of ordered domains found on cellular membranes. A raft is considered to have a particular lipid and protein composition, to be transient in existence (London 2005; Dietrich et al. 2002) and to be, at least in non-clustered form, small enough to avoid detection by optical imaging (Prallea et al. 2000; Almeida et al. 2005; Varma & Mayor 1998). Nomenclature for the phenomenon, however, remains to be confusing and terms such as liquid-ordered membrane domain, raft and detergent-resistant membrane (DRM) are still often used interchangeably.

Clustering of rafts into larger aggregates occurs through oligomerisation of proteins (Paladino et al. 2004; Simons & Vaz 2004). Clustering can be induced artificially (Harder et al. 1998; Janes et al. 2000), but it is an ongoing natural process which allows the small rafts to form larger platforms for intracellular functionality (Simons & Ehehalt 2002; Simons & Vaz 2004). Raft clustering

has been proposed to be a way to couple the outer leaflet and inner leaflet rafts (Gri et al. 2004). One of the best characterised clustering events on the plasma membrane is the formation of caveolae. Caveolae are plasma membrane cavities of 50-100 nm in size which can detach from the membrane to form vesicles (Peters et al. 1985). Caveolae are lined with caveolin-1 protein (Rothberg et al. 1992). The lipid composition of caveolae is thought to match that of lipid rafts (Meder & Simons 2006). The view is supported by the strong binding of caveolin-1 to cholesterol (Murata et al. 1995). Caveolin-1 can also be cross-linked by the ganglioside GM1 (Fra et al. 1995), which gives further evidence on the strong presence of raft lipids in caveolae. Caveolar invaginations are formed through oligomerisation of the caveolin-1 protein (Monier et al. 1995; Sargiacomo et al. 1995) and internalised in a regulated manner triggered by the ingoing cargo, such as Simian virus 40 or cholera-toxin binding to GM1 molecules (Parton et al. 1994; Pelkmans et al. 2001; Orlandi et al. 1998). Caveolae, like other clustered raft regions (Pierce 2002), have also been noted to act as signalling platforms (Li et al. 1996; Okamoto et al. 1998). In addition of the general nature of the signalling in caveolae, caveolae-based signalling is also used to trigger their own internalisation process (Aoki et al. 1999).

2.2 Endocytosis and endosomes

2.2.1 An overview of endocytic routes

Mammalian cells have various ways by which they internalise material, all of them collectively called endocytosis. These cellular internalisation pathways can be divided roughly into phagocytosis and pinocytosis (see Figure 6). In phagocytosis large particles (>0.5 μm), such as pathogens or apoptotic cells, are taken in into the cell (Aderem & Underhill 1999). Phagocytosis is triggered by receptor recognition on the cell surface followed by internalisation of the particle and subsequent fusion of the vesicle with lysosome to form a phagolysosome (Stuart & Ezekowitz 2005). Monocytes, macrophages and neuthophils, collectively also known as professional phagocytes, are responsible for the majority of the ongoing phagocytosis. Consequently, phagocytosis has a strong role in triggering defence mechanisms (Aderem & Underhill 1999; Aderem 2003).

Pinocytosis delivers extracellular fluid, macromolecules and membrane into the cell. The different pinocytic methods are summarised in Figure 6. Macropinocytosis is characterised by membrane ruffling, i.e. membrane protrusions which collapse and fuse with the plasma membrane generating large vesicles, or macropinosomes (0.2 - 5 μm), containing extracellular fluid and molecules residing in the fluid phase (Swanson & Watts 1995; Swanson 2008). Although the mechanism for particle intake by macropinocytosis is rather unspecified, it is nevertheless strictly controlled. The formation of membrane ruffles is actin-dependent and regulated through the GTPases of the Rho-family such as Rac1 and Cdc42

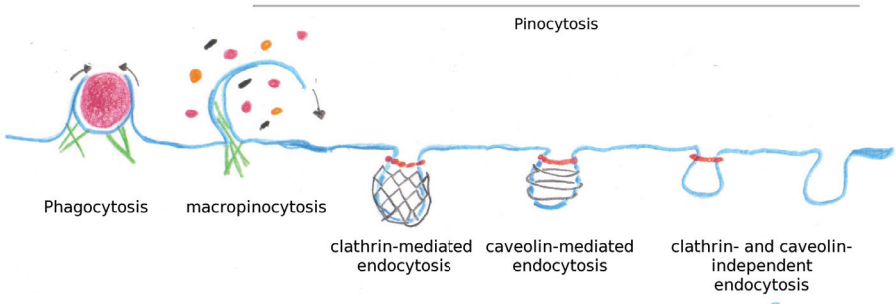

FIGURE 6 Different modes of endocytosis. Phagocytosis is utilised mainly by professional phagocytes while pinocytosis, including clathrin-mediated, caveolin-mediated and clathrin- and caveolin-independent pathways, is a ongoing process in majority of cell types. Figure modified from (Conner & Schmid 2003). Illustration by Lars Duelund. Reproduced with artists' permission.

(Ridley et al. 1992; Garrett et al. 2000; Conner & Schmid 2003).

Clathrin-mediated endocytosis is responsible for the constitutive uptake of nutrients into cells. The continuous internalisation process, where receptors are endocytosed irrespective of ligand-binding, involves for example low density lipoprotein receptor (LDLR) (Anderson et al. 1982) and transferrin receptor (TfR) (Watts 1982). The non-constitutive internalisation of receptors is triggered by specific ligands binding to their receptors, as examplified by the intake of the epidermal growth factor receptor (EGFR) (Beguinot et al. 1984). During the process the receptors and their bound ligands are gathered into clathrin-coated pits on plasma membrane. The pit is lined by clathrin triskelions, complexes of three heavy chains of the clathrin protein and supplemented with bound light chains, which self-assemble into caged structures aided by adaptor protein (AP) complexes. The coated pits invaginate into the cell and eventually pinch off as clathrin-coated vesicles with the help of the GTPase dynamin. Two mechanisms for the cleavage process has been proposed. One model presents dynamin as "pinchase" which constricts the vesicle neck resulting in severing of the vesicle from plasma membrane (Hinshaw & Schmid 1995; Sweitzer & Hinshaw 1998) and the other as "poppase" which in a spring-like manner detaches the vesicle (Stowellet al. 1999).

Caveolar endocytic pathway does not require clathrin. It begins from caveolae, plasma membrane cavities lined with caveolin-1 protein (Peters et al. 1985; Rothberg et al. 1992). In non-induced conditions caveolae either reside motionless on the plasma membrane (Parton et al. 1994; Pelkmans & Zerial 2005) or make rapid cycles in the vicinity of the plasma membrane without starting onto the vesicular delivery route (Pelkmans & Zerial 2005). This short cycle can be triggered into endocytosis where the enclosed cargo is delivered to caveosomes. Regulation of the short- and long-distance circulation appears to be kinase-based

(Pelkmans & Zerial 2005). In addition to fusion with caveosomes, caveolar vesicles have been shown to be able to dock onto other organelles such as early endosomes where they maintain their original lipid and protein composition. This peculiar behaviour of the caveolar vesicles has been proposed to link endocytic and exocytic routes and to permanently ensure the identity of caveolar domains (Pelkmans et al. 2004).

Clathrin-independent endocytosis can also occur through mechanisms which do not include participation of caveolin and which can be either dependent or independent of dynamin. These pathways are, however, poorly understood compared to other pinocytic routes for internalisation (Conner & Schmid 2003). The dynamin-dependent, clathrin- and caveolin independent internalisation pathway is proposed to be regulated by RhoA and the dynamin-independent variants by either Arf6 or Cdc42 (Conner & Schmid 2003; Mayor & Pagano 2007).

2.2.2 Travelling through the clathrin-mediated endocytic pathway

When endocytic cargo embarks on it's journey along the clathrin-mediated pathway, it is first internalised into the cell in a vesicle coated with clathrin (see section 2.2.1). Soon after the original clathrin-coated vesicle has detached itself from the plasma membrane, it is uncoated enzymatically in an ATP-dependent manner (Braell et al. 1984). The uncoated vesicle delivers the cargo to an early endosome onto which it fuses. Early endosomes are also called sorting endosomes based on their function to sort cargo to their appropriate destinations (Mayor et al. 1993). In the mildly acidic lumen of the early endosome the cargo molecules are disengaged from their receptors (Yamashiro et al. 1984; Mellman 1996; Mukherjee et al. 1997). The cargo is proposed to be sorted to futher locations on the endocytic route by retention in the vesicular areas, whereas the receptors, proposedly due to their larger fractional surface area, accumulate in the tubular regions of the early endosomes. From these tubules the receptors are subsequently sent back to the plasma membrane (Mayor et al. 1993; Mellman 1996). Although this general scheme of sorting applies to many receptor-ligand pairs, alternate fates for receptors occur. Some of them, like EGFR can be sorted forward for degradation (Herbst et al. 1994), while others, such as the cation-independent mannose 6-phosphate receptor (Ci-MPR), have distinct intracellular destinations to go to (Jin et al. 1989; Mukherjee et al. 1997). Transit through the early endosome is rapid: the cargo continues onwards together with the intraluminal vesicles in 2-3 minutes (Mellman 1996). Some of the recycled material is not returned directly to the plasma membrane, but shuttled through recycling endosomes. The recycling endosomes are located deeper in the cell, close to the microtubule organising center (MTOC) (Perret et al. 2005). Passage through the recycling vesicles is slower than the direct route from sorting endosomes to plasma membrane (Schmid et al. 1988; Mellman 1996).

Two alternate models have been proposed on the progression of cargo from early to late endosomes. The carrier vesicle approach presents large multivesicular structures which are derived from vacuolar regions of sorting endosomes

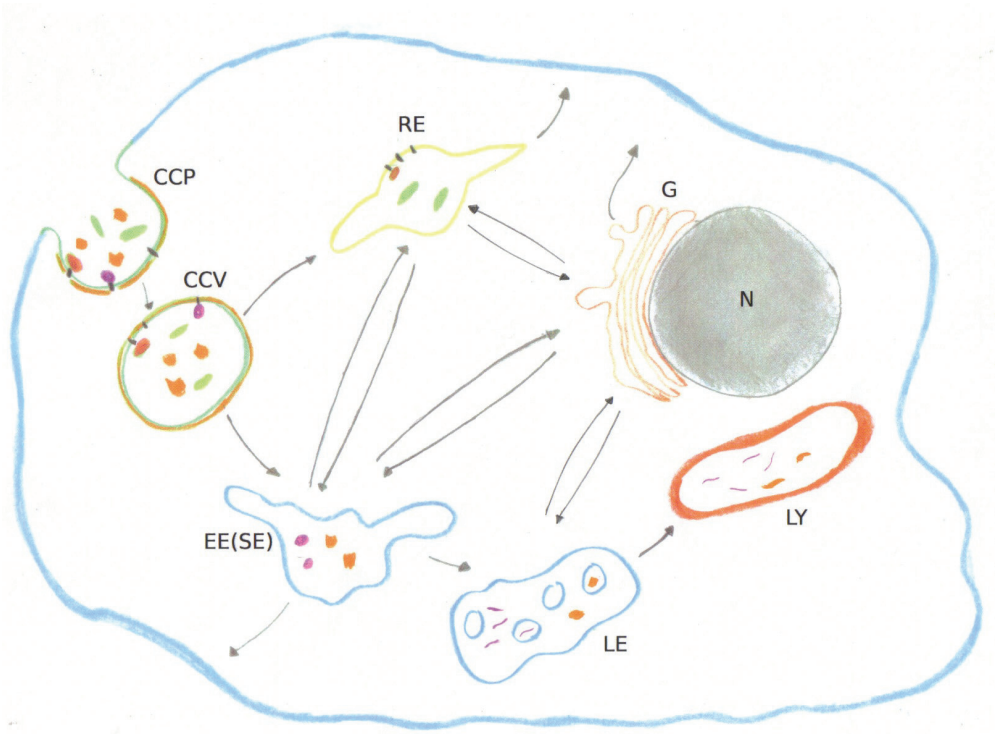

FIGURE 7 Clathrin-mediated endocytic route. Cargo, bound to receptor, is internalised into the cell through the clathrin-coated pit (CCP), after which the formed clathrin-coated vesicle (CCV) is uncoated. The vesicle fuses with the early (sorting) endosomes (EE/SE), where some of the receptors bound for recycling, and cargo destined to proceed forward are sorted into separate areas. The recycling endosome (RE) contributes to further sorting and recycling of the endocytosed material. The onwards sorted cargo is delivered from early endosomes to late endosomes (LE) and further to lysosomes (LY), where the molecules are degraded. Arrows represent delivery between organelles. G, Golgi; N, nucleus. Figure adapted from (Mukherjee et al. 1997; Sieczkarski & Whittaker 2002) based on (Kornfeld & Mellman 1989; Mellman 1996). Illustration by Lars Duelund. Re-produced with artists' permission.

and contain internal vesicles. The carrier vesicles, travelling along microtubules, deliver forward sorted cargo to late endosomes (Gruenberg et al. 1989; Aniento et al. 1993). The other model suggests the same large multivesicular structures, initially early (sorting) endosomes, to maturate into late endosomes (Stoorvogel et al. 1991; Dunn & Maxfield 1992; Woodman & Futter 2008). ESCRT protein complex facilitates the sorting of ubiquitin-tagged gargo to lysosomes for degradation. It is also found to be connected to the formation of internal vesicles in multivesicular bodies (Conibear 2002).

Like the delivery of material from early endosomes to late endosomes, transfer of endocytic cargo from late endosomes to lysosomes remains elusive. An early model, maturation, assumed lysosomes to be formed from late endosomes in a gradual process (Roederer et al. 1987; Murphy 1991). Later, evidence of content mixing between late endosomes and lysosomes contradicted the maturation theory (Bright et al. 1997; Mullock et al. 1998). Three mechanisms for content mixing have been proposed, although one of them, vesicular transport between late endosomes and lysosomes, relies merely on experimental results in yeast (Vida & Gerhardt 1999). The kiss-and-run model explains content mixing to occur through transient fusion and fission events, or "kisses", between the two compartments (Storrie & Desjardins 1996). The third model proposes the fusion of the late endosomal and lysosomal vesicles to be complete and lysosomes to be reformed from the hybrid organelles formed in fusion (Bright et al. 1997; Mullock et al. 1998; Pryor et al. 2000). The fusion-fission theory has been seen as an elaboration of the kiss-and-run model (Luzio et al. 2000). In addition, evidence has been presented that these two methods of cargo delivery to lysosomes appear simultaneously in a cell (Bright et al. 2000). Once in lysosomes, the delivered molecules are degraded by hydrolytic enzymes (Kornfeld & Mellman 1989). The clathrin-mediated endocytosis pathway is summarised in Figure 7.

2.2.2.1 Early and recycling endosomes

In many cultured cell types early endosomes form a network of tubules and vesicular regions dispersed in the cytoplasm (Hopkins et al. 1990; Tooze & Hollinshead 1991; Mellman 1996). The vesicular compartments of the organelle have a diameter of 250-400 nm, whereas the tubules have been measured to be 50-60 nm in diameter and reach out up to 4 μm outwards. Up to 70% of the volume of the organelle has been estimated to be in the vesicular areas and 50-80 % of the surface area in the tubules (Mukherjee et al. 1997; Gruenberg et al. 1989; Marsh et al. 1986). The structures are mildly acidic with a pH of 6.3 - 6.8 (Yamashiro et al. 1984; Mellman 1996).

Small GTPases of the Rab family are found throughout the endosomal system. Both Rab4 and Rab5 are present in early endosomes. Rab4 regulates recycling of receptors to the plasma membrane directly from early endosomes and possibly also through a slower route through the recycling endosomes (Daro et al. 1996; Mohrmann et al. 1999). Rab5 is important for fusion of clathrin-coated vesicles into early endosomes (McLauchlan et al. 1998) and for fusion

events between the early endosomes. This homofusion is facilitated by Rab5 together with effector proteins phosphatidylinositol-3 kinase (PI(3)K) and early-endosomal autoantigen (EEA1) (Simonsen et al. 1998; Christoforidis et al. 1999). EEA-1 is classically used as a identification marker for the early endocytic compartment (Mu et al. 1995). In addition to the fusion functions, Rab5 has been linked with the movement of the early endosomal structures along microtubules (Nielsen et al. 1999). Cooperative actions of Rab4 and Rab5 have been suggested to orchestrate the influx into and efflux out of endosomes (Mohrmann et al. 1999).

The early endosomes are sometimes referred to as sorting endosomes based on their primary function, the sorting of endocytic cargo to appropriate locations (Mayor et al. 1993) (see section 2.2.2). Nomenclature of the early compartment is complicated by recycling endosomes, which are sometimes grouped under the name early endosomes together with the sorting compartment to emphasise their early occurance in the endocytic pathway and to differentiate them clearly from late endosomes. The recycling endosomes are formed, similar to sorting endosomes, by interconnected tubular structures of 50-70 nm in diameter and function likewise in recycling (Mellman 1996; Mukherjee et al. 1997; Perret et al. 2005). The lumen of recycling endosomes is slightly more acidic than that of early (sorting) endosomes. Their pH is in the order of 6.2 - 6.4, depending on cell type (Perret et al. 2005; Gagescu et al. 2000), which further underlines that the organelle is physically distinct from early (sorting) endosomes. Rab11 is a prominent marker for recycling endosomes. It has been suggested to govern the return of recycling receptors to the plasma membrane as well as delivery from Golgi to plasma membrane through the endosomal system (Somsel Rodman & Wandinger-Ness 2000; Ullrich et al. 1996; Ren et al. 1998; Chen et al. 1998). In apical recycling endosomes at least two other Rab proteins are encountered in addition to Rab11. Rab17 is connected to transcellular trafficking through recycling endosomes (Hunziker & Peters 1998), whereas Rab25 has been proposed to maintain homeostasis of the organelle together with Rab11 and possibly to have a role in retrograde traffic from the recycling compartment to Golgi (Somsel Rodman & Wandinger-Ness 2000).

2.2.2.2 Late endosomes - multivesicular bodies

Late endosomes were named generically based on their late participation in the endocytic route. Delivery of material into late endosomes takes in mammalian cells 4 - 30 minutes (Piper & Luzio 2001). In contrast to early endosomes, which have a tubular appearance, late endosomes are distinctly more vesicular. Their size, on the other hand, is in the same range with early endosomes (Mukherjee et al. 1997). On the basis of their more detailed morphology, which features prominent internal vesicles and membrane invaginations, the late endosomes are sometimes referred to as multivesicular bodies (MVBs) (Piper & Luzio 2001). However, the nomenclature of the late endocytic organelles is somewhat confusing, as some authors consider MVBs to be merely delivery intermediates between early and late compartments and to differ

distinctly from the actual late endosomes by their lipid and protein content (Gruenberg 2001). The late endosomal compartments are markedly more acidic than early endosomes, and have their pH around 5.5 - 6.0 (Mukherjee et al. 1997; Gruenberg 2001).

Discrimination between late endosomes and lysosomes by using electron microscopy is usually straightforward as the late endosomal morphology is seen distinctly different from that of electron dense lysosomes. Late endosomes are seen as pleiomorphic structures with cisternal, tubular and multivesicular regions (Gruenberg & Stenmark 2004). With biochemical methods the differences seen between the the organelles are not as clear-cut, but nevertheless certain hallmarks characterising the organelles are evident. When centrifuged in a density gradient, such as Percoll, late endosomes appear at a distinctly lower density than lysosomes (Kornfeld & Mellman 1989; Mellman 1996). Ci-MPR facilitates the delivery of lysosomal hydrolases from trans-golgi network to late endosomes. Lysosomes lack both Ci-MPR and it's small variant, cation-dependent MPR (Cd-MPR) and therefore MPR is sometimes used as a marker for late endosomes. In addition to the endosomal compartments the two MPRs are found in the trans-Golgi network, which can compromise the use of MRP for identification of late endosomes (Kornfeld & Mellman 1989; Klumperman et al. 1993; Mukherjee et al. 1997).

Like other endocytic structures, also late endosomes contain certain Rab-GTPases. Rab7 has a strong role in regulating traffic from early to late endosomes (Feng et al. 1995; Vitelli et al. 1997). In addition, there is evidence to support the view that the lipid composition of the endosomal membranes could master Rab7 function to facilitate late endosomal motility (Lebrand et al. 2002). Rab9 governs trafficking from late endosomes towards the trans-golgi network (TGN) and has been found to have a crucial role in the delivery of Ci-MPR and furin to the TGN (Lombardi et al. 1993; Mallet & Maxfield 1999). Rab24 is also found in late endosomes. However, it provides a much less specific identification method for the organelle than for example Rab7, as Rab24 is found also in the endoplasmic reticulum and in the Golgi (Olkkonen et al. 1993). In addition to the characteristic proteins, also a unique lipid enriched in late endosomes, bis(monoacylglycero)phosphate (BMP), known also as lysobisphosphatidic acid (LBPA), can be considered as a marker for the organelle. Unfortunately, BMP cannot be used as a ubiquitous identifier for late endosomes as it has been also found in lysosomes of human B cells (Kobayashi et al. 1998; Kobayashi et al. 2002; Möbius et al. 2003; Matsuo et al. 2004).

2.2.2.3 Lysosomes

The name lysosome was first posed by de Duve and co-workers in 1955 (de Duve et al. 1955). Systematic use of biochemical methods, namely tissue fractionation followed by enzymatic tests, led to the discovery of a novel intracellular organelle (those days still called a particle) lined by a membrane and filled with freely diffusing hydrolytic enzymes (de Duve et al. 1955; Appelmans et al. 1955; Wattiaux et al. 1956). Later, direct evidence for the existence of lysosomes

and insight into their mophology was given by electron microscopy, which pinpointed the ambiguous granules as sack-like, electron dense organelles (Novikoff et al. 1956; Baudhuin et al. 1965). Later, in different cell types lysosomes with multilamellar and tubular morphologies have been captured (Swanson et al. 1987; Mukherjee et al. 1997).

In the early days of lysosome research two different populations of lysosomes were found in the preparative density gradients. The low density lysosomes were later identified as their own endosome type, late endosomes, and this renders some of the earliest results of lysosome research somewhat inaccurate in today's terms (Kornfeld & Mellman 1989; Mellman 1996). Nevertheless, the early measurements on the size of the dense lysosomes, with a diameter of 0.13 - 0.4 μm, represent well the current view on the size range of lysosomes (de Duve et al. 1955; Appelmans et al. 1955; Novikoff et al. 1956; Wattiaux et al. 1956).

The lumen of lysosomes is acidic, pH is as low as 4.6- 5.5 (Yamashiro et al. 1984; Luzio et al. 2007). The acidic environment is maintained by ATP-dependent proton pumps, vacuolar ATPases (Luzio et al. 2007). Even though already in the early days of lysosome studies the organelle was considered difficult to define in clear terms (Kornfeld & Mellman 1989) and the debate on lysosome biogenesis is still ongoing (Storrie & Desjardins 1996; Luzio et al. 2000; Luzio et al. 2007), there are certain undisputed features of lysosomes, which are used for their identification. From the very beginning lysosomes have been known to contain hydrolytic enzymes (de Duve et al. 1955). There are numerous enzymes entrapped within lysosomes, but in particular enzymes such as acid phosphatase, β-glucuronidase, and cathepsin are often used as biochemical markers for the organelle (Essner & Novikoff 1961; Miller et al. 1981; Löffler et al. 1984; Oliver et al. 1989; Izagirre et al. 2009).

Lysosomes can be identified in negative terms as MPR negative structures to differentiate them from late endosomes. Lysosomal, as well as late endosomal, membranes are rich in glycoproteins. Particularly certain highly glycosylated integral proteins have become distinctive markers for lysosomes. These can be broadly classified into two categories: lysosome associated membrane proteins (LAMPs) lysosomal integral membrane protein (LIMPs), of which LAMPs are the most abundant. LAMPs and LIMPs have been suggested to constitute as much as 50 % of the membrane proteins in lysosomes (Marsh et al. 1987; Eskelinen et al. 2003). Classically the lysosomal glycoproteins were considered to have a role mainly in protecting the lysosomal membrane from degradation by forming a clycocalyx, a carbohydrate lining on the lumenal side of the membrane (Neiss 1984). In agreement with this suggestion, more recent results have emphasised the role of asparagine-linked oligosaccharides in the protection of lysosome integrity (Kundra & Kornfeld 1999). In addition to maintaining lysosomal stability, LAMPs and LIMPs have been suggested to be connected to several functions of lysosomes. LIMPs have been associated with vesicle fusion and fission events as well as lysosome biogenesis. In addition, LIMP-2 has been

recently reported to function as a receptor for β-glucocerebrosidase trafficking from ER to lysosomes (Reczek et al. 2007). Although LAMP-1 is abundant in lysosomal membranes, deficiency of LAMP-2 protein has been shown to result in far more drastic malfunctions of lysosomes, including impaired recycling of MPRs to TGN, cholesterol retention and accumulation of autophagic vacuoles (Tanaka et al. 2000; Eskelinen et al. 2003; Eskelinen et al. 2004; Eskelinen 2006).

In addition to the endogenous markers for lysosomes also functional ways to identify the structures within cells exist. Fluorescent weak bases such as acridine orange and quinacrine accumulate in lysosomes through protonation and can be used for example in imaging (Canonico & Bird 1969; Goren et al. 1984). Also, fluid-phase markers such as dextran and horseradish peroxidase (HRP) accumulate in lysosomes and can be used for their identification (Marsh et al. 1986; Baravalle et al. 2005).

2.2.3 Endosomal membranes

Not only does the protein composition and morphology of different types of endosomes differ, the lipid composition of their membranes has also some significant and controlled variation. The particular lipid composition of membranes is reflected in their physical properties and thus, the lipid composition of endosomal membranes can be seen as an important factor in determining many of the attributes of the organelles.

Phosphatidylinositols have strong functional role in the early steps of endocytosis. Phosphatidylinositol-4,5-biphosphate (PI(4,5)P_2) facilitates the formation of clathrin coated vesicles on the plasma membrane (Jost et al. 1998). Phosphatidylinositol-3-phosphate (PI3P) is highly enriched in early endosomes and recent evidence suggests PI3P to have an important role in determining endosome morphology as well as governing cargo recycling and delivery onwards (Gillooly et al. 2000; Fili et al. 2006). Phosphatidylinositols have been proposed to form domains, or platforms, on early endosomal membranes together with Rab5 efector proteins phosphatidylinositol 3-kinase (PI3K) and PI3P-binding proteins (Zerial & McBride 2001; Gruenberg 2001). PIKFyve, a phosphoinositide 5-kinase containing a Fyve finger domain (Bondeva 1998), found on late endosomal structures (Sbrissa et al. 2002) generates phosphatidylinositol-3,5-biphosphate (PI(3,5)P_2), which has been shown to have a role in maintaining the integrity of the endosomal membrane (Ikonomov et al. 2002).

Apart from the enrichment of phosphatidylinositols, the lipid composition of early endosomes is thought to resemble that of the plasma membrane (Kobayashi et al. 1998). Recycling endosomes have been found to be particularly rich in cholesterol and other typical raft-components (Gagescu et al. 2000; Möbius et al. 2003). Similar to the plasma membrane, also early endosomes are thought to contain lipid rafts (Ikonen 2001; Gruenberg 2001) and correspondingly, cholesterol-stabilised Annexin II domains have been detected on early endosomal membranes (Harder et al. 1997). The endosomal raft domains have been postulated to have a role in cargo sorting, similar to their functions on

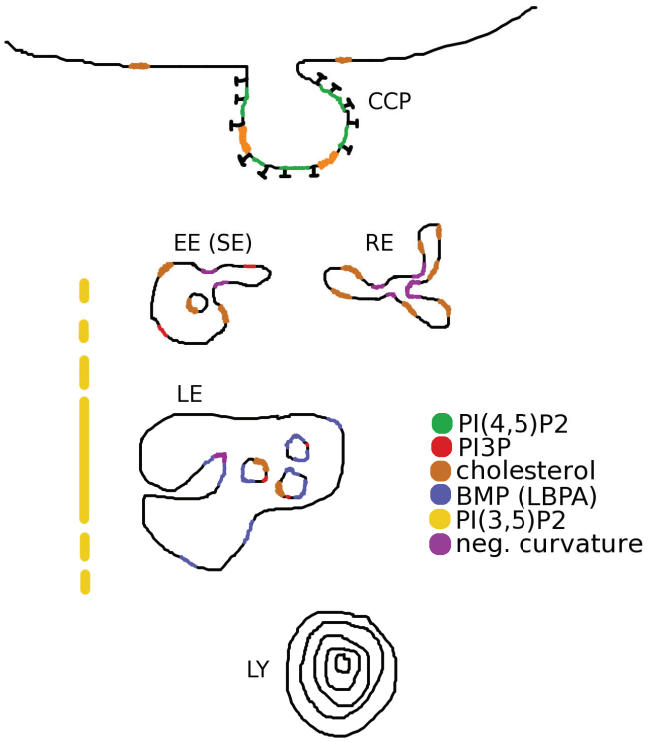

FIGURE 8 Functional membrane domains on the clathrin-mediated endocytosis route. Phosphatidylinositols (PI(4,5)P_2, green; PI3P, red) are present mainly in the beginning of the pathway. Localisation of PI(3,5)P_2 (yellow) is not precisely known, but it has been found to be produced in late endosomes. Plasma membrane, early and recycling endosomes and the inner vesicles of MVBs contain significant amounts of cholesterol (orange), which is assumed to form raft-like domains also on the membranes of the endosomal structures. BMP (LPBA; blue) is highly enriched in late endosomal membranes. Areas of high negative curvature (pink) in early sorting endosomes have been proposed to have a role in sorting. Size and number of membrane domains is only illustrative. CCP, clathrin coated pit; EE (SE), early endosome (sorting endosome); RE, recycling endosome; LE, late endosome; LY, lysosome. Size and number of domains merely illustrative. The picture is modified from (Gruenberg 2003) based on the text in section 2.2.3 (see references in text).

plasma membrane and trans-Golgi (Gruenberg 2001). GPI-anchored proteins have been found to be recycled in a cholesterol-dependent manner and thought to be mediated by rafts (Mayor et al. 1998). Fluidity and curvature of the sorting endosome membrane has been proposed to have a role in lipid sorting. The tubules of the endosome could be more fluid than the vesicular regions, or alternatively, the areas of high curvature stress (negative curvature) in the necks of the tubules could function as gates for partition of lipids into tubules (Mukherjee & Maxfield 2000).

The phospholipid composition of late endosomes/MVBs has been found to be unique. The structures, and especially their internal membranes, have been show to harbour bis(monoacylglycero)phosphate (BMP; known also as LBPA) in large amounts (Kobayashi et al. 1998; Kobayashi et al. 2002). BMP has been suggested to have an important role in governing trafficking of proteins and particularly cholesterol through the late endosomes (Kobayashi et al. 1998; Kobayashi et al. 1999; Gruenberg & Stenmark 2004; Delton-Vandenbroucke et al. 2007). *In vitro*, in acidic conditions mimicking late endosomes, BMP has been shown to induce multivesicularisation. This suggests BMP to have a role in the biogenesis of late endosomal structures (Matsuo et al. 2004). In addition, BMP seems to be connected to particular microheterogeneity of the late endosomal membranes, as membrane fractions with different phospholipid composition and varying amounts of BMP have been isolated (Kobayashi et al. 2002). BMP itself is poorly degradable based on its unique stereochemistry, but interestingly it has been been shown to effectively facilitate the enzymatic degradation of glycolipids (Gruenberg 2001; Hepbildikler et al. 2002).

Whether BMP is present on lysosomal membranes was for long somewhat unresolved, as the early results where BMP was detected in lysosomes were obtained with methods unable to distinguish between late endosomes and lysosomes (Wherrett & Huterer 1972; Brotherus & Renkonen 1977). Gruenberg reviewed the point in 1998 stating that the early observations of "light lysosomal fractions" containing BMP and neutral lipids such as triglycerides and cholesterol esters support the results obtained later with late endosomes (Kobayashi et al. 1998). Recently, however, BMP was reported to be present also on lysosomal membranes as well as in MVBs (Möbius et al. 2003). Similar to neutral lipids, such as triglycerides and cholesterol esters found in lysosomes (Wherrett & Huterer 1972; Brotherus & Renkonen 1977; Ruiz & Ochoa 1997), also dolichol has been associated with the lysosomal compartment (Wong et al. 1982). Apart from triglycerides (Pakkanen et al. unpublished), no recent confirmation for the presence of these lipids on lysosomal membranes have been provided. In general, the comprehensive lipid composition of lysosomes is still obscure, over 50 years after their discovery.

While the earlier endosomal structures have been shown to contain significant amounts of cholesterol, view on the cholesterol content of late endosomes and lysosomes is still somewhat unclear. Schoer et al. suggested lysosomes to have intermediate amounts cholesterol: less than on plasma

membrane but more than on cholesterol-poor ER (Schoer et al. 2000). On the other hand, Möbius et al. reported the internal membranes of MVBs to contain cholesterol while only little cholesterol was found on the limiting membrane (Möbius et al. 2002; Möbius et al. 2003). The presence of cholesterol on the inner membranes, but not on the limiting membranes of MVBs (Möbius et al. 2002) is reasonable when one considers the view that multivesicular structures could be derived from the vesicular areas of the early endosomes rich in cholesterol (Gruenberg et al. 1989; Aniento et al. 1993). However, MBVs have been reported to contain different types of raft-like membrane domains both on their limiting membrane and their intraluminal vesicles (Sobo et al. 2007).

Cholesterol released in lysosomes from low density lipoprotein particles is translocated to the plasma membrane and to the endoplasmic reticulum (ER) (Lange et al. 1997; Möbius et al. 2003). Reasonably low cholesterol content seems to be important for proper function of lysosomes as, conversely, cholesterol accumulation is connected to various deleterious effects. Increased cholesterol amount in lysosomes has been shown to increase lysosomal pH by inhibiting vacuolar ATPase-dependent pumping of H+ ions (Cox et al. 2007), to cause swelling (Jerome et al. 1998) and to inhibit degradation of lipoprotein cholesteryl ester in macrophages (Jerome et al. 2008). In short, cholesterol accumulation impairs normal lysosomal and late endosomal functions (Sobo et al. 2007; Ganley et al. 2006; Liao et al. 2007).

Accumulation of cholesterol in lysosomes is caused by disabled function of Niemann-Pick C protein 1 (NPC1) caused by mutation in the respective gene npc1. The condition is known as Niemann-Pick C disease and originates from mutation in the NPC gene (Liscum 2000). In addition, lysosomes become loaded with free cholesterol in macrophages during foam cell development. In this process free cholesterol generated by hydrolysis of phagocytosed cholesteryl ester droplets is not esterified and becomes retained in lysosomes (Mahlberg et al. 1990; Tangirala et al. 1993). Interestingly, cholesterol accumulation in lysosomes has also been found to occur in LAMP-1/LAMP-2 double negative fibroblasts (Eskelinen et al. 2004). Experimentally cholesterol accumulation in lysosomes can be produced by treating the cells for example with U18666A, an agent that blocks LDL-cholesterol egress from lysosomes (Liscum & Faust 1989) or progesterone (Butler et al. 1992). Also other lipids than cholesterol cause problems when they accumulate in lysosomes. Pathological conditions known as lysosomal lipid storage diseases typically arise from lysosomal enzyme deficiency leading to accumulation of lipids, and most typically sphingolipids, in lysosomes (Futerman & van Meer 2004).

2.3 Viruses and membranes: barrier penetration in cellular conditions

Viruses are intracellular parasites which have no other means of producing offspring than relying obligatorily on the cellular machinery of their host cells. From the selfish point of view of the virus this can lead to only one result: complete invasion and takeover of the cell and all it's functions. There are two main ways for viruses to enter the cell, either to directly pass through the plasma membrane into the cytosol or exploit endocytic internalisation routes to get a free ride inside the cell. Utilisation of endosytosis, as attractive and easy as it might appear, does not remove the need for membrane penetration (Sieczkarski & Whittaker 2002; Marsh & Helenius 2006). Typically, the virus or the viral capsid has to penetrate into the cytosol before replication can take place (Marsh & Helenius 2006). Thus, in every viral infection there is need for successful interplay between the virus, either viral membrane or viral capsid, and cellular membranes, either the plasma membrane or endosomal membranes. This crucial step is a promising and variable target for development of antiviral therapies. Inhibition of fusion between the viral envelope membrane and the host cell membrane, for example, provides means for specific inhibition of infection. Enfuvirtide, a synthetic peptide which binds to the fusion protein of the human immunodeficiency virus (HIV), has been found effective in treating patients with drug-resistant HIV infections (Lalezari et al. 2003). Another victorious example is amantadine, which blocks the ion channel activity of influenza virus type A M2 protein and is used for treatment and prophylaxis of influenza (Wang et al. 1993; Fleming 2001). To further develop strategies for preventing and treating viral diseases detailed understanding on the fundamental mechanisms and practical functions of virus-membrane interactions is needed. Not only is it crucial to increase the comprehension on membrane-membrane interactions between the cellular membranes and the virus envelope but also to elucidate the reciprocal actions between viral proteins and membranes. This fascinating area of virus-membrane interactions remains for the most part still to be unravelled.

2.3.1 Membrane interactions of enveloped viruses

Many clinically significant viruses are covered by an outer layer of membrane, or envelope. Viruses acquire their envelopes from cellular membranes. The process can be complex as seen with herpes simplex virus 1 (HSV1), which undergoes an elaborate envelopment procedure where some capsids are wrapped into membrane on Golgi, some on rough endoplasmic reticulum and some get their envelopes on either inner or outer nuclear membrane (Leuzinger et al. 2005). On the other hand, for some viruses envelopment is a fairly straightforward part of their life cycle. This, however, does not imply that the interactions between the virus capsid and the envelope-to-be governing the process would be any less fine-tuned.

Even though the viral membrane is derived from the host cell membranes, it does not necessarily present the same lipid or protein composition. Influenza viruses, for example, bud out from the plasma membrane, and during the process selectively incorporate cholesterol-rich liquid-ordered regions into their envelope (Scheiffele et al. 1999). In addition to influenza viruses, many viruses such as canine distemper virus, hepatitis B virus (HBV) and borna disease virus (BDV) have cholesterol as an important part of their envelope membrane (Sun & Whittaker 2003; Imhoff et al. 2007; Bremer et al. 2008; Clemente et al. 2009). The role of cholesterol has been reported to be crucial for simian immunodeficiency virus (SIV) and human immunodeficiency virus (HIV), which require cholesterol to be present in the envelope to maintain the virion integrity (Graham et al. 2003).

TABLE 3 Examples of viruses utilising class I and class II proteins for membrane fusion (Kielian & Rey 2006).

Virus family	Virus	Fusion protein
Class I		
Orthomyxoviridae	Influenza virus	Hemagglutinin (HA2)
Paramyxoviridae	Simian virus 5	F1
Filoviridae	Ebola virus	GP2
Retroviridae	Human immunodeficiency virus	gp41
	Moloney murine leukemia virus	TM
Coronaviridae	Mouse hepatitis virus	S2
	SARS virus	S2
ClassII		
Flaviviridae	Tick-borne encephalitis virus	E protein
	Dengue virus	E protein
Togaviridae	Semliki Forest virus	E1

The envelope of influenza viruses contains two important viral proteins, hemagglutinin (HA) and neuraminidase (NA), which both have been found to interact strongly with rafts through their transmembrane domains (Scheiffele et al. 1997; Barman & Nayak 2000). Similarly, respiratory syncytial virus (RSV) fusion protein (protein F) has been reported to associate with raft domains (Fleming et al. 2006). Viral proteins can also interact with membranes to modulate the lipid composition of the envelope. The Nef protein of HIV alters the lipid composition of both virions and host cell plasma membranes. In T lymphocytes Nef was found increase the amount of sphingomyelin and decrease the amount of polyunsaturated phosphatidyl cholines in membranes, but interestingly had no effect on cholesterol concentration on either viral or host cell membranes (Brügger et al. 2007). Incorporation of additional sphingomyelin into the

HIV membrane, which has been shown to have particularly high cholesterol content, is in good accordance with early results reporting the envelope of HIV to be highly ordered (Aloia et al. 1988; Aloia et al. 1993). Similar to the Nef protein function also RSV has been shown to alter to the composition of host cell membranes. During RSV infection an increase in the amount of phosphatidyl inositol and phosphorylated phosphatidyl inositol in the membrane has been detected (Yeo et al. 2007).

Particularly pronounced membrane interactions take place during the viral entry. Enveloped viruses gain access into the cellular interior by penetrating the cellular membrane either at the plasma membrane or within endosomes. At the plasma membrane the fusion event is typically triggered by binding of the virus to its receptor in neutral conditions (Smith & Helenius 2004; Kielian & Rey 2006). For example, in the case of HIV, the initiation of the fusion event requires complex interactions between the virus envelope glycoprotein gp120 and receptor molecules, including immunoglobulin CD4 and chemokine receptors. Furthermore, dissociation of p120 from gp41 protein is needed (Gallo et al. 2003). The fusion protein of HIV belongs to the class I fusion proteins, as well as the fusion proteins of many other viruses such as influenza virus, Ebola virus and SARS virus (Kielian & Rey 2006). Class I fusion proteins are homotrimeric glycoproteins which have their subunits joined by coiled coils. When triggered, the metastable subunits expose a hydrophobic peptide which preferentially inserts into the host cell membrane. Free energy is gained when the protein returns to it's most stable conformation and this is used to drive the membrane fusion (Baker et al. 1999; Melikyana et al. 2000). In the case of HIV, the fusion peptide gp41 inserts into the host cell membrane forming a pre-hairpin structure, followed by emergence of a six-helix bundle (Gallo et al. 2003). The formation of a six-helix bundle alone has been estimated to release more than enough free energy to make the membrane fusion possible (Melikyana et al. 2000). Examples of class I viral fusion proteins can be seen in Table 3 and a schematic presentation of a model for membrane fusion mediated by a class I fusion protein in Figure 10A.

Not all fusion proteins act at the plasma membrane level. Some enveloped viruses use endocytosis to by-pass the plasma membrane penetration step. Consequently, the membrane fusion of these viruses occurs inside endosomes and the acidic pH of the organelles is typically required to trigger the fusion event (Smith & Helenius 2004; Marsh & Helenius 2006). Classical examples of enveloped viruses fusing with the endosomal membranes are influenza virus and Semliki Forest virus (SFV) (Helenius et al. 1980; Doms et al. 1985). The hemagglutinin protein of influenza virus is a class I fusion protein, whereas the E1 protein of SFV is a well-chracterised example for class II proteins (Kielian & Rey 2006). Class II fusion proteins exist as heterodimers bound together with another membrane protein. In response to low pH cue the fusion subunits dissociate from the dimers and form fusion competent homotrimers in the host cell membrane (Kielian 2006). Examples of class II viral fusion proteins

are listed in Table 3. Illustration of the fusion event mediated by a class II fusion protein in Figure 10B.

Lipid composition of both the viral envelope and the host cell membrane can have an important role in mediating fusion between the two membranes. For example, the presence of cholesterol on the host cell membrane facilitates the fusion of SFV and hepatitis C virus (HCV) envelopes with the cellular membranes (Phalen & Kielian 1991; Bron et al. 1993; Lavillette et al. 2006). In addition to cholesterol, sphingolipids on the target membrane have been found to be important for SFV fusion (Nieva et al. 1994). Modulation of the host cell membrane has been also found to be able to stop viruses from infecting the cell, as seen with HIV. Treating the host cells with sphingomyelinase, an enzyme generating ceramide by cleavage of sphingomyelin, inhibits HIV infection by blocking the membrane fusion. This has been proposed to be a fascinating possibility for membrane-based antiviral therapy (Finnegan et al. 2004) and emphasises further the crucial role of composition and organisation of the host cell membranes in the viral life. Sometimes, though, the need for the correct envelope membrane composition exceeds the requirement for the perfect fusion site on the host cell membrane. Depletion of cholesterol from the viral envelope, decreases markedly the infectivity of human herpes virus 6 (HHV6), compared to only a mild effect achieved by cholesterol depletion of the host cells (Huang et al. 2006).

2.3.2 Membrane interactions of non-enveloped viruses

Non-enveloped viruses have protein shells which protect the genetic material stored within them. The evident lack of viral membrane does not prevent the non-enveloped viruses from experiencing significant interactions with the host cell membranes. Non-enveloped viruses naturally cannot utilise membrane fusion to deliver their capsid inside the cell, but, interestingly, viral proteins with fusogenic potential have been reported also amongst the non-enveloped viruses. The N-terminal ectodomain of p10 protein of avian (ARV) and Nelson Bay (NBV) reoviruses has been found to structurally resemble fusion peptides of enveloped viruses and facilitate membrane fusion (Shmulevitz et al. 2004). The role of membrane fusion in the life cycle of ARV and NBV is not connected to the entry phase, unlike in the case of enveloped viruses. Cell-cell fusion promoted by the fusogenic p10 leads to formation of syncytia, which seem to improve the egress of the virus. However, the syncytia seem not to be essential for the virus egress (Duncan et al. 1996; Shmulevitz & Duncan 2000). Similarly, Bluetongue virus, another reovirus, encodes a protein, VP5, which facilitates cell-cell fusion when expressed on the cell surface. The same protein is also utilised during the virus entry. In acidic environment of endosomes VP5 undergoes conformational changes and permeabilises the endosomal membrane (Forzan et al. 2004). Utilisation of fusogenic protein in the entry of rice dwarf virus, a phytoreovirus, has also been proposed (Zhou et al. 2007).

Most non-enveloped viruses are internalised into host cells by endocytosis. Hence, studies on membrane interactions of non-enveloped viruses have

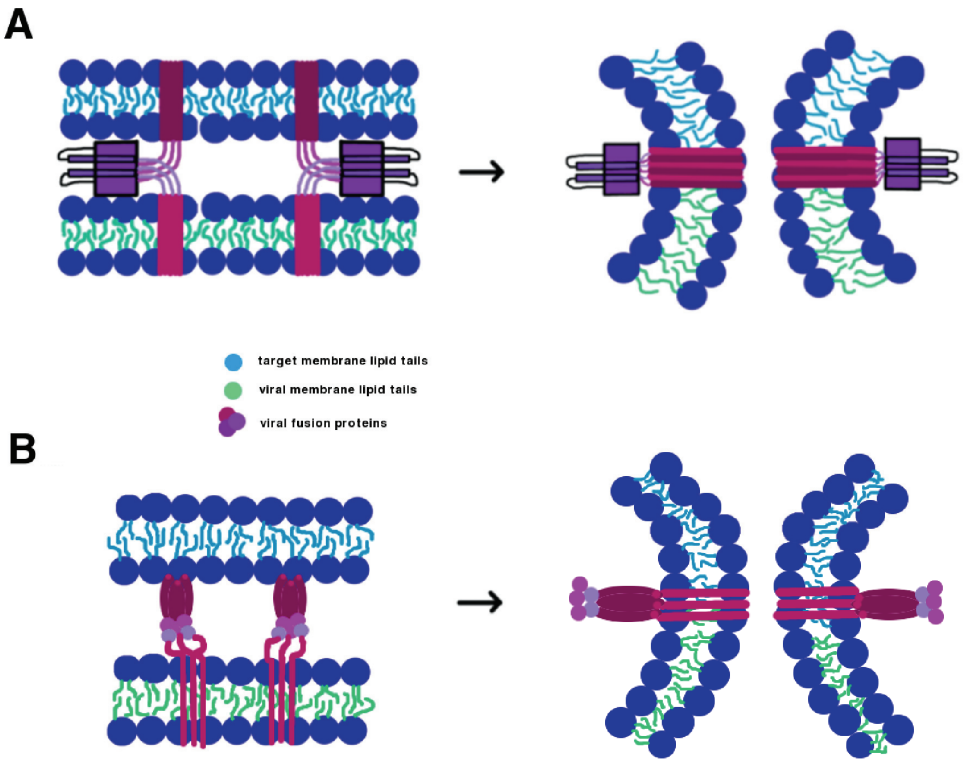

FIGURE 9 (A) Membrane fusion mediated by viral fusion proteins. A schematic presentation of membrane fusion facilitated by a class I viral fusion protein. The generalised fusion model is based on the crystal structures of influenza virus HA and HIV gp41 fusion proteins. The model includes conformational transitions of the fusion protein (drawn in magenta and purple) embedded in the viral membrane (blue lipid tails) followed by insertion of the fusion peptide into the host cell target membrane (cyan lipid tails). The model suggests flexible polypeptide linkers between the fusion peptide or TM anchor and the fusion protein to have an important role in the fusion (Baker et al. 1999). (B) Illustrative drawing of membrane fusion facilitated by a class II viral fusion protein. The fusion between the envelope of SFV and the endosomal membrane is initiated by the low pH of the endosome which exposes the fusion loop. Insertion of the loop into the membrane as well as trimerisation of the E1 fusion protein is promoted by both acidicity and cholesterol. The E1 trimers interact cooperatively to distort the target and virus membranes. Finally, E1 reaches a completely folded hairpin conformation (on the right) when the fusion is completed (Kielian 2006). Colours as in A. Illustrations for A and B modified from (Baker et al. 1999) and (Kielian 2006), respectively.

concentrated in large extend on membrane penetration in endosomes. The endosome penetration is essential for successful infection, as the virus inside endosomes, although in one sense is inside the cell, cannot access the cellular machinery required for replication. Nonenveloped viruses have in principle two main methods for endosomal breakout: they either lyse the endosomal membrane altogether or generate pores in it (Smith & Helenius 2004). Typically, as in the case of Bluetongue virus (Forzan et al. 2004), the low intraendosomal pH triggers conformational changes in the capsid proteins of the virus. Also for human rhinovirus 2 (HRV2) the acidic conditions (pH 5.0) are enough to trigger necessary rearrangements in protein conformation (Brabec et al. 2003). On the other hand, in some cases multiple factors in addition to proper pH are needed to facilitate the endosomal penetration. In early studies adenovirus was found to require pH of 6.0-6.5 for membrane penetration (Seth et al. 1985). However, acidicity alone was later found to be insufficient to facilitate the rupture of early endosomal membranes. Penton base of the adenovirus capsid requires the help of α_v integrins, $\alpha_v\beta_5$ in particular, as well as a protease encoded by the virus itself to interact with the early endosomal membranes and facilitate the lysis (Wickham et al. 1994; Cotten & Weber 1995). Protein VI of adenovirus, which dissociates from the peripentonal hexons and inserts itself into the endosomal membrane, has been proposed to be the final cause of the membrane lysis (Wiethoff et al. 2005). In addition to protons altering the pH, also other ions can function as cues for endosomal penetration. Decrease in endosomal Ca^{2+} concentration has been proposed to be critical for the breakout of rotavirus from endosomes (Ruiz et al. 1997; Chemello et al. 2002).

Pore formation is another main strategy for non-enveloped viruses to penetrate the endosomal membrane (Smith & Helenius 2004). In the case of reovirus T1L, proteolytic digestion of the outer capsid proteins by endosomal enzymes exposes μ1 protein and generates infectious subvirion particles (ISVPs). Pore in the endosomal membrane is formed by μ1 onto which the viral particle docks (Agosto et al. 2006; Ivanovic et al. 2008). The pores, however, are very small, even smaller than the virus itself, and it is still unclear how in detail the virus is released from the endosome. Models for pore enlargement by host cell or endosome rupture through osmotic swelling have been proposed (Agosto et al. 2006). Membrane permeabilisation also can be undertaken by using lipolytic enzymes. Parvoviruses harbour in their capsid phospholipase A_2 (PLA_2) enzyme, which they utilise for penetration through the endosomal membranes. The endosomal escape of parvoviruses is presumably initiated by conformational changes of the capsid triggered by the acidic conditions within endosomes. This externalises the N-terminus of the VP1 protein containing the PLA_2 (Zádori et al. 2001; Suikkanen et al. 2003b; Farr et al. 2006). PLA_2s cleavage phospholipids at the *sn*-2 position generating a lysophospholipid and a fatty acid. The parvoviral PLA_2 has been found not to have preference for substrate in terms of saturation of the fatty acids in the *sn*-2 position. Nevertheless, it has been found to release arachidonic acid from cellular membranes (Canaan et al. 2004). Perforation of the membrane does not create openings big enough for the virus

to pass through, resembling in that respect the situation in reovirus penetration. However, in the case of parvoviruses the endosomes are not likely to lyse, as both larger dextran and α-sarcin are retained within the structures during virus entry (Parker & Parrish 2000; Suikkanen et al. 2003b).

Poliovirus takes a different approach on membrane perforation. Having an RNA genome makes life easier for poliovirus as, like many other RNA viruses, it does not need to travel all the way to the host cell nucleus to proliferate. A model for poliovirus membrane penetration suggests the virus capsid to undergo conformational transition triggered by receptor binding after which the capsid proteins, VP1 and VP4 playing a major role, form a pore in the host cell membrane through which the viral genome is released to the cytoplasm (Belnap et al. 2000). Current model of poliovirus entry suggests the virus penetrate directly through plasma membrane, as it does not require a low pH step for its conformational alterations (Pèrez & Carrasco 1993; Stewart et al. 2003).

Also other cellular membranes than endosomal membranes and the plasma membrane can be attacked by incoming viruses. Polyomavirus uses a clever entry tactic where it passes into the nucleus through the endoplasmic reticulum (ER). Polyomavirus is internalised into the host cells through caveolae in cholesterol-dependent manner. The virus passes through the cell along with intracellular traffic and finally reaches the ER. Presence of the ganglioside receptor for polyomavirus, GD1a, facilitates the correct delivery of the virus to the ER (Gilbert et al. 2004). In the ER lumen, ERp29, a protein structurally related to the ER oxido-reductase protein disulfide isomerase (PDI), exposes the C-terminus of the polyomavirus VP1 protein. This renders the viral particle hydrophobic and ready to bind to the ER membrane and to perforate it (Magnuson et al. 2005; Rainey et al. 2007). Simian virus 40 (SV40), a virus closely related to polyomavirus, follows the same internalisation route from plasma membrane to ER, although it uses a different ganglioside, GM1, as its receptor (Kartenbeck et al. 1989; Tsai et al. 2003). SV40 utilises a rather convoluted strategy for delivery into nucleus, as it has been found to pass to the nucleus through the cytoplasm and not directly from the ER as polyomavirus is thought to do (Nakanishi et al. 1996; Magnuson et al. 2005).

As well as for many enveloped viruses, cholesterol has been found to be crucial also for the entry of some non-enveloped viruses. Very typically cholesterol dependency is seen at the plasma membrane level for viruses which require caveolae-mediated endocytosis for their internalisation. SV40 (Pelkmans et al. 2001), echovirus 1 (EV1) (Marjomäki et al. 2002; Pietiäinen et al. 2004), polyomavirus (Ricterova et al. 2001) and human papillomavirus type 31 (HPV-31) (Bousarghin et al. 2003) for example utilise caveolae for their entry into host cells. In addition, raft regions distinct from caveolae have been connected to the entry of some non-enveloped viruses. The coxsackie B virus and adenovirus receptor (CAR) has been shown to reside in rafts negative for caveolin-1 and GPI-anchored proteins but positive for the low density lipoprotein receptor (LDLR) (Ashbourne et al. 2003). This suggests a novel connection between plasma membrane rafts and internalisation

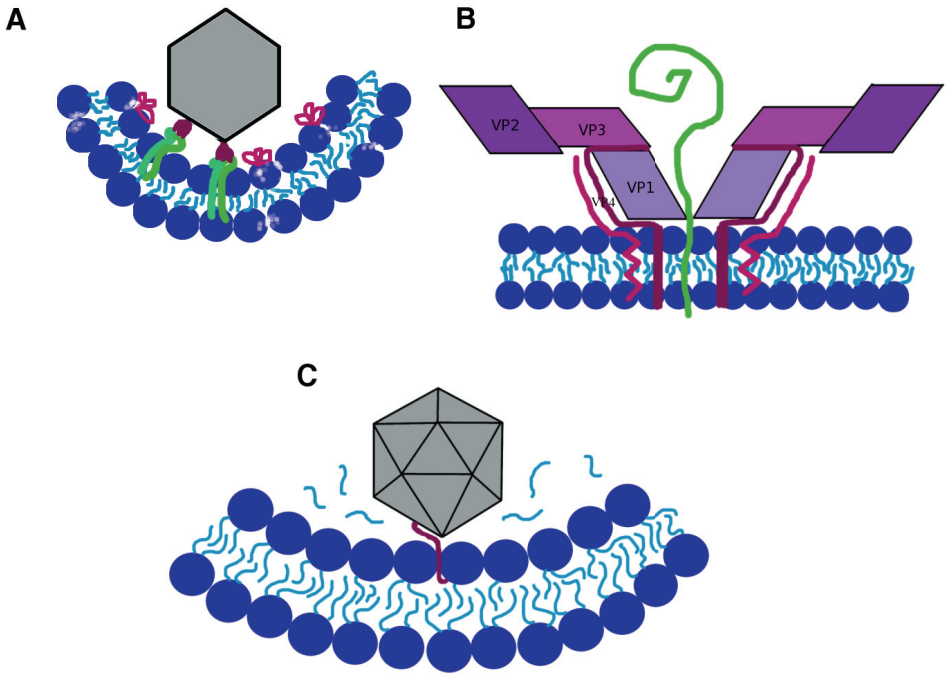

FIGURE 10 Different ways of endosome penetration by non-enveloped viruses. (A) Hypothetical model for adenovirus-mediated endosomal membrane disruption. Low pH in endosome induces partial disassembly of the capsid. Protein VI inserts itself into the endosomal membrane which leads to disruption of the membrane (Wiethoff et al. 2005). $\alpha_v\beta_5$ integrins drawn in green, penton bases and protein VI in dark and light magenta, respectively. (B) Model for poliovirus membrane penetration. Attachment of poliovirus to its receptor triggers conformational changes in the virus capsid. VP1 and VP4 play a major role in formation of a pore through which the RNA genome (green) of the virus eventually passes into the cytoplasm (Belnap et al. 2000). (C) Penetration of parvoviruses through the endosomal membrane is facilitated by the PLA_2 activity of the VP1 protein N-terminus (drawn in magenta) (Zádori et al. 2001; Suikkanen et al. 2003b; Farr et al. 2006). Action of the PLA_2 releases fatty acids (cyan) from the phospholipids. Illustrations for A and B modified from (Wiethoff et al. 2005; Belnap et al. 2000). Illustration for C drawn based on (Zádori et al. 2001; Suikkanen et al. 2003b; Canaan et al. 2004).

of coxsackie virus B and adenovirus. To attach to host cells, coxsackie B virus employs also another receptor, the decay accelerating factor (DAF), also known as CD55 (Shafren et al. 1995). DAF is coupled to lipid bilayers through a GPI-achor, which renders it willing to partition into rafts on the plasma membrane (Low 1989; Legler et al. 2005) and thus creates yet another connection between rafts and viral entry. In addition to different strains of coxsackie B virus also coxsackie A21 virus (Newcombe et al. 2004), several echoviruses (Bergelson et al. 1994; Stuart et al. 2002) as well as hantaviruses Hantaan and Puumala (Krautkramer et al. 2008) have been found to use DAF as a receptor. A rare example of raft-interactions in late stages of the life cycle of non-enveloped viruses is rotavirus assembly. Rafts has been proposed to function as platforms for the assembly of rotavirus and viral protein VP4 to be particularly pronouncedly associated with rafts (Sapin et al. 2002; Delmas et al. 2007).

2.4 Summary of the entry of canine parvovirus

Canine parvovirus (CPV) is a small, non-enveloped virus belonging to the autonomous Parvovirus genus of the *Parvoviridae* family (Cotmore & Tattersall 1987). The entry of CPV is mediated by the transferrin receptor, onto which the virus binds on the plasma membrane, followed by internalisation through clathrin-mediated endocytosis through the early and recycling endosomes to lysosomal associated membrane protein 2 (LAMP-2) positive vesicles (Parker et al. 2001; Suikkanen et al. 2002). The major protein of the parvovirus virion is VP2 and only 10 % of the capsid subunits are VP1 proteins. VP1 contains an N-terminal nuclear localisation signal and a phospholipase A2 (PLA_2) motif essential for infection (Cotmore & Tattersall 1987; Vihinen-Ranta et al. 1997; Zádori et al. 2001; Suikkanen et al. 2003b; Canaan et al. 2004). The N-terminus of VP1 is hidden inside the capsid subunits in intact capsids, but is exposed in acidic conditions such as those encountered in endosomes, or experimentally by treatment with heat or urea (Weichert et al. 1998; Cotmore et al. 1999; Vihinen-Ranta et al. 2002; Suikkanen et al. 2003b). When the N-terminus is exposed, the phospholipase site is activated (Zádori et al. 2001; Suikkanen et al. 2003b). Although the PLA_2 motif is active during the endosomal escape of CPV, the virus only partly permeabilizes the endosomal vesicles without complete disruption of the structures. Interestingly, the openings formed by the action of the PLA_2 have been shown to be smaller than the viral capsid itself (Parker & Parrish 2000; Suikkanen et al. 2003b). This suggests that some other mechanism or mechanisms, in addition to phospholipase action of PLA_2, facilitate the endosomal escape of CPV.

CPV is released from endosomal vesicles seemingly intact (Vihinen-Ranta et al. 2000) and it travels towards the nucleus along microtubules in a dynein-dependent manner (Suikkanen et al. 2003a;

Vihinen-Ranta et al. 2000). The N-terminus of the VP1 structural protein contains a nuclear localisation signal, which is exposed already within the acidic endosomal compartments. The whole CPV capsid might be able to enter the nucleus through the nuclear pore complex as antibodies against intact capsids recognise the capsids in the nucleus (Vihinen-Ranta et al. 2000).

3 AIMS OF THE STUDY

In this thesis virus-membrane interactions and endosomal membranes were studied with a broad multidisciplinary focus. The interactions between membranes and canine parvovirus (CPV) were studied both from the point of view of the viral capsid as well as from the point of view of the membranes. Cholesterol was found to have a role in the entry of the virus. A simplified model of lysosomal membranes, was used to understand the role of rare lipids in lysosomal membranes. In addition, the late steps of CPV infection were investigated. The underlying themes and aims of the thesis were:

1. To characterize membrane-capsid interactions of a non-enveloped model virus, canine parvovirus, and to investigate the functional role of these interactions.

2. To learn how manipulation of the membranes can be used to hinder the entry of canine parvovirus.

3. To understand better the protective function of endosomal and lysosomal membranes which could have a role in guarding the cell against pathogens.

4 SUMMARY OF MATERIALS AND METHODS

This chapter provides a concise overview of the main methods used in the thesis. Comprehensive descriptions of the methods used can be found in the original publications.

4.1 Cell culture, virus culture and preparation

Norden laboratory feline kidney (NLFK) cells (II, III, V) and canine fibroma A72 (V) cells were both grown and maintained in Dulbecco's modified Eagle's medium (PAA Laboratories GmbH, Pasching, Austria) supplemented with 10% fetal calf serum, non-essential amino acids (PAA Laboratories GmbH) and antibiotic mixture. Spodoptera frugiperda (*Sf*9) insect cells (II) were maintained in monolayer and/or suspension cultures at 28 °C using serum-free Insect-Xpress culture medium (Cambrex, Walkersville, MD) without antibiotics. Human cervical carcinoma, HeLa MZ, cells (II) were grown in Dulbecco's modified Eagle's medium (Invitrogen, Carlsbad, CA) supplemented with 10% inactivated fetal bovine serum (FBS) and 1% penicillin-streptomycin (Invitrogen).

Canine parvovirus (CPV-2d) was originally derived from the infectious plasmid clone of the virus (Parrish 1991) and subsequently cultured and purified as previously described (Suikkanen et al. 2002; Suikkanen et al. 2003b). For infection experiments, the cells were grown to a 90% confluency (or lower in case of control cells for long infections, see article V) on glass coverslips (II, III, V).

4.2 Expression, purification and characterization of His-VP2 virus-like particles

His-tagged CPV VP2 protein was engineered to be used as a control capsid (II) without the PLA_2 activity present in native CPV. The 1755 bp coding sequence

of CPV VP2 was amplified by PCR from the infectious CPV clone pBI265 (Parrish 1991) using AAA TCT AGA TAT GAG TGA TGG AGC AGT TCA AC -forward and AAA CTC GAG TTA ATA TAA TTT TCT AGG TGC TAG TTG AG -reverse primers containing XbaI and XhoI restriction sites, respectively. The PCR product was subcloned into pFastBac HTA transfer vector downstream of the polyhedrin promoter in frame with the N-terminal 6xHis tag to create the expression vector encoding His-VP2 fusion protein (631 amino acids). The recombinant virus was generated using the Bac-to-Bac baculovirus expression system (Invitrogen) and named AcHis-VP2. S*f*9 cells (2 x 106 cells/ml) were infected with an MOI (multiplicity of infection) of 5 using AcHis-VP2. The infected cells were harvested at 72 h post infection (p.i.) by centrifugation. The cells were lysed with Triton X-100 on ice after which cell debris was pelleted by centrifugation. Supernatant was centrifuged through a sucrose cushion and the resulting pellet was resuspended in PBS by gentle agitation. The suspension was centrifuged in a 40 to 10% sucrose gradient. The gradient was fractioned and fractions analyzed with SDS-PAGE and Western blotting. The final purification was conducted chromatographically using affinity resin (Streamline chelating, GE Healthcare, Uppsala, Sweden) with $NiSO_4$ (J.T. Baker, Deventer, The Netherlands). The His-VP2-containing fractions were pooled and concentrated

Expression of His-VP2 in S*f*9 cells was visualized with immunofluorescence labeling using antibodies to both His-tag and CPV VP2. The purified protein was analysed both with SDS-PAGE and Western blotting. For visualisation of proteins bands on Western blots antibodies to both His-tag and CPV VP2 were used. Visual analyses of His-VP2 VLPs were performed by transmission electron microscopy (JEOL JEM-1200 EX, Jeol Ltd., Tokyo, Japan) with phosphotungstic acid (PTA) staining. Binding and internalisation of the VP2 virus-like particles was studied in HeLa and NLFK cells. The samples were prepared similar to the cell samples with CPV infections (see below).

4.3 Microscopy: sample preparation and visualisation

The cells grown on cover slips were infected with approximately $2x10^9$ CPV particles by first attaching the virus to the cell surface in small amount of culture medium after which medium was added and the infection was allowed to progress. At appropriate time points the cells were fixed with ice-cold methanol (Sigma-Aldrich, St. Louis, MO) (III, V). For visualisation the fixed cells were labelled with standard immunofluorescence methods, using antibodies appropriate for each case. Cell viability was confirmed using Hoechst 33342 (Sigma-Aldrich) staining. The samples were imaged with a confocal microscope (LSM510, Zeiss Axiovert 100M, Jena, Germany) with appropriate settings for each fluorophore. Calculations for capsid positive nuclei were performed manually with a epifluorescence microscope (Leitz DM RBE, Leica, Wetzlar, Germany). Length of cellular extensions was measured using ImageJ software (Rasband,

W.S., ImageJ, U.S. National Institutes of Health, Bethesda, MD) and the number of cellular extensions manually from confocal microscope images. Fluorescence emission spectra of the di-4-ANEDPPHQ probe was measured in live cells to evaluate whether the fluidity of the membranes of intracellular vesicular structures changed during CPV infection. For live cell spectra acquisition the cells were treated with the di-4-ANEDPPHQ probe for 5 min and washed with phosphate buffered saline prior to spectroscopy with a confocal microscope (see section 4.4). A list of antibodies and probes can be found in Table 5.

4.4 Spectroscopical methods

Intrinsic tryptophan fluorescence was used to evaluate structural changes in CPV capsids. The fluorescence emission of tryptophan is highly affected by solvent polarity. Consequently, tryptophans residing in hydrophobic environment away from water have a structured emission spectrum with a strong blue contribution and emission maxima close to 330 nm, whereas in hydrophobic environment the tryptophan residues display emission at longer wavelengths with maximum around 350 nm (Lakowicz 2006).

The intrisic fluorescence of CPV capsids (I) and fluorescence spectra of the di-4-ANEDPPHQ probe (II) were recorded using using a Perkin Elmer LS55 fluorescence spectrophotometer and a cuvette with 10 mm path length (Perkin Elmer Industries, Wellesley, MA). Temperature was kept stabile with Thermo Haake water bath and circulator (Thermo Electron Corporation, Waltham, MA). For tryptophan fluorescence studies the samples were excited at 290 nm and emission was gathered at 310-430 nm (I). For di-4-ANEDPPHQ the exitation and emission wavelengths were 475 nm and 500-750 nm, respectively (II). The wavelength of maximum emission was analysed manually after subtraction of background scattering (measured without the probe) from the data. Intracellular spectra of di-4-ANEDPPHQ (II) were measured in live cells using a confocal microscope (Olympus Fluo-View 1000, Olympus Optical Co., Tokyo, Japan). The emission spectra were gathered from perinuclear vesicular populations at 500-750 nm with excitation at 488 nm.

Laurdan fluorescence is very sensitive to the polarity of the surrounding environment. It is used to assess water penetration into the glycerol backbone level of the membrane. This further gives information of either polarity or fluidity of the membrane (Parasassi et al. 1990; Parasassi et al. 1998). Laurdan (Invitrogen) fluoresence emission spectra and DPH (Invitrogen) anisotropy (IV) were measured using a Chronos ISS fluorometer (ISS, Champaign, IL) and a Starna quartz cuvette of 3 mm path length (Starna Cells, Inc. Atascadero, CA). Temperature was maintained at 25°C with a water bath (Julabo Labortechnik GmbH, Seelbach, Germany). When using Laurdan the samples were excited at 375 nm and non-corrected emission was measured at 420-520 nm. For DPH the exitation wavelength was 375 nm. Unpolarised emission was gathered at 450 nm.

The anisotropy values were calculated automatically by the Vinci software (ISS) operating the fluorometer.

To quantify the shift in Laurdan emission, general polarization (GP; IV) was measured with a BMG FLUOstar Omega plate reader (BMG LABTECH, Offenburg, Germany). The temperature control unit of the FLUOstar plate reader was used to heat the samples and to maintain the temperature at a desired value. A 10 minute incubation time was used between each measurement to equilibrate the temperature in the sample. Excitation wavelength of 360 nm ($\pm$ 5 nm) was used for both 440 nm and 490 nm emissions. The pathlength of the measurement was determined by the volume (150 μl) of liquid in the measurement well. GP was calculated from emission intensities at 440 nm (I_B) and 490 nm (I_R), based on the equation (Parasassi et al. 1990)

$$GP = \frac{I_B - I_R}{I_B + I_R} \tag{3}$$

and normalized to the GP of free Laurdan in DMSO.

To study the physical properties of the model membrane in short time and length scale we used electron paramagnetic resonance (EPR) spectroscopy (IV). The EPR spectra with Me-5-DSA spin probe (Sigma-Aldrich) were measured with a Bruker EMX Plus spectrometer (Bruker Biospin, Rheinstetten, Germany) equipped with a PremiumX microwave bridge and Bruker internal variable temperature unit. The samples were measured in a micro hematocrit tube (Vitrex Medical A/S, Herlev, Denmark) which was positioned in a standard EPR tube. All spectra obtained were X-band spectra (frequency $\approx$ 9.43 GHz) recorded with a power of 20 mW, a modulation frequency of 100 KHz, modulation amplitude 1G and time constant of 20.48 ms. The spectra were simulated with the program EPRSIM, ver 4.99-2005 (Štrancar et al. 2000)

To get detailed information on the structure of viral capsid proteins circular dichroism spectroscopy (I) was performed in far UV region using a Jasco J-720 spectropolarimeter (JASCO Corporation, Tokyo, Japan) and a cylindrical quarz cuvette (Helma GmbH & Co KG, Müllheim, Germany) of 1 mm pathlength. The spectra were recorded from 240 to 190 nm with bandwidth of 2.0 nm and 0.5 s response time. Speed for scanning was 10 nm/min.

Absorption spectroscopy was used to monitor the activity of PLA_2 based on a commercial kit (Cayman Chemicals, Ann Arbor, MI). Absorbances at 405 nm were measured using a Lambda 850 spectrophotometer and quartz cuvette with pathlength of 10 mm (Perkin Elmer Industries,Wellesley, MA). Temperature was maintained at +25°C using a water bath and circulator (Thermo Electron Corporation). The PLA_2 activities were measured and calculated according to manufacturer's instructions.

4.5 Quantitative thin-layer chromatography and differential scanning calorimetry

Thin-layer chromatography (TLC; IV) of lipids was performed using silica gel plates (VWR, Copenhagen, Denmark). Water was removed from the samples by evaporation on a rotary evaporator (Heidolph VV micro, Heidolph Instruments, Schwabach, Germany). The resulting dry lipids were dissolved in chloroform. Standards of appropriate ratios were applied on each plate. The plates were developed using the solvent systems for non-polar lipids described previously (Yao & Rastetter 1985). The plates were charred in an oven (model Digiheat, J.P. Selecta s.a., Barcelona, Spain) at 180°C after which they were scanned (Lexmark X75, Lexmark, Birkeroed, Denmark) to create a high-resolution RGB coded colour image. Unspesific charring was removed and the images inverted. Integrated densities of the spots were measured and normalised against standards on each plate. Image processing and analysis was performed with ImageJ software (Rasband, W.S., ImageJ, U. S. National Institutes of Health, Bethesda, MD).

Thermotropic behaviour of the membranes was analysed using differential scanning calorimetry (DSC; IV). DSC was performed either with Calorimetric Sciences Corp. model 4100 MC-DSC (TA-Instruments, Lindon, UT) or with TA-Instrument NANO-DSC equipped with cylindrical gold cells (TA-Instruments). For the MC-DSC the scan rate was 5 K/h and a solid metal insert was used as a reference sample. For the NANO-DSC a scan rate of 30 °C/h and a pure water reference were used. The thermograms were analysed in Origin 7 (OriginLab Corporation, Northampton, MA) by first subtracting the baseline and determining the start and end temperatures of the phase transition using the method described by Mabrey and Stutewant (Mabrey & Sturtevant 1976). The enthalpies of the phase transitions were calculated by integration of the DSC trace, by the use of a linear baseline from the Origin 7 DSC module. The obtained enthalpies were then normalised with respect to the total lipid concentration.

4.6 Atomistic molecular dynamics simulations

Molecular dynamics (MD) computer simulations were utilised to study interactions between desipramine and membranes in atomistic detail. A previously validated united-atom model (Chiu et al. 1995; Berger et al. 1997; Ollila et al. 2007) was used for palmitoyloleoyl phosphatidylcholine (POPC). For cholesterol the model by Höltje et al. (Höltje et al. 2001) based on a modified version of the united-atom GROMOS87 force field (van Gunsteren & Berendsen 1987; van Buuren et al. 1993; Daura et al. 1996) was employed. The simple point charge (SPC) model (Berendsen et al. 1981) was used for water.

The model for desipramine was developed for this work. As in the case of the cholesterol model used, the bonded and Lennard-Jones parameters for

the desipramine model were taken from the modified GROMOS87 force field. Only the protonated form of desipramine was considered. The atomic partial charges were obtained by quantum-mechanical calculations with the Gaussian03 software package (Frisch et al. 2004). The model was further detailed by optimising the structure of 20 random desipramine conformations at the Hartree-Fock level of theory by employing a 6-311G* basis set. The resulting electronic distributions were then fitted to produce atomic partial charges with the ChelpG method (Breneman & Wiberg 1990). The final partial charges for the model were obtained by averaging over the respective values for the different desipramine conformations.

In the MD simulations fully hydrated POPC/cholesterol bilayers with a total of 128 lipids were used. The membranes contained either 5 mol% or 40 mol% cholesterol. A total of 6 or 14 (5 mol-% or 10 mol-%, respectively) desipramine molecules were positioned evenly and symmetrically in the plane of the bilayer, at a distance of 2.7 nm from the bilayer center. The remaining free volume in the simulation cell was filled with water molecules. The simulation systems were made charge neutral by randomly replacing a number of water molecules, corresponding to the number of desipramine molecules in the system (6 or 14), with Cl^- ions.

The simulations were carried out with the GROMACS package (Lindahl et al. 2001; van der Spoel et al. 2005), version 3.3.1. The system temperature was maintained at T = 310 K with the Nosé-Hoover thermostat (Nosè 1984; Hoover 1985). The molecules in the bilayer, including desipramine, and the subsystem comprising water and Cl^- ions were separately coupled to thermostats with a time constant of 0.5 ps. The system pressure, p = 1 bar, was maintained independently in the direction parallel to the bilayer normal and in the plane of the bilayer with the Parrinello-Rahman barostat (Parrinello & Rahman 1981), with a coupling time constant of 2.0 ps. The simulation time step length was 2 fs and the total simulation time for all the bilayer systems 100 ns.

TABLE 4 Alphabetical summary of methods used in this thesis. Detailed descriptions can be found in the articles indicated in the table by Roman numerals.

Method	Article
Cell culture and virus infections	II, III, V
Cellular protrusion quantitation by the ImageJ program	V
Circular dichroism spectroscopy	I
Confocal microscopy and spectra acquisition	II, III, V
Differential Scanning Calorimetry (DSC)	IV
DPH anisotropy	IV
Electron paramagnetic resonance spectroscopy (EPR)	IV
Fluorescence spectroscopy	I, II, IV
Immunofluorescence labelling	II, III
Kinetics of PLA_2 enzymatic activity	I
Kruskall-Wallis analysis for variance	II, III, V
Large unilamellar vesicles (LUVs), extrusion method	V
Laurdan general polarisation	IV
Mann-Whitney U-test	II, III, V
Multilamellar vesicles (MLVs), shaking method	IV
Molecular dynamics simulations	III
Protein production with the baculovirus expression system	II
Purification and analysis of His-tagged proteins	II
Protein concentration assay (Bradford method)	I
Quantitation of virus marker positive nuclei	III
Small unilamellar vesicles (SUVs), sonication method	I
Student's t-test	I
Thin-layer chromatography (TLC)	IV
Virus culture and purification	I, II, III, V

The antibodies and probes used in the thesis are summarised below.

TABLE 5 Antibodies and probes used in this thesis

Antibody or probe	Source	Article
Alexa Fluor 488, 555 anti mouse / rabbit	Molecular Probes, Eugene, OR / Invitrogen	V
Alkaline phosphatase conjugated secondary antibodies	Promega, Madison, WI	II
Di-4-ANEDPPHQ	L. M. Loew, University of Connecticut Health Center, Farmington, CT	II
1,6-diphenyl-1,3,5-hexatriene (DPH)	Invitrogen	IV
Hoechst 33342	Sigma-Aldrich	V
Laurdan	Invitrogen	IV
Mouse monoclonal antibody to alpha-tubulin	Sigma-Aldrich	V
Mouse monoclonal antibody to CPV capsid (Mab8)	(Strassheim et al. 1994), C. R. Parrish, Cornell University, Ithaca, NY	II, III, V
Mouse monoclonal antibody to LAMP2	Developmental Studies Hybridoma Bank, The University of Iowa City, Iowa City, IA	II
Mouse monoclonal antibody to His-tag	Serotech, Oxford, UK	II
Northern Lights NL-557 donkey anti-mouse	R&D Systems Inc., Minneapolis, MN	II, III, V
Methyl-5-doxylstearic acid (Me-5-DSA)	Sigma-Aldrich	IV
Rabbit polyclonal antibody to transferrin receptor	Cymbus Biotechnology, Hampshire, UK	II
Rabbit polyclonal antibody to CPV capsid	C. R. Parrish, Cornell University, Ithaca, NY	II

5 REVIEW OF THE RESULTS

5.1 Interactions of parvovirus capsid with model membranes

5.1.1 Alterations in the CPV capsid structure

We studied how acidic conditions and the presence of membranes affect the structure of the CPV capsid. The icosahedral (T=1) capsid of CPV is built with structural proteins, VP2 and VP1, the latter comprising only 10% of the 60 subunits of the capsid (Paradiso et al. 1982; Cotmore & Tattersall 1987). The capsid has a diameter of 26 nm (Agbandje et al. 1993; Chapman & Rossmann 1993). In DNA-containing viruses the VP2 N-termini exposed outside the capsid are cleaved by host cell proteases to form VP3 protein (Paradiso et al. 1982; Weichert et al. 1998). The protein monomers are organised into eight-stranded antiparallel barrels with the loops connecting the strands at the surface of the capsid (Tsao et al. 1991). 143 additional amino acid residues differentiate parvoviral VP1 protein from the VP2 protein forming the so-called unique N-terminus of VP1, which contains a phospholipase A_2 motif and a nuclear localisation signal (Paradiso et al. 1982; Vihinen-Ranta et al. 1997; Weichert et al. 1998).

As CPV capsid is known to bind Ca^{2+} ions (Simpson et al. 2000), the measurements were performed in the presence of $CaCl_2$. Red shifts in the maximum emission wavelength of CPV capsid tryptophans were detected when the sample was supplemented with small unilamellar vesicles (SUVs) composed of bovine brain sphingomyelin or bovine brain phosphatidyl serine (I, Fig. 1A). However, phosphatidyl choline, phosphatidyl ethanolamine and phosphatidyl inositol were found to not cause any pronounced changes in the emission (data not shown). Acidic conditions, pH 5.5, combined with sphingomyelin induced a significant red shift (3.8 ± 0.3 nm; $P = 0.002$) in the tryptophan emission of CPV capsids compared to $CaCl_2$ alone. A similar, but less significant, shift in emission towards higher wavelength was seen with sphingomyelin at pH 7.4. With phosphatidyl serine a trend in red shift resembling the changes seen with sphingomyelin was seen both at pH 5.5. and pH 7.4. The change, however, was deemed

statistically insignificant. Interestingly, the acidicity alone was not sufficient to induce a significant change in the maximum emission wavelength. Only a minor strengthening in the emission at the red end of the measured spectra was seen at pH 5.5 when compared with pH 7.4 (I, Fig. 1A). The results suggest increased water penetration between the subunits of the CPV capsid proteins. This can originate for example from structural changes in the capsid.

The red shift detected in CPV capsids at low pH in the presence of sphingomyelin can be assumed to arise through conformational rearrangements which either bring tryptophan containing motifs of the structural proteins to the capsid surface or loosen the capsid to become more penetrable to water. It is important to note as well that even though acidicity did not have an effect alone, together with sphingomyelin it contributed to a significant red shift in the capsid. The fluorescence emission of free tryptophan in water is not sensitive to changes in pH (Luykx et al. 2004), which implies the pH-related changes in the capsid fluorescence to indeed stem from the conformational changes resulting from exposure of tryptophans to water.

Each VP2 protein of the CPV capsid contains 14 and each VP1 protein 15 tryptophan residues, all of them more or less shielded from water by their hydrophobic location inside the capsid subunits (Chapman & Rossmann 1993; Xie & Chapman 1996). This variable access of water molecules to the tryptophan residues of the capsid proteins can be clearly seen in a Stern-Volmer plot calculated from acrylamide quenching experiments (Pakkanen et al. unpublished, see Fig. 11). No pH variation in the water accessibility of CPV tryptophans was detected.

To further investigate the interactions of phosphatidyl serine and sphingomyelin with CPV capsids, circular dichroism (CD) spectroscopy in far UV region was used. Measurements were again performed in the presence of $CaCl_2$ and the effect of phosphatidyl serine/sphingomyelin SUVs as well as acidicity on the capsid protein conformation was analysed. In general terms the spectra contained a wide negative valley at 220-200 nm and a narrower positive peak at 190 nm. Without vesicles, in the presence of $CaCl_2$ only, the positive 190 nm peak was lower at pH 5.5 compared to pH 7.4. The wide valley at 220-200 nm was slightly shallower and shifted to red at pH 5.5 (I, Fig. 1 B, C).

Vesicles composed of phosphatidyl serine/sphingomyelin markedly changed the CD spectra of the capsids. Similar to acidic conditions only, the 220-200 nm valley became less negative with the vesicles. Differences seen in the 220-200 nm valley without vesicles at pH 5.5. and pH 7.4 seemed to lessen when the vesicles were present, making the two spectra resemble more each other than the spectra measured at each pH without vesicles. Surprisingly, also the blue shift seen with pH 5.5 was corrected with the presence of the vesicles. The differences in the spectra with vesicles were evident mainly in the raise up to the 190 nm peak: the 205-195 nm slope at pH 7.4 was not as steep as at pH 5.5 ((I, Fig. 1B-C). The circular dichroism data were not interpreted in terms of secondary structure. However, the data strongly suggests the presence of phosphatidyl serine and sphingomyelin to result in different kind of conformational changes in the

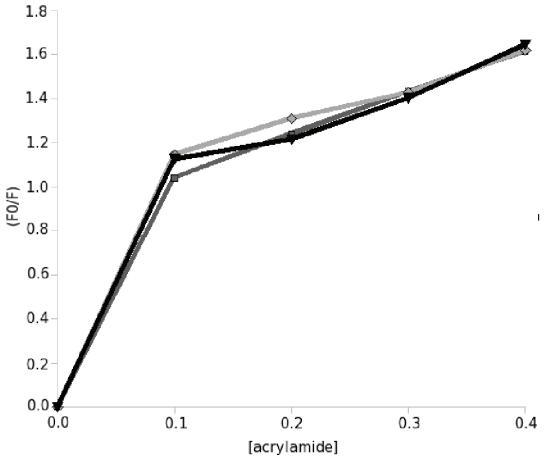

FIGURE 11 A Stern-Volmer plot of CPV capsid tryptophan fluorescence in the presence of phosphatidyl serine vesicles (K. Pakkanen unpublished). The plot deviates from the linearity towards the x axis, which is indicative of different populations of tryptophan residues, each accessed differently by the quencher (Lakowicz 2006). Light grey pH 5.5, dark grey pH 6.5 and black pH 7.4.

CPV capsids than acidicity alone can do.

In addition to the effects produced by acidicity and membranes, we also elucidated the reversibility of the acid-induced structure alterations. This might have a role in the viral life just after the endosomal membrane penetration, when the virus is released to the neutral cytoplasm. For the experiments, the virus capsid was incubated at pH 5.5 for 10 min after which the sample was immediately neutralised. The tryptophan fluorescence emission was again used to report on changes in the capsid proteins. No statistically significant changes in tryptophan fluorescence emission maxima were detected when acid-treated neutralised capsids were compared with native capsids (I, Fig. 1D). In the CD spectrum of the acid-treated capsids, however, some marked differences were seen. In acid-treated capsids the valley at 220-200 nm was less profound than in native capsids, and there was a distinct shoulder at 225 nm (I, Fig. 1E). This difference between neutralised acid-treated and native capsids could relate to long-term effects of those structural rearrangements the CPV capsid undergoes when it it first influenced by the acidicity of the endosomes and then subsequently escapes from the endosome lumen to the cytoplasm. The remaining neutralised conformation of the capsid could have a role later in the viral life. For example, minute virus of mice (MVM), a parvovirus related to CPV, has been shown to damage the nuclear envelope, possibly helping the virus to gain entry into the nucleus (Cohen & Panté 2005).

5.1.2 Sphingomyelin does not affect the function of CPV PLA_2

The unique part of parvoviral VP1 protein harbours the phospholipase A $_2$ activity of the viral capsid and contains two motifs found conserved throughout the phospholipase A_2 family. Similar to secretory type PLA_2s, the parvoviral phospholipase is not partial in choosing its substrates in respect to lipid species or fatty acid saturation (Zádori et al. 2001; Canaan et al. 2004). The enzyme requires Ca^{2+}, is especially active towards aggregated lipids (Canaan et al. 2004) and is only available for functioning when the N-terminus of the VP1 protein is exposed from inside the viral capsid (Weichert et al. 1998; Vihinen-Ranta et al. 2002; Suikkanen et al. 2003b).

Sphingomyelin has previously been connected with inhibiting the function of group V secretory PLA_2 (Singh et al. 2007). We tested the effect of sphingomyelin on the activity of CPV PLA_2. Thiol-conjugated phosphatidyl choline, supplemented when applicable with bovine brain sphingomyelin SUVs, was used as a substrate in the assay. The activity of CPV PLA_2 was not significantly affected by the presence of sphingomyelin in the reaction mixture. The activity decreased from 0.0019 ± 0.0003 μmol/ml/min without sphingomyelin to 0.0016 ± 0.0003 μmol/ml/min with sphingomyelin, which in essence was similar to the behaviour of bee venon PLA_2 used as a control (I, Fig. 2). These results, together with the findings on the effect of sphingomyelin and acidicity on the capsid protein conformation, suggest that the changes in the capsid structure are most likely not involved in facilitating the function of the CPV PLA_2. The changes in structure may, however, have some previously unknown function in the endosomal escape of the virus.

5.1.3 CPV capsid modifies fluidity of membranes *in vitro*

Membranes can function as trigger to induce changes in the viral capsid, but it is also important to understand how the virus alters the membrane it interacts with. We studied the effect of CPV capsids on the rigidity of ordered cholesterol-rich phosphatidyl choline membranes and very fluid phopshatidyl choline membranes without cholesterol. For this we utilised fluorescence spectroscopy and di-4-ANEPPDHQ probe. Di-4-ANEPPDHQ is a styryl probe which is sensitive to the molecular ordering of its local environment and has been shown to exhibit pronounced spectral shifts in respect to transition from liquid disordered phase to liquid ordered phase (Jin et al. 2006)

The emission spectra of di-4-ANEPPDHQ (II, Fig. 1) were all in all in good accordance with previously published results (Jin et al. 2006). In the case of the DPPC:cholesterol vesicles (7:3 molar ratio) CPV capsids induced at pH 5.5 a statistically significant red shift (2.1 nm; $P = 0.035$) in the emission of the probe compared to vesicles without the virus (II, Fig. 2A). This implies increase in disorder in the the vicinity of di-4-ANEPPDHQ. At neutral pH the virus capsid did not seem to be able to induce any significant shifts in the emission (II, Fig. 2B). At either acidic or neutral environment neither bee venom PLA_2 nor CPV His-VP2

protein induced any significant shifts in the emission of di-4-ANEPPDHQ (II, Fig. 2 A-B).

Characteristically, with DOPC vesicles the general form of the spectra was wider and the emission appeared at higher wavelengths than with DPPC:cholesterol vesicles (II, Fig. 1). No significant shifts in emission were detected in either acidic or neutral conditions with either CPV or with His-VP2 and PLA2 used as controls (II, Fig. 3 A-B).

Similar to the emergence of the PLA_2 activity at low pH (Suikkanen et al. 2003b), the present results show that acidicity is required for the fluidising function of the capsid. It is important to note that the His-VP2 capsids lacking the VP1 protein, and subsequently the PLA_2 activity, did not have a fluidising effect on DPPC:cholesterol vesicles. This implies that the fluidising domain in the CPV capsid is located in the VP1 unique N-terminus. However, as secretory type PLA_2 used as a control did not pose any disordering effect on the vesicles, it is plausible that the classical lipase activity of the parvoviral PLA_2 is not responsible for the fluidising effect. Nevertheless, it is possible that there is an additional functional domain in the VP1 N-terminus responsible for the disordering of membranes. In addition, one cannot exclude possibility that the PLA_2 domain would have additional abilities outside the normal action of the enzyme.

5.2 Interactions of the parvoviral capsid with endosomal membranes

5.2.1 Membrane fluidisation is a part of the entry strategy of CPV

Similar disordering effect as seen *in vitro* at acidic pH with DPPC:cholesterol membranes (see 5.1.3) was also detected in perinuclear intracellular compartments during CPV entry. The disordering was again monitored using fluorescence spectroscopy and di-4-ANEPPDHQ probe, but this time the spectra were gathered from live cells by using a confocal microscope. At 3 h and 4 h post infection (p.i.) the form of the emission spectrum was wider than at 5 h p.i. or without virus (II, Fig. 4 A). At 3 h p.i. the emission was clearly red shifted in comparison to cells without virus and at 4 h p.i. significantly red shifted in respect to both cells without virus (15.4 nm; $P = 0.007$) and 5 h p.i. (8.8 nm; P=0.04) (II, Fig. 4 B). These results imply increase in the fluidity of the membrane and a clear-cut difference between the time points 4 h and 5 h p.i.

5.2.2 Disintegration of cholesterol-rich areas affects parvoviral entry

Cholesterol itself or the ordering effect it poses on membranes seems to function as some kind of trigger for the membrane fluidisation by the CPV capsid (II, see sections 5.1.3 ad 5.2.1). As the role of cholesterol on cellular membranes is

very closely connected to the emergence of lipid rafts (Simons & Ikonen 1997), we tested the effect of raft disrupting compounds on CPV entry. All the tested compounds have previously been reported to disrupt cholesterol-rich membrane domains, or lipid rafts (Gidwani et al. 2003; Awasthi-Kalia et al. 2001; Klingenstein et al. 2006; Kamata et al. 2008). In experiments with CPV the drugs were found to hinder the progression of the virus from intracellular vesicles to nucleus. The virus was internalised into the cell and no clear virus labelling was detected at the plasma membrane at 24h p.i (III, Fig 5), indicating that the effect of the tested compounds was indeed intracellular. In all cases where CPV traffic was perturbed, the virus was found arrested in intracellular vesicular structures.

Ceramide C2 (30 μM) caused the most pronounced reduction in the CPV traffic efficiency. Only 1.6% (P= 0.021) of cells were infected with the virus at 24 h (III, Fig. 5 D, G). U18666A (7μg/ml), which in addition to causing cholesterol and sphingolipid accumulation in lysosomes (Liscum & Faust 1989; Lusa et al. 2001; te Vruchte et al. 2004) has been reported to be able to disrupt detergent resistant membranes (DRMs) (Klingenstein et al. 2006), also had an inhibiting effect on the intracellular progression of CPV. With U1866A only 12% (P= 0.021) of cell nuclei were positive for CPV at 24 h p.i. (III, Fig. 5 C, G). Desipramine (10 μM) , a putative raft-breaker, had also a clear effect in hindering the intracellular traffic of CPV, decreasing the percentage of capsid positive nuclei down to 38% (P= 0.021) (III, Fig. 5 B, G) compared to untreated cells, where 87% of cells were positive for the virus at 24h p.i. Although the hindering effect on CPV infection brought about by lidocaine (0.2%) did not reach the significance level (5%), perturbation of normal CPV infection was evident. Gentamicin, a lysosomotropic antibiotic with no known raft disintegrating function was used as a control and it was found not to affect CPV entry (III, Fig. 5 F, G).

In addition to the various compounds used, we also tested how removal of cholesterol from the membranes by using 10 mM methyl-β-cyclodextrin (MβCD) affected CPV entry. Previously, MβCD has been found to inhibit internalisation of CPV on the plasma membrane level (data not shown) and therefore it was added to cells 3 h p.i. After one hour of treatment with MβCD, CPV was not able to proceed beyond perinuclear vesicular structures (III, Fig. 6A) Following the MβCD treatment, only 5.9% (P= 0.053) of nuclei were detected to be CPV positive after 24 h incubation in fresh medium compared to nearly 30% of infected cells in the untreated control (III, Fig. 6C).

To learn more on the effects of cholesterol and sphingomyelin, crucial raft components, on CPV infection, we tested how CPV is able to infect cells supplemented with additional cholesterol or sphingomyelin. Addition of 20 μg/ml cholesterol to cells did not seem to influence the course of CPV infection, 88.7 % of the cell nuclei were positive to CPV at 24 h p.i (III, Fig. 7 B,C). Additional sphingomyelin, 50 μg/ml, on the other hand, seemed to hinder the progression of the virus. Only 36.1 % of the cells were infected at 24 h p.i. in the presence of supplementary sphingomyelin (III, Fig. 7 A, C). The virus marker was seen localised primarily inside the cells, implying that also with sphingomyelin the effect on CPV entry was at the intracellular stage, and not at the plasma membrane level. We

also tested whether cholesterol could enhance the viral entry in cells first supplemented with additional sphingomyelin. The cells were given 50 μg/ml sphingomyelin and infected for 24 h after which cholesterol, 20 μg/ml, was added for 3 h time and the number of CPV positive nuclei quantified. Cholesterol was indeed found to counteract the effect of sphingomyelin: there was a significant increase in the percentage of CPV positive nuclei (49.1%; P= 0.036) in cells treated with cholesterol after sphingomyelin supplementation when compared to cells with added sphingomyelin only (36 %; III, Fig. 8).

5.3 Antidepressant desipramine disorders cholesterol-rich membranes

Desipramine, 3-(5,6-dihydrobenzo[b][1]benzazepin-11-yl)-N-methylpropan-1-amine (DMI, for structure see III, Fig. 1), is a tricyclic antidepressant known to accumulate in lysosomes through protonation (Stoffel et al. 1987; Lemieux et al. 2004). In cell studies desipramine was found to inhibit the entry of CPV (III, Fig. 5) along with other molecules known to disrupt the integrity of raft domains on cellular membranes. Desipramine itself has also been previously connected to destabilisation of DRMs (Klingenstein et al. 2006).

The effect of desipramine on lipid bilayers was studied in atomistic detail with molecular dynamics simulations. The model membrane consisted of palmitoyloleoyl phosphatidylcholine (POPC) and cholesterol. Two membrane models were constructed, one with 5 mol% and the other with 40 mol% cholesterol. The former corresponded to cholesterol-depleted disordered domains, and the latter one to highly ordered raft-like domains in cell membranes (Niemela et al. 2007). The concentrations of desipramine in the simulations were 0, 5 or 10 mol%.

Addition of desipramine in the membrane with 5 mol% cholesterol resulted in a clear increase in the deuterium order parameter (S_{CD}) values close to the glycerol backbone of the lipids (III, Fig.2 A-B). However, the membrane was still clearly in fluid state. A detailed study on the localisation of desipramine in the membrane confirmed, that the regions with the most pronounced increases in S_{CD}, around carbons 5 in both chains, coincided with the position of the desipramine tricyclic ring in the membrane (III, Supplementary Fig. S1, S2). In the lipid bilayer with low cholesterol desipramine affected only little the area of the membrane and did not seem to alter the membrane phase. For both 0 and 5 mol% DMI the calculated areas per lipid were 0.64 $\pm$ 0.01 nm^2 and for 10 mol% DMI 0.65 $\pm$ 0.01 nm (III, Fig. 3 A). These resemble area per lipid values published previously for neat POPC bilayers (Ollila et al. 2007).

The influence of desipramine on the cholesterol-rich membrane was indeed found to differ from the effect seen with membranes poor in cholesterol. The buckling of the S_{CD} curves around the centers of the lipid chains, a feature typical for highly ordered cholesterol rich bilayers (Falck et al. 2004), was significantly

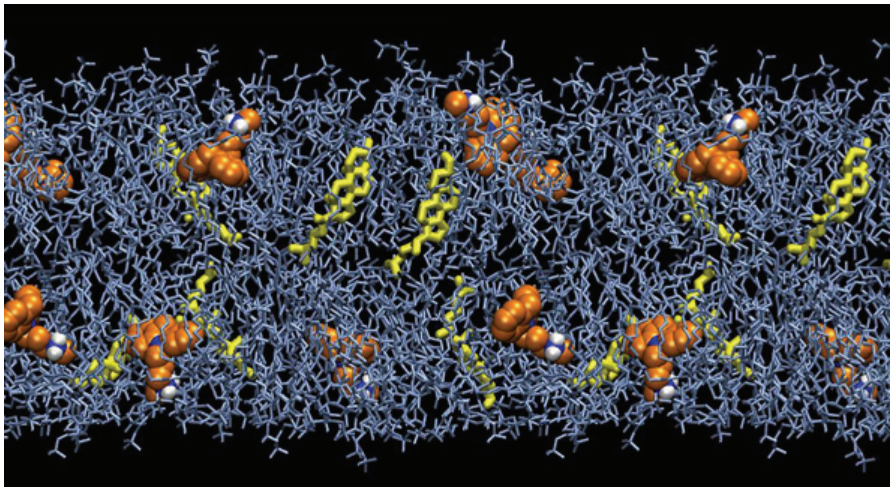

FIGURE 12 A snapshot of desipramine embedded in a cholesterol-rich membrane. POPC molecules are drawn with grey and cholesterol with yellow. Desipramine is presented as a space-fill model in orange with its nitrogens marked in blue. Picture with permission from Emppu Salonen. For the detailed structure of DMI see III, Fig. 1

reduced by desipramine. Correspondingly, the S_{CD} values for POPC in the high cholesterol membranes decreased substantially when desipramine was present in the membrane (III, Fig. 2 C, D). This was also seen as an increase in the membrane area, which allowed the POPC fatty acid chains to twist into less ordered conformations. For 0, 5, and 10 mol% DMI the calculated areas per lipid were 0.418 $\pm$ 0.004 nm^2, 0.431 $\pm$ 0.004 nm^2, and 0.444 $\pm$ 0.005 nm^2. These results indicate that desipramine induced a fluidising effect on the cholesterol-rich membranes. DMI molecules were not positioned all that deeply in the membrane: the calculated electron density profiles revealed the tricylic ring of desipramine to reside at the level of the lipid carbonyl groups (III, Supplementary Fig. S1). Interestingly, desipramine showed no preference of residing close to cholesterol in either high or low cholesterol concentration (data not shown).

5.4 Lysosomal membrane properties - a simplistic approach

5.4.1 Physical properties of triglyceride-containing membranes

Lysosomal membranes have been reported to contain triglycerides (Brotherus & Renkonen 1977; Ruiz & Ochoa 1997) and even tolerate uptake of triglycerides for storage (Schoonderwoerd et al. 1990). Hence, it is likely that triglycerides participate in determining the behaviour of the lysosomal membranes. But how do triglycerides affect the properties of a phospholipid

membrane, such as the lysosomal membrane? So far only little is known about the properties of triglyceride-phospholipid bilayers. The few studies so far have mainly concentrated on the solubility of triglycerides in phospholipid membranes (Spooner & Small 1987; Hamilton & Small 1981) and on the hexagonal phase transitions of phosphatidylethanolamine-triglyceride systems (Lee et al. 1996; Prades et al. 2003). In addition to triglycerides, we have also found monoglycerides in the lysosomal membranes (data not shown, Pakkanen et al. unpublished).

To elucidate the contribution of triglycerides in the properties of phospholipid membranes, we studied the effect of triolein (TO) on simple phospholipid membranes (POPC) by fluorescence and electron paramagnetic resonance spectroscopy as well as differential scanning calorimetry. In addition to the influence of triolein alone, possible synergistic effects of monopalmitin (MP) and TO on POPC membranes were analysed. Ratios of lipids were 10 mol% TO, 90 mol% POPC for the two-component system and 10 mol% TO, 10 mol% MP and 80 mol% POPC for the three component system. Intriguingly, both the TOPOPC system and the MPTOPOPC system were found to undergo macroscopical phase separation into a lighter floating phase and a pellet. The pellet was expected to be a multilayer phase, while the supernatant was considered a dilute vesicular phase (Janiak et al. 1979). The phase separation was most pronounced when the samples were centrifugated, but the same phenomenon could clearly be seen also in normal gravity after over night storage. The floating fraction and the pellet were named light phase (LF) and heavy phase (HF), respectively.

The composition of the two phases was analysed by quantitative thin-layer chromatography. There were only subtle differences in the compositions of the LF and HF. In TOPOPC system both the LF and the HF contained 5% TO and 95% POPC. In MPTOPOPC system, the amount of TO in LF seemed to be higher than in TOPOPC LF, 9%. The percentages for MP and POPC in MPTOPOPC LF were 4% and 87%, respectively. However, in the MPTOPOPC HF TO, only 2%, made a minor contribution to the composition. Correspondingly, the amount of MP was higher, 8%. Some oil-like drops were seen on the membrane-water interface of the sample. However, these droplets were separated from the sample (LF and HF) and therefore are not included in the quantitations (IV, Fig 1 A). Differential scanning calorimetry of the different phases further supported the view that no major compositional difference was responsible for the phase separation of HF and LF. Only some minor variation was seen in the DSC traces of the different phases. Furthermore, the DSC results demonstrated that in both TOPOPC and MPTOPOPC LFs the TO in the membrane was in equilibrium with another TO containing phase, namely the oily drops at the water surface, (IV, Fig. 2), analogously to a microscopic interaction model proposed for foreign molecules which partition into the membrane (Jørgensen et al. 1991).

The two phases were analysed in detail with spectroscopical methods. EPR spectroscopy showed the LF and HF of the TO containing systems to differ clearly from the membranes of MPPOPC or POPC alone. The EPR spectra of all the samples measured showed clearly the spin probe, Me-5-DSA, to reside in a fluid

environment. The spectra of TO and MPTO HFs were clearly representative of a more fluid environment than those of MPPOPC or POPC (for TOPOPC see IV, Fig. 5). Phase separation like that seen with the TO systems did not take place in the systems without TO as indicated by the very weak EPR signal in the LF of these systems and similarity of DSC thermograms of HF and LF (IV, Fig. 2).

To extract more information from the EPR data, we simulated the spectra using the EPRSIM program (Štrancar et al. 2000; Kavalenka et al. 2005). The program can simulate EPR spectra assuming the presence of one or several domains. None of the samples analysed bore any indication for more than one domain in their spectra and the goodness of fit in the simulation did not improve by allowing one or several domains. Therefore, all of the spectra were simulated based on one domain. The TOPOPC and MPTOPOPC LFs were found to be nearly isotropic with their order parameters, S_z, around 0.03. Interestingly, the order parameters for the LFs presented almost no temperature variation. Between different HFs only minor differences in order were seen (IV, Fig. 6 A). The correlation time, τ_c, which is inversely proportional to the viscosity of the membrane, confirmed the TOPOPC and MPTOPOPC LF to be considerably more fluid than the HFs (IV, Fig. 6 B). Furthermore, the simulations were used to obtain information on the polarity of the membrane-water interface. Only minor differences in polarity were seen between the different HFs, but the polarity in LFs of TOPOPC and MPTOPOPC was markedly different (IV, Fig. 6 B). The EPR spectra and the simulation of the EPR data show the studied membrane systems to be in fluid phase and TO to further increase the fluidity of the membranes, particularly in the case of the LF. In addition TO seemed to lower the polarity of the membrane-water interphase in LF.

We utilised both Laurdan and 1,6-diphenyl-1,3,5-hexatriene (DPH) as probes for fluorescence spectroscopy. Laurdan was used to assess water penetration to the glycerol backbone region of membrane and DPH anisotropy measurements to gain more information on the viscosity of membranes. However, unlike with EPR, only minor differences in anisotropy were seen between the LFs and HFs (IV, Fig. 7). In addition, the anisotropy values measured were not on an isotropic level, unlike values measured with neat olive oil (data not shown), which is different to the near-to-isotropic behaviour of TOPOPC and MPTOPOPC LFs seen with EPR spectroscopy (IV, Fig. 6 A). The DPH results imply the microviscosity in the fatty acid region of the TO-containing membrane to resemble pure POPC membranes.

Marked differences in the spectra of the two phases of the TO containing systems compared to neat POPC membranes were seen with Laurdan. The emission spectrum of POPC membranes followed the general features of Laurdan emission in fluid membranes and had a clear emission maximum in the region of 470 nm. Compared to POPC HF, the emissions of TOPOPC and MPTOPOPC LFs as well as MPTOPOPC HF were clearly blue-shifted (IV, Fig. 3). Laurdan general polarisation (GP) was measured to gain quantified information on the Laurdan fluorescence sensitive to local molecular environment. Most striking differences in Laurdan GP were seen between the TO containing LFs and POPC.

The GP values for TOPOPC LF ranged from 0.24 at 25°C to 0.11 at 40°C and those for MPTOPOPC LF from 0.29 at 25°C to 0.15 at 40°C , whereas GP for POPC was at its lowest, at 40°C , only -0.09 (IV, Fig. 4). Statistical testing using the non-parametric Kruskall-Wallis and Mann-Whitney U tests ensured the GP values for both TOPOPC LF and MPTOPOPC LF to be indeed significantly higher than those for POPC at all temperatures tested. P values for the difference between TOPOPC LF and POPC were 0.0006 for all temperatures measured and for MP-TOPOPC and POPC 0.023, 0.029, 0.029 and 0.041 for 25°C, 30°C, 35°C and 40°C, respectively. The higher GP values of LFs of TO-containing systems indicate that water was less able to penetrate to the upper part of the membrane. This is well in accordance with the EPR results on lower polarity of the TO-containing LFs.

5.5 At the far end of the parvovirus infection

5.5.1 Long cellular protrusions as potential means of parvovirus egress

The entry of CPV into its host cells has been characterised in detail (Parker & Parrish 2000; Parker et al. 2001; Suikkanen et al. 2002; Suikkanen et al. 2003b), but so far next to no information has been available on the late steps of the infection. A parvovirus related to CPV, minute virus of mice (MVM) has been proposed to have a non-lytic and potentially active vesicular egress mechanism (Salome et al. 1989; Bär et al. 2008). To shed light on the egress phase of CPV infection, we explored the late steps of the infection process of CPV.

The morphology of the infected Norden laboratory feline kidney (NLFK) cells differed markedly from that of the uninfected cells at 72 h p.i., whereas the morphology was essentially unchanged at in the infected cells at 24 h p.i. The uninfected cells and infected cells at 24 h p.i. were characteristically flat and triangular. However, when the cells were infected for a longer period of time, the shape of the cells begun to change. Already at 42h p.i. some differences to the uninfected cells were seen (data not shown) but more pronouncedly the striking difference in the cell morphology became evident at 72 h p.i. (V, Fig. 1A, C, E, G). The infected cells had become rounder, but were nevertheless still attached to the cover slip surface. They had grown protrusions which reached out from the cell body and sometimes fused with other cells or protrusions of other cells. In NLFK cells the longest protrusions streched out to an astonishing length of 130 μm. Changes in cell morphology similar to those seen in NLFK cells at late time points in infection, at 42 h p.i. (data not shown) and particularly at 72 h p.i. were apparent also in another cell line, canine fibroma A72 (see Fig. 13). For A72 cells the maximum length of protrusions measured was even longer than the longest protrusions seen in NLFK cells; 200 μm (V, Fig. 2). In addition to long neurite-like protrusions, the infected NLFK (V, Fig. 1I) and A72 cells (Fig. 13) featured short, filopodia-like extensions.

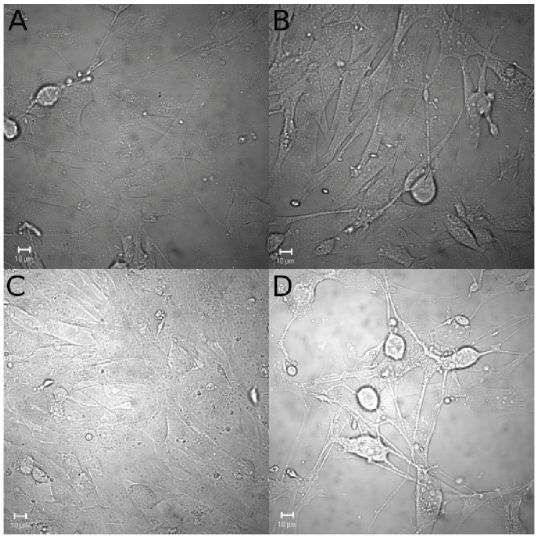

FIGURE 13 Morphology of A72 cells during CPV infection and in uninfected control cells. (A) Uninfected control cells grown for 24 h and (B) infected cells at 24 h p.i. (C) Uninfected control cells grown for 72 h and (D) infected cells at 72 h p.i. The morphology of the infected cells at both time points differs clearly from that of the uninfected control cells.

Some roundness and shorter protrusions were visible also in uninfected control cells grown in subconfluency for 72 h but the changes were much more subtle and seemingly less uniform than in the infected cells. Hoechst 33342 staining revealed that some of the NLFK cells infected for 72 h were undergoing apoptosis or necrosis, but the occurrence of protrusions did not correlate with the viability of the cell at the time of imaging (data not shown).

NLFK cells were also visualised with confocal fluorescence microscopy. Antibody to tubulin was found to stain effectively the long protrusions seen in cells infected for 72 h. As with differential interference contrast (DIC) imaging, short extensions in control cells grown for 24 h or 72 h were also seen with tubulin staining (V, Fig. 1 B, D, F and H). The long protrusions of the infected cells seemed to be primarily dependent on tubulin and no major participation of two other cytoskeletal proteins tested, actin and vimentin, was detected with immunofluorescence methods (data not shown). In addition to the striking long protrusions seen in cells infected for 72 h, the staining pattern of the infected and uninfected cells differed interestingly. In control cells grown for 24 h the characteristic spindle-like organisation of tubulin was clearly visible, but in at 24 h p.i. tubulin in the infected cells was anomalously mainly localised on the rim of the cells. Similarly, at 72 h p.i. the most intense fluorescence was seen in the cell periphery, as well as in the long protrusions, which were the most intensively stained parts of the cells (V, Fig. 1 B, D, F and H). At 24 h p.i. CPV capsid marker localised distinctively in the nuclei of the cells, but at 72 h p.i. some of the virus

marker was present also in the long tubulin-stained structures (V, Fig. 1J).

In cells infected for 72 h both the length of individual protrusions and the number of protrusions per cell were greater than in control cells grown for 72 h. In NLFK cells at 72 h p.i. the protrusions had an average length of 79.9 μm and in A72 cells 158.1 μm. In both cell lines the protrusions were significantly longer than those seen in uninfected cells (V, Fig. 2). Protrusions at 24 h p.i. were considerably shorter than those emerging at 72 h p.i, but still significantly longer than extensions seen in uninfected cells grown for 24 h (V, Fig. 2). At 72 h p.i. the number of protrusions was significantly higher in infected cells in both cell lines used compared to uninfected control cells. Each NLFK cell had in average 3.62 ($P = 0.001$) and each A72 cells 4.27 ($P < 0.0001$) long protrusions, whereas for the control cells grown for 72 h the average number of extensions were 2.08 and 2.89, for NLFK cells and A72 cells, respectively (V, Fig. 3). Also compared to infected cells at 24 h p.i., the cells infected for 72 h had significantly more protrusions in both cell lines. At 24 h p.i. the protrusions in A72 cells were significantly more numerous ($P = 0.04$) than in the uninfected control cells. The average number of protrusions was 3.07 for infected and 2.59 for uninfected cells. Difference between the number of protrusions per cell at 24 h was not found to be significant in NLFK cells (V, Fig. 3). These quantitative results on the number and spectacular length of the cellular extensions formed during CPV infection suggest that the processes that drive the formation of the protrusions start already early in infection and the alteration of cell morphology is a gradual process.

6 DISCUSSION

6.1 Interactions of parvovirus capsid with membranes

The membrane-capsid interactions of non-enveloped viruses are for the virus a crucial step towards a successful infection. As non-enveloped viruses typically are internalised into the host cells through endocytosis (Smith & Helenius 2004), some of the most critical interactions take place in the vicinity of the endosomal membranes. Studying these events is challenging as the physical size of viruses is well below the optical resolution limit and the intracellular location of events provides further methodological challenges for the studies. In general, the interactions between virus capsid and the endosomal membranes fall into two categories: the virus either perforates the membranes so that the whole organelle lyses, or it generates well-defined pores into the membrane through which the virus particle or its genome passes into the cytoplasm (Wickham et al. 1994; Belnap et al. 2000; Smith & Helenius 2004; Wiethoff et al. 2005; Ivanovic et al. 2008). In both cases, it is clear that these membrane penetration events contain multiple individual interactions which put together make it possible for the virus exert the desired effect on the endosomal membrane.

Some of the important interactions facilitating the penetration of a virus through the endosomal membrane may not necessarily bear signs as clear as pore formation or full-blown organelle lysis. The endosomal release of CPV is dependent of the action of the viral PLA_2, which is triggered to surface from inside the capsid by the acidic environment of endosomes (Parker & Parrish 2000; Suikkanen et al. 2003b). It would be easy to assume that the action of PLA_2 would permeabilise the limiting endosomal membrane altogether and the virus particles would be released when the vesicles lyses. However, this does not seem to be the case, as endosomes of CPV infected cells retain their integrity even when the virus passes through them. In fact, only particles up to 10-20 kDa in size can get through the endosomal membranes as result of the virus-induced membrane permeabilisation (Parker & Parrish 2000; Suikkanen et al. 2003b). Thus, it seems

that there is more to the endosomal penetration of parvoviruses than the function of the phospholipase. Our results implied the CPV capsid to react differently to the presence of membranes composed of different lipids at acidic pH. While phosphatidyl choline, phosphatidyl ethanolamine and phosphatidyl inositol had practically no influence on the CPV capsid, the presence of sphingomyelin and, to a lesser extent phosphatidyl serine, seemed to trigger changes in the capsid subunit organisation in terms of water penetration into the capsid (I, Fig. 1A) as well as secondary structure (I, Fig. 1B-C). Interestingly, the water penetration of the capsid was not affected by acidity alone, without the membranes (I, Fig. 1A), but marked changes were visible in the secondary structure of the virus proteins at acidic pH (I, Fig. 1 B, C).

The solvent sensitive fluorescence emission of tryptophan reports on the hydrophobicity of the local environment around the amino acid (Lakowicz 2006). Water penetration into the capsid can be thought to result from loosening of the capsid, facilitated by structural changes in the capsid subunits. These changes were found to be partly irreversible by neutralisation, as still some of the changes were visible after the capsids were brought back to pH 7.4 (I, Fig. 1E). These results suggest that the changes acidity induces in the capsid, presumably including at least the exposure of the VP1 N-terminus (Weichert et al. 1998; Vihinen-Ranta et al. 2002; Suikkanen et al. 2003b), differ from those induced by the presence of sphingomyelin and phosphatidyl serine. Based on the fact that the capsid interior becomes more accessible to water in the presence of the two lipids, these structural rearrangements can be thought to change the capsid more profoundly than the exposure of the VP1 N-terminus. However, the low pH-triggered conformational changes in the capsid are a prerequisite for the membrane- induced changes. The changes in the capsid structure brought about by sphingomyelin and, to lesser extent, phosphatidyl serine membranes could for example bring additional protein domains to the capsid surface to further facilitate the endosomal penetration process. Futhermore it seems, that some of the structural changes the virus undergoes in the endosomal lumen might persist in the virus capsid and possibly are of use also in further steps of the viral life. Although also other parvoviruses have been previously reported to react to low pH in endosomes (Mani et al. 2006; Ros et al. 2006), and to possess the acidicity-triggered PLA_2 domain (Zádori et al. 2001), our results show for the first time that a membrane can affect the parvovirus capsid and that these membrane- induced structural changes require low pH as a mediator.

We also reported CPV to be able to actively alter membranes by increasing water penetration into the upper part of the membrane. This is generally considered to be a sign for disordering, or fluidisation, of the membrane. Again, the virus required acidity to exert the fluidising effect. The change in the membrane was seen only in rigid DPPC:cholesterol membranes, but not in fluid DOPC membranes (II, Fig. 2, 3). This can imply two points. Firstly, cholesterol as such is needed for the fluidisation exerted by CPV or, secondly, the rigidity of the membrane *per se* could function as a trigger. Interestingly, the fluidisation ability of the capsid seemed to be located in the unique N-terminal part of the

VP1 protein. We constructed virus-like particles (VLPs) composed only of CPV VP2 protein which, consequently, lacked the N-termini of VP1, the part differing between VP2 and VP1 proteins (Paradiso et al. 1982; Xie & Chapman 1996). These VP2 VLPs did not have a fluidising effect on either of the used membranes. Futhermore, the activity for membrane fluidisation could, based on our results, be different from the classical hydrolysis activity of secretory PLA_2. Bee venom PLA_2 used as a control did not influence the fluidity of the membranes used, when analysed spectrophotometrically with di-4-ANEDPPHQ probe (II, Fig. 2, 3). Therefore it is reasonable to assume that the fluidising effect did not arise from the normal phospholipase function of the enzyme. But there is, in fact, only little sequence homology between the secreted type PLA_2 and the parvoviral enzyme. The homology is mainly limited to histidine and aspartate residues in the catalytic region and the calcium-binding motif GXG (Canaan et al. 2004). Therefore it is possible that the enzymatic domain could contain motif or motifs capable of membrane fluidisation. In addition to the VP1 N-terminus which is known to interact with membranes through the PLA_2 domain (Zádori et al. 2001; Canaan et al. 2004), large part of the external surface of the CPV capsid is hydrophobic (Xie & Chapman 1996), which can assist the whole capsid to interact with membranes. Hence, one cannot exclude the possibility that both VP1 and VP2 might be simultaneously needed for the membrane fluidisation.

6.2 Interactions of parvoviral capsid with endosomal membranes

One interesting goal in our studies was to elucidate, how CPV can penetrate the endosomal membrane through holes smaller than itself. CPV is not the only virus to encounter the problem of the undersized pore. During entry reovirus virions are modified by endosomal proteases resulting in infectious subvirion particles (ISVPs) of 45-50 nm in diameter (Silverstein et al. 1970; Sturzenbecker et al. 1987). However, when reovirus penetrates the endosomal membrane it passes through size-selective pores formed presumably by one of the viral proteins, μ1N (Agosto et al. 2006; Ivanovic et al. 2008). These pores have been both shown to be of only few nanometers in diameter (Tosteson et al. 1993; Agosto et al. 2006). Agosto and co-workers speculated the pores to be enlarged either by host cell factors or the whole organelle to undergo lysis because of osmotic swelling (Agosto et al. 2006). In the case of CPV the osmotic lysis of endosomes does not seem to be the way for the virus to get to the cytoplasm as both cytotoxic α-sarcin and dextran are retained in endosomes during CPV infection (Parker & Parrish 2000; Suikkanen et al. 2003b).

Despite some similarity in their problems to get through the endosomal membrane, the penetration process for CPV and reovirus differ. The PLA_2 of CPV contributes to the endosomal escape process (Suikkanen et al. 2003b). Our results suggest membrane fluidisation to have a role in squeezing CPV capsid

from the endosome lumen to the cytoplasm. During the entry phase of the infection CPV imposes a clear fluidising effect on the membranes of perinuclear endosomal vesicles (II, Fig. 4). The results showed a clear-cut difference between time points 4 h and 5 h post infection, which as such could suggest for example that the virus might need to accumulate in the endosomal vesicles before the capsids could penetrate the organellar membrane in bulk. The time points for the shift in spectra in infected cells, 3 to 4 h p.i., corresponds well with earlier published CPV entry kinetics (Suikkanen et al. 2002; Suikkanen et al. 2003b). Our *in vitro* results showed cholesterol, in addition to acidity, to trigger the CPV-induced fluidisation in model membranes (II, Fig. 2).

Furthermore, a second suggestion to cholesterol's particularly important role in CPV infection was given with our study on drugs influencing CPV entry. We found desipramine, U18666A and C2 ceramide to significantly inhibit CPV infection (III, Fig. 5) and to arrest the virus in intracellular vesicular structures. A similar trend was seen with methyl-β-cyclodextrin and lidocaine, which also seemed to perturb the intracellular trafficking of the virus. In addition, in the same study we provided atomistic scale evidence on the disordering effect of desipramine on phospholipid membrane rich in cholesterol by molecular dynamics simulations (see section 6.3).

We must take into account that lysosomotropic compounds, such as lidocaine and desipramine (Honegger et al. 1983; Vandenbroucke-Grauls et al. 1984), are known to alter lysosomal pH (Poole & Ohkuma 1981) and to perturb infection of viruses requiring acidic step in their entry (Helenius et al. 1982). In addition, U18666A and imipramine, a metabolic precursor of desipramine (Madsen et al. 1997), have been shown to induce cholesterol accumulation in lysosomes (Liscum & Faust 1989; Lange et al. 2000; Lange et al. 2002; Klingenstein et al. 2006). However, lysosomotropic antibiotic gentamycin, which has no known effect on lipid raft integrity, was found not to hinder CPV infection (III, Fig. 5). In cellular experiments the numerous and sometimes even opposing effects of one compound typically render interpretation of results difficult. In our case, however, we provided multiple lines of evidence for the importance of correct organisation of intracellular membranes in CPV infection. Not only did we find different types of raft-disrupting compounds to inhibit CPV infection, we also showed how cholesterol can rescue CPV infection after a block caused by sphingomyelin addition to cells (III, Fig. 8). The mechanism of cholesterol to relieve the sphingomyelin-induced block in CPV traffic remains unclear. However, the fact that addition of cholesterol is favourable for CPV infection further underlines the special role of cholesterol in the infection process. In addition, the ability of cholesterol to enhance domain formation could also have an effect on rescuing the infection. The activity of PLA_2 has been shown to be enhanced by the presence of interfacial regions of membrane domains.

CPV's requirement for cholesterol during it's entry does not seem to be a typical case of cholesterol-dependent entry for a non-enveloped virus. CPV is internalised by clathrin-mediated endocytosis (Parker et al. 2001; Suikkanen et al. 2002), and therefore does not rely directly on plasma membrane

cholesterol domains unlike viruses utilising for example caveolae-mediated endocytosis (Marsh & Helenius 2006). Although CPV internalisation is perturbed by cholesterol-depletion of the plasma membrane (data not shown), this effect is likely to originate from cholesterol's role in facilitating internalisation of clahtrin-coated pits (Subtil et al. 1999) rather than direct interactions between the virus and cholesterol of the plasma membrane. Based on our results it seems that the role of cholesterol in CPV entry is particularly pronounced at 3 to 4 hours after the virus is internalised (III, Fig. 6). This corresponds well with the time CPV has been shown to reside in the endosomal system and especially in LAMP-2 positive vesicles (Suikkanen et al. 2002). Our results obtained with fluorescence spectroscopy in live cells reveal the CPV-induced fluidisation to be present at 3 to 4 h p.i. Furthermore, the fluidisation was found to be triggered by cholesterol and low pH in *in vitro* experiments. In conclusion, we propose that cholesterol and correct cholesterol-based organisation of intracellular membranes are important for the endosomal penetration of CPV and, consequently, are needed for successful infection.

6.3 Antidepressant desipramine disorders cholesterol-rich membranes

Results of the atomistic molecular dynamics simulations with the antidepressant desipramine (DMI) relate to the experimental studies, where DMI was found to inhibit CPV infection. The membrane interactions of desipramine, and other known drugs, are interesting also from a broader view point. Understanding the way these compounds function outside their immediate scope of action can complement the current clinical based view on their side effects and potentially render new ways to utilise existing drugs.

The MD simulation results showed the fused three-ring moiety of desipramine to introduce disorder into phospholipid membranes with high cholesterol content. Especially pronounced this effect was in the centre of the membrane (III, Fig. 2 C-D). Nevertheless, the ring triplet was interestingly not situated very deep in the membrane. This was revealed by the calculated electron density profiles (III, Supplementary Fig. 1). Conversely, in membranes with only 5 mol% cholesterol the effect of desipramine was moderately ordering (III, 2 A-B). Cholesterol affects the permeability of phospholipid membranes by altering the physicochemical properties of the membrane. In particular the ability of cholesterol to lower the free volume of membranes corresponds to lower permeability of the membrane. Moreover, a membrane in lo phase has particularly reduced membrane free volume, and consequently, permeability (Mouritsen & Jørgensen 1994; Barenholz 2002). Introduction of disorder into the cholesterol-rich membrane by desipramine can thus be assumed to increase the permeability of the membrane.

Desipramine as well as the serotonin receptor 5-HT_3 have been reported

to colocalise with caveolin-2 and flotillin-1 in cell membranes. This suggests accumulation of desipramine in lipid rafts on the plasma membrane (Eisensamer et al. 2005). Interestingly however, in our simulations the molecular radial distribution functions showed no preference of desipramine to localise in close vicinity of cholesterol at the molecular level at either low or high cholesterol concentrations. However, localisation of desipramine in the light buoyant density (LBD) fraction, a density gradient fraction considered to contain membrane rafts, of isolated membranes could have other background than direct association with cholesterol. For example, ligand-receptor interactions could attract desipramine to the site. DMI exerts its function through inhibition of norepinephrine uptake (Bauer & Tejani-Butt 1992; Zhu et al. 2004) and norepinephrine transporter (NET) has been found to be present in lipid rafts (Jayanthi et al. 2004). Disordering of the membrane and dilation of the membrane area in raft regions by desipramine can be assumed to lead to disintegration of the raft domains leading possibly to changes in proteins embedded in rafts and, consequently, in cellular functions, such as signalling, connected to rafts.

The intracellular effect of desipramine is focused on the endosomal system and in particular to the late structures. Because of it's lysosomotropic nature desipramine, like other cationic amphiphilic drugs, becomes trapped inside the acidic vesicles by protonation (Honegger et al. 1983; Lemieux et al. 2004). We utilised this property of desipramine to be inherently targeted to the endosomal route and found the drug to inhibit CPV entry by arresting the virus into intracellular vesicles (III, Fig. 5; see section 6.2). In addition to the potential antiviral use of the drug, loosening the ordering of cholesterol-rich membranes, and potentially other highly ordered membranes, give also different view points to use of tricyclic antidepressants like desipramine outside their classical mode of action.

Using desipramine as and intracellular raft-breaker has, however, some inherent challenges. Imipramine, another tricyclic antidepressant closely related to desipramine, have been found to induce cholesterol accumulation in lysosomes mimicing the cholesterol strorage disorder Niemann-Pick C disease (Lange et al. 2000; Lange et al. 2002). Imipramine is metabolised into desipramine through N-demethylation by cytochrome P450s (Madsen et al. 1997). In addition to imipramine (desipramine), also another cationic (class 2) amphiphile, U18666A, has been found to cause accumulation of cholesterol in lysosomes and to disrupt DRM domains (Liscum & Faust 1989; Klingenstein et al. 2006). However, the effect on cholesterol accumulation by class 2 amphiphiles seems to originate from direct effects on the NPC1 protein or it's pathway (Lange et al. 2000). How the direct influence of tricyclic antidepressants and other cationic amphiphiles on cholesterol-rich membranes contribute to the lysosomal cholesterol accumulation, whether promoting or counteracting it, remains to be seen.

6.4 Lysosomal membrane properties - a simplistic approach

We studied in a well controlled model system how triglycerides alter the physical properties of phospholipid membranes. This relates to our interest to understand the physical properties of lysosomal membranes. In the study the model membranes used were simple, but the systems containing TO and POPC turned out to behave in a complex way and exist in two different macroscopical phases both in centrifugal field and in normal gravity. Interestingly, the two phases seemed nevertheless to have more or less the same composition, rich in POPC (IV, Fig. 1). In addition, their thermal behaviour analysed with DSC appeared to be nearly identical (IV, Fig. 2).

Neither inverted hexagonal phase, which has been reported previously for triglyceride-phosphatidyl ethanolamine systems (Lee et al. 1996; Prades et al. 2003), nor micellar phase, where TO droplets would be covered with POPC, would give adequate explanation to the formation and strikingly different behaviour of the LFs. Both DPH anisotropy results and the TLC quantitations contradicted the view that the systems would form POPC-coated micelles of TO. On the other hand, inverted hexagonal phase, a hexagonally arranged 3D structure of inverted micelles (for inverted micelles see Section 2.1.2), would not have allowed such extreme fluidity close to the membrane-water interphase as seen with EPR in the TO-containing systems (IV, Fig. 6 B).

Based on our spectroscopical results we presented a model (IV, Fig. 8; see Fig. 14) on how triglycerides could be positioned in a phospholipid bilayer. We proposed these two different orientations to account for formation of the light and heavy phases (LF and HF, respectively) in TO containing systems and for their different behaviour. The model can be used as a first approximation to understand the contribution triglycerides make in the material properties of lysosomes.

In the model a triglyceride molecule is assumed to be able to adopt two main conformations. Either the triglyceride lies on the membrane with the three fatty acid side chains inserted into the membrane in a conformation which we, based on the caricatural letter it resembles, named E (Fig. 14; IV, Fig. 8B) or the triglyceride is fully embedded in the membrane. This latter option, what we call the h configuration would, unlike lipids in general in a membrane, find a most suitable place for itself upright in the membrane with two of it's fatty acids pointing to one direction and the last one to opposite direction (Fig. 14; IV, Fig. 8B). Both E and h conformation have also been described previously. Triolein has been shown to reside in conformation corresponding that of our E conformation in an NMR study (Hamilton & Small 1981). Similar conformation has also been suggested for tristearin (Teixeira et al. 2008). The h conformation, or "tuning fork" as it has also been named, has been noted to appear in both crystalline triglyceride and fluid tristearin (Callaghan 1977; Akita et al. 2006). In addition, both E and h conformations have been seen in molecular dynamics simulations. According to the simulations 88% of tripalmitins in crystalline phase are in conformations corresponding h (tuning fork and chair conformations) and mere 9% in the E

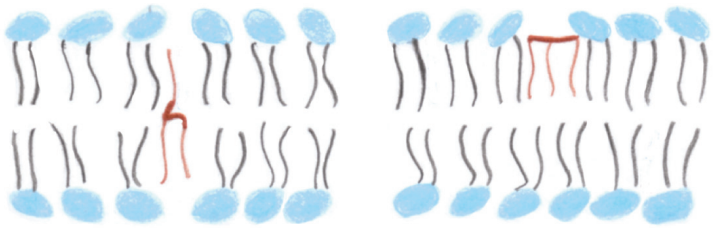

FIGURE 14 Model on triglyceride orientation in phospholipid membranes. On the left, triglyceride (brown) in h conformation and on the right in E conformation.

(trident) conformation. In fluid phase on the other hand, the simulations showed tripalmitin to adopt mainly random conformations (Hall et al. 2008).

Our spectroscopical results support the idea of h-type orientation of TO in the phospholipid membrane. Viscosity (IV, Fig. 6 B) and order (IV, Fig. 6 A) of the light phase membranes with TO were considerably lower at the membrane-water interphase than in the heavy phase membranes of the same systems. At the same time, viscosity deeper in the membrane was unchanged in the light phase. This corresponds well to our model of E and h conformations. If TO was positioned in h conformation in the light phase membranes, the spin probe would have more freedom to rotate as the lack of head group in the upward pointing fatty acids would generate space in the uppermost part of the membrane. At the same time the core of the membrane would remain practically unchanged if the glycerol backbone of the TO would reside in the middle of the membrane. This was confirmed with the DPH anisotropy measurements (IV, Fig. 7). DPH has been shown in molecular dynamics simulations to reside deep in the membrane, in the middle of the fatty acid region (Repáková et al. 2004). Polarity of the upper part of the membrane at the level of the glycerol-fatty acid ester bonds was also seen to be changed in the light phase (IV, Fig. 6 C). This is explained by the h conformation when the fatty acids pointing upwards in the membrane would bring a non-polar contribution to the phase. Furthermore, our GP data support the results on low polarity of the light phase. Decreased polarity repels water from the upper part of the membrane and this affects directly the GP measured in light phase. The increase in GP (IV, Fig. 4) cannot be explained by decrease in the membrane area due to ordering of the membrane as the EPR results at the same time tell the membrane to be greatly fluidised. Therefore we assume the significant raise in GP in the light phase compared to the heavy phase to originate from the water repelling effect the fatty acids of the TOs in h conformation bring to the membrane, and consequently affect the emission of Laurdan by decreasing solvent dipolar relaxation.

These previous studies on triglyceride confomations in crystalline and fluid phase (Callaghan 1977; Akita et al. 2006) were, apart from the NMR study

(Hamilton & Small 1981), made with pure triglycerides. However, in our case the system contained mainly POPC: over 90% in the two-component systems and over 80 % in the three-component system. The systems were in fact saturated with triolein, as with 10 % addition only 5 % of TO partitioned into the POPC membrane in the two-component system (IV, Fig. 1B). In a phospholipid membrane the phospholipids could provide a molecular scaffold for the triglycerides to orient in a more crystal-like manner in a phospholipid membrane. Correspondingly, in our systems, the triglycerides would first orient in the membrane mainly in E conformation. When the amount of TO in the membrane would increase, more and more of the triolein molecules would flip into h conformation and this would promote the formation of the light phase (LF). This view is also supported by our most recent results. POPC membranes supplemented with only 2% TO did not present phase separation into light and heavy phase. However, POPC membranes with either 4%, 6%, 8% or 10% TO, that is to say amounts close to or above the saturation limit, formed the two phases (for 2, 4, 6 and 8 % data not shown, Pakkanen et al. unpublished; for 10% see IV).

Triglycerides are in cellular context sparse components of membranes. Typically triglycerides reside in cells as lipid droplets. The lipid droplets have a core of triglycerides and cholesterol esters covered by a layer of phospholipids and they are most abundantly found in adipose tissue in mammals (Zweytick et al. 2000; Tauchi-Sato et al. 2002). In addition, in cells and in blood circulation, triglycerides are transported inside two classes of triglyceride-rich lipoproteins, chylomicrons (CM) and very low density lipoproteins (VLDL). These are, after enzymatic modification by the lipoprotein lipase, taken into cells by receptor-mediated endocytosis and delivered into lysosomes for degradation (Heeren & Beisiegel 2001). Consequently, triglycerides have been found in lysosomes of normal healthy cells (Brotherus et al. 1977; Ruiz et al. 1997, Pakkanen et al. unpublished). As a highly hydrophobic molecule, triglycerides can be expected to partition into the lysosomal membrane during the degradation of triglyceride-containing lipoproteins. Our recent studies suggest triglycerides to indeed partition to phospholipid membranes and the isolated membranes to contain triglycerides (Pakkanen et al. unpublished). In fact, the presence of triglycerides is one of the few facts which actually have been established regarding the composition of the lysosomal membranes.

All in all, the lysosomal membrane composition is still, after decades of research, somewhat obscure. In addition the the suggestion of triglycerides in the membranes, lysosomal membranes have been shown to be poor in cholesterol (Möbius et al. 2003). As the composition remains unclear, also the properties of the lysosomal membranes are, to date, more or less unknown. Studying the detailed physical properties of native lysosomal membranes is challenging because of difficulties in obtaining highly purified membrane material in sufficient amounts. In addition, lysosomal membranes like all native cellular membranes contain innumerable amount of different lipid species. Each of the lipid species contribute to the properties of the membrane and this makes the interpretation of the results from a biophysical perspective unreliable, as one does not know

which property originates from which component. Our approach here was to bring the system complexity to the minimum and investigate the properties of lysosomes one part at the time. It is of course true, that a simplistic approach like ours does not give any information on the synergistic effects of different lipids on to the properties of the membrane nor direct evidence on the behaviour of native membranes. Nevertheless, we have gained by studying this simple model membrane new insight into how the lysosomal membranes could with the help of the triglycerides they contain function as a barrier against the harsh conditions of the lysosomal lumen and for retaining the acidic conditions inside the vesicles.

Low amounts of cholesterol in the lysosomal membrane pose a requirement for additional protection against leakage, as the permeability of membranes without cholesterol has been proposed to be compromised (Finkelstein 1976; Lande et al. 1995) and the mid-plane of a fluid membrane without cholesterol to contain appreciable amounts of water (Marsh 2001). It so seems that the cholesterol-poor lysosomes have a challenge in keeping water out and solutes in to retain the pH gradient over the limiting membrane. We therefore postulate, that accumulation of triglycerides in lysosomes leads to saturation of lysosomal membranes with triglycerides. This, then promotes the formation of the light phase membranes, where the triglycerides are in h conformation. Consequently, decrease in polarity repels water from the membrane interphase and reduces the permeability of the membrane to water. At the same time as promoting the barrier properties triglycerides allow the membrane to be highly fluid, which differs from the situation achieved by sealing the membrane with cholesterol.

6.5 At the far end of the parvovirus infection

Exit of viruses from cells is a critical step for the virus to efficiently transfers its offspring to neighbouring cells in the tissue. Viruses have optimised the transit from one cell to another to maximise the efficiency of spreading the infection. Some viruses utilise the host cell cytoskeleton to firstly move from inner parts of the cell to the plasma membrane and secondly, to reach out to other cells. Typically, viruses induce the host cell normal outgrowth, filopodia, for means of transfer to the next cell. Viruses such as Marburg virus, Semliki Forest virus (SFV), Sindbis virus and Murine leukemia virus have been found to induce filopodia-formation in host cells (Kolesnikova et al. 2007; Laakkonen et al. 1998; Sherer et al. 2007). Interestingly, in the case of Semliki Forest virus (SFV) and Sindbis virus, the abnormal growth of filopodia is induced by the viruses nonstructural proteins (Laakkonen et al. 1998).

In our study CPV was found to induce the formation of cellular protrusions late in infection. Although some smaller, filopodia-like extensions of the host cell cytoskeleton appeared on the infected cells (V, Fig. 1 I), dominated long protrusions the scene at 72 h p.i (V, Fig. 1). The long, neurite-like protrusions did not seem to be actin-based (V, data not shown) but contained tubulin (V,

Fig. 1J). Dramatically long cellular protrusions similar to those induced by CPV has been reported also to be formed during pseudorabies virus infection. These protrusions, however, contained both actin and tubulin (Favoreel et al. 2005). The protrusions emerging during CPV infection were more solitary, whereas the protrusions associated with pseudorabies virus infection appeared more branched (Favoreel et al. 2005). The staining pattern of tubulin, on the other hand, was similar in both: tubulin was localised mainly at the rim of the cell and in the long protrusions. For pseudorabies virus it has been cleared that the formation of the long protrusions is dependent on a viral protein kinase, US3. The US3 kinase affects directly the cytoskeleton by inducing disassembly of actin fibers (Van Minnebruggen et al. 2003; Van den Broeke et al. 2009). Similar actin rearrangements leading to formation of cellular protrusions during viral infections are seen also with HIV and vaccinia virus (Fackler et al. 1999; Valderrama et al. 2006). For vaccinia virus the actin fiber loss is induced by the viral effector protein F11L, which hampers RhoA signalling in the cell (Valderrama et al. 2006).

The long protrusions were the dominating feature seen in cells infected with CPV (V, Fig. 1) and this suggests that similar to e.g. vaccinia virus and pseudorabies virus some interactions between the viral proteins and the host cell cytoskeleton are likely take place during infection. Although actin was not found to be present in the long protrusions during CPV infection, RhoA signalling could still have a role in the formation of the cellular protrusions. Sceife et al. have reported microtubule to be rearranged into bundles and fibroblasts to grow out extensive tubulin-based protrusions when Rho effector protein ROCK and the multiadaptor proto-oncoprotein Cbl were simultaniously inhibited (Scaife et al. 2003). These tubulin-containing extensions bear striking resemblance to the extensions seen in CPV infected cells.

Presence of tubulin in the long protrusions in CPV infection is highly interesting. Previously, CPV has been shown to associate with microtubules and microtubule motor protein dynein both *in vitro* and *in vivo*. Both dynein and microtubules seem to be indispendable for the cytoplasmic transport of CPV from endosomal region towards the nucleus. (Suikkanen et al. 2003a). In our study, CPV was found to partially localize in tubulin-stained structures of the cells (Fig. 1J). This suggests that CPV might utilise microtubules not only in its entry but also in egress from the host cells. In both cases travelling along the microtubule is a good way for the virus to avoid the slowing effect of viscose cytoplasm.

Our results propose CPV to have a tubulin-mediated egress strategy. A related parvovirus, MVM has been previously suggested to leave the host cell by using a vesicular mechanism including vesicles, which contain markers for late endosomes/ lysosomes. (Bär et al. 2008). Although the actin network of the host cell seemed to have a role in MVM exit, it does not exclude the possibility of microtubules to participate in facilitating the movement of the virus towards the cell perifery. In addition, both early and late endosomes have been shown to move along microtubules with the help of motor proteins kinesin and dynein (Nielsen et al. 1999; Murray et al. 2000; Bananis et al. 2004). This

provides another way to interpret the results of our study, namely that CPV could during the exit phase of the infection travel onboard endosomal vesicles along microtubules which stretch out as long protrusions towards the neighbouring cells.

7 CONCLUSIONS

The main conclusions of this thesis are:

1. CPV interacts strongly with lipid bilayers both *in vitro* and *in vivo*. The capsid structure is affected by sphingomyelin and the virus is capable of fluidising membranes. This fluidisation effect is triggered by cholesterol and present only in low pH.

2. Cholesterol is important for successful CPV infection. In particular cholesterol seems to be needed at the intracellular membranes to facilitate CPV entry.

3. Tricyclic antidepressant desipramine disorders cholesterol-rich membranes. Desipramine also inhibits CPV infection.

4. At or above their saturation limit in membranes, triglycerides promote macroscopic phase separation in fluid phospholipid membranes. In the light floating phase triglyceride fluidises the membrane and repels water from the membrane-water interface. As triglycerides are found in lysosomal membranes we propose them to decrease the water permeability of lysosomal membranes and thus, contribute to maintaining the pH gradient over the membrane.

5. Late in infection CPV induces the growth of tubulin-based neurite-like protrusions in host cells. These are likely to contribute to the egress of the virus.

Acknowledgements

This study was carried out at the University of Jyväskylä, at the Department of Biological and Environmental Science. One of the projects connected to the thesis, the Lysosome Project, was conducted as a collaborative study at MEMPHYS – Center for Biomembrane Physics at the University of Southern Denmark in Odense.

I wish to thank my supervisor professor Matti Vuento for providing me the opportunity for this thesis. I thank Matti for introducing me to the secrets of spectroscopy and for teaching me many valuable lessons - in science and in life. I thank my second supervisor professor Henrik Kunttu especially for the much needed support at the end of my PhD studies. I am grateful to professor Ole G. Mouritsen for providing me the opportunity to work at MEMPHYS. I thank my opponent docent Pentti Somerharju and the reviewers of this thesis, professor J. Peter Slotte and docent Eeva-Liisa Eskelinen.

To all my co-workers, past and present, I want to give my warmest thanks. Lars Duelund, John H. Ipsen, Tuula Jalonen, Pirjo Kauppinen, Jenni Karttunen, Sanna Kirjavainen, Eila Korhonen, Anna Mäkelä, Jonna Nykky, Christian "Kricke" Oker-Blom, Nina Rintanen, Emppu Salonen, Ilpo Vattulainen and Salla Virtanen - working with all of you has been inspiring and enjoyable. Antti-Juhani Kaijanaho is acknowledged for troubleshooting the thesis typesetting.

In addition to hard work there has been many unforgettable moments. Anna, thank you for all the help and support! You got it right: "Kerranhan täällä vaan eletään – ja silleen!" Elina and Valtteri, thank you!! Sanna and Jonna, you were there right in the beginning of my life in science - thank you. Thank you Nina for great company by the Mediterranean. Kiitos Pirjo monista neuvoista ja yhteisistä juttutuokioista! Tuula, thank you for opening new ways of thinking for me. Lars, thank you for sharing the attitude that science should be fun. As unbelievable as it is, we actually were doing science! And furthermore, thank you for all your help with this thesis. Thank you, John, for being my tour guide to physical chemistry and membrane science. And especially, thank you for all our inspiring discussions – with and without a coffee cup – throughout the thesis process. Thank you everybody at MEMPHYS for welcoming me into the crowd! Riikka, in addition to everything else, thank you teaching me statistics and for revising the logic of thought in this thesis.

For the people in my real life outside science I want to express my deep appreciation and gratitude. Your love and friendship remind me constantly on the important things in life. Thank you, all of you, for supporting me each in your own way. I dedicate this book to my wonderful parents. Kiitos äiti ja isä!

This thesis has been supported financially by the Finnish National Graduate School in Nanoscience (NGS-NANO) and Letterstedska foundation. MEMPHYS – Center for Biomembrane Physics is supported by the Danish National Research Foundation.

YHTEENVETO (RÉSUMÉ IN FINNISH)

Endosomeista eteenpäin. Lipidikalvoja, lysosomeja ja viruskapsidin vuorovaikutuksia

Solut tarvitsevat ulkopuoleltaan materiaalia, joka kuljetetaan soluun solukalvolta lähtevän rakkulakuljetusjärjestelmän, endosytoosin, avulla. Endosytoosissa pieni osa solukalvoa kuroutuu tarkan signaalikoneiston säätelemänä rakkulaksi eli vesikkeliksi solun sisään. Sisään kuljetettu materiaali, niin reseptorit, niihin kiinnittyneet ligandit kuin soluväliaineen nestefaasissa mukaan tulleet molekyylitkin, lajitellaan lipidikalvojen rajaamissa osastoissa joko jatkamaan matkaansa syvemmälle soluun yhä happamampiin kalvorakkuloihin, tai kuljetettavaksi takaisin solukalvolle uudelleen käytettäväksi.

Vaikka endosytoosi on soluille elintärkeä, se on solulle myös turvallisuusuhka. Monet mikrobit, kuten esimerkiksi virukset, ovat kehittäneet tapoja kaapata solun oma endosytoosikoneisto käyttöönsä. Tällöin solu huomaamattaan itse kuljettaa mikrobit sisäänsä kalvorakenteiden sisällä muun endosytoosissa soluun sisään otettavan materiaalin mukana. Viruksen päästyä tarpeeksi syvälle solun sisään – mahdollisimman lähelle tumaa – sen tarvitsee vain murtautua endosytoosivesikkelejä rajaavan lipidikaksoiskalvon läpi päästäkseen solulimaan ja yhä edelleen tumaan monistamaan genomiaan ja tuottamaan uusia viruspartikkeleita. Endosomikalvon läpäisy on tärkeä virusinfektion onnistumiselle. Jos virus ei jostain syystä pääsekään ulos kalvojen rajaaman, tyypillisesti hyvin happaman vesikkelin sisältä ei se voi infektoida solua eikä siten synny myöskään uusia viruspartikkeleita. On tärkeää oppia ymmärtämään mitkä kalvon ja viruksen ominaisuudet määrittelevät onnistuuko viruksen läpäistä kalvo.

Tässä väitöskirjatyössä tutkittiin koiran parvoviruksen (CPV) ja kalvojen vuorovaikutuksia: kuinka CPV vaikuttaa kalvoihin sekä kuinka kalvot vaikuttavat CPV:hen ja sen toimintaan solussa. Lisäksi tutkittiin mallikalvosysteemin avulla kuinka triglyseridit vaikuttavat fosfolipidikalvon ominaisuuksiin. Tämä osa väitöskirjaa edesauttaa ymmärtämään lysosomien, endosytoosireitin viimeisten rakenteiden, kalvojen ominaisuuksia ja antaa erityisesti uutta informatiota lipidikoostumuksen vaikutuksesta lysosomikalvojen eheyteen. Viimeisenä kokonaisuutena tässä väitöskirjassa tutkittiin CPV-infektion loppuvaihetta, jossa virus on jo valmis hylkäämään isäntäsolunsa ja siirtymään ulos solusta voidakseen infektoida yhä uusia soluja.

Lipidikalvojen koostumuksella havaittiin olevan vaikutusta CPV:n rakenteeseen ja toimintaan. Erityisesti sfingomyeliinin todettiin aiheuttavan viruksen proteiinialayksiköissä muutoksia, jotka johtivat kapsidin rakenteen väljentymiseen. Sfingomyeliini ei kuitenkaan vaikuttanut CPV:n kapsidissa sijaitsevan lipideitä hajottavan fosfolipaasi A_2 entsyymin toimintaan. Fosfolipaasi-entsyymi ei näyttänyt olevan ainoa alue kapsidissa, joka aktiivisesti osallistuu kalvojen

muokkaamiseen viruksen haluamaan suuntaan. Happamissa olosuhteissa CPV:n todettiin muuttavan jäykkien, kolesterolirikkaiden kalvojen juoksevuutta. Samankaltaisia juoksevuusmuutoksia havaittiin myös solun sisällä endosomirakenteissa CPV infektion aikana. Tulostemme perusteella vaikuttaa siltä, että CPV tarvitsee jäykkiä kolesterolirikkaita kalvoalueita voidakseen päästä endosomien sisältä solulimaan.

On tärkeää löytää uusia tapoja pysäyttää virusinfektion kulku solussa. Me tutkimme tarkemmin yhtä lääkeainetta, desipramiinia, joka on jo kliinisessä käytössä mielialalääkkeenä. Atomitarkkuudella toteutetuissa tietokonesimulaatioissa havaitsimme desipramiinin notkistavan kalvoja, joiden kolesterolipitoisuus on korkea. Solukokeissa havaitsimme desipramiinin myös haittaavan CPV infektiota. Tämä antaa uuden näkökulman viruslääkkeiden kehitykseen: muuttamalla solun kalvoja virukselle haitalliseen suuntaan voi viruksen kenties saada pysäytettyä.

Neljännessä osatutkimuksessa opimme että triglyseridit muuttavat fosfolipidikalvojen ominaisuuksia. Triglyseridin lisäys kalvoon sai aikaan kahden erilaisen kalvofaasin muodostumisen. Toinen näistä kalvoista erosi juoksevuudeltaan ja polaarisuudeltaan fosfolipidikalvosta ilman triglyseridiä. Lysosomien kalvon voi karkeasti ottaen ajatella olevan fosfolipidikalvo, jossa on mukana myös triglyseridejä. Näin yksinkertaisen mallikalvon avulla saadut tulokset triglyseridejä sisältävien kalvojen ominaisuuksista liittyvät läheisesti ymmärtämykseemme lysosomikalvojen ominaisuuksista. Triglyseridien tehtävä lysosomien kalvoissa saattaakin liittyä juuri kalvon polaarisuuteen, jolloin kalvosta tulee tavallista enemmän vettähylkivä.

Väitöskirjan viimeinen osatyö käsitteli CPV infektion loppuvaiheita. Havaitsimme CPV infektion aihettavan pitkien, tubuliinia sisältävien ulokkeiden muodostumisen soluissa. CPV nähtiin myös näiden ulokkeiden sisällä, joten on perusteltua olettaa että nämä naapurisoluja kohti kurottelevat ulokkeet voisivat luoda reitin, jota pitkin virus voi siirtyä uuteen soluun tai ainakin aivan sen lähistölle.

REFERENCES

Aderem, A. & Underhill, D. M. 1999. Mechanisms of phagocytosis in macrophages. Annu. Rev. Immunol. 17: 593–623.

Aderem, A. 2003. Phagocytosis and the Inflammatory Response. J. Inf. Dis. 187: S340–S345.

Agbandje, M., Mckenna, R., Rossmann, M.G., Strassheim, M. L. & Parrish, C. R. 1993. Structure determination of feline panleukopenia virus empty particles. Proteins 16(2): 155–171.

Agosto, M. A., Ivanovic, T. I. & Nibert, M. L. 2006. Mammalian reovirus, a nonfusogenic nonenveloped virus, forms size-selective pores in a model membrane. Proc. Natl. Acad. Sci.103(44): 16496–16501.

Akita, C., Kawaguchi, T. & Kaneko, F. 2006. Structural study on polymorphism of cis-unsaturated triacylglycerol: triolein. J. Phys Chem. B 110(9): 4346–4353.

Almeida, P. F. F., Vaz, W. L. C. & Thompson, T. E. 1992. Lateral diffusion in the liquid phases of dimyristoylphosphatidylcholine/cholesterol lipid bilayers: a free volume analysis. Biochemistry 31(29): 6739–6747.

de Almeida, R. F. M., Loura, L. M. S., Fedorova A. & Prieto, M. 2005. Lipid rafts have different sizes depending on membrane composition: a time-resolved fluorescence resonance energy transfer study. J. Mol. Biol. 346(4): 1109–1120.

Aloia, R. C., Jensen, F. C., Curtain, C. C., Mobley, P. W. & Gordon, L. M. 1988. Lipid composition and fluidity of the human immunodeficiency virus. Proc. Natl. Acad. Sci. 85(3): 900–904.

Aloia, R. C., Tian, H. & Jensen, F. C. 1993. Lipid composition and fluidity of the human immunodeficiency virus envelope and host cell plasma membranes. Proc. Natl. Acad. Sci. 90(11): 5181–5185.

Anderson, R. G., Brown, M. S., Beisiegel, U. & Goldstein, J. L. 1982. Surface distribution and recycling of the low density lipoprotein receptor as visualized with antireceptor antibodies. J. Cell Biol. 93: 523–531.

Aniento, F., Emans, N., Grittiths, G. & Gruenberg, J. 1993. Cytoplasmic dynein-dependent vesicular transport from early to late endosomes. J. Cell Biol. 123(6): 1373–1387.

Aoki, T., Nomura, R. & Fujimoto, T. 1999. Tyrosine phosphorylation of caveolin-1 in the endothelium. Exp. Cell Res. 253(2): 629–636.

Appelmans, F., Wattiaux, R. & De Duve, C. 1955. Tissue fractionation studies. 5. The association of acid phosphatase with a special class of cytoplasmic granules in rat liver. Biochem. J. 59(3): 438–445.

Ashbourne Excoffon, K. J. D., Moninger, T. & Zabner, J. 2003. The coxsackie B virus and adenovirus receptor resides in a distinct membrane microdomain. J. Virol. 77(4): 2559–2567.

Awasthi-Kalia, M., Schnetkamp, P. P. & Deans, J. P. 2001. Differential effects of filipin and methyl-beta-cyclodextrin on B cell receptor signaling. Biochem. Biophys. Res. Comm. 287(1): 77–82.

Baker, K. A., Dutch, R. E., Lamb, R. A. & Jardetzky, T. S. 1999. Structural basis for Paramyxovirus-mediated membrane fusion. Mol. Cell 3(3): 309–319.

Baker, K. A., Dutch, R. E., Lamb, R. A. & Jardetzky, T. S. 1999. Structural basis for paramyxovirus-mediated membrane fusion. Mol. Cell 3(3): 309–319.

Bananis, E., Nath, S., Gordon, K., Satir, P., Stockert, R. J., Murray, J. W. & Wolkoff, A. W. 2004. Microtubule-Dependent Movement of Late Endocytic Vesicles In Vitro: Requirements for Dynein and Kinesin. Mol. Biol. Cell 15(8): 3688–3697.

Baravalle, G., Schober, D., Huber, M., Bayer, N., Murphy, R. F., Fuchs, R. 2005. Transferrin recycling and dextran transport to lysosomes is differentially affected by bafilomycin, nocodazole, and low temperature. Cell Tissue Res. 320(1): 99–113.

Barenholz, Y. 2002. Cholesterol and other membrane active sterols: from membrane evolution to ÒraftsÓ. Prog. Lipid Res. 41(1): 1–5.

Barman, S. & Nayak, D. P. 2000. Analysis of the transmembrane domain of influenza virus neuraminidase, a type II transmembrane glycoprotein, for apical sorting and raft association. J. Virol. 74(14): 6538–6545.

Barnett, R. E., Furcht, L. T. & Scott, R. E. 1974. Differences in Membrane Fluidity and Structure in Contact-Inhibited and Transformed Cells. Proc. Natl. Acad. Sci. 71(5): 1992–1994.

Baudhuin, P., Beaufay, H. & de Duve C. Combined biochemical and morphological study of particulate fractions from rat liver: Analysis of preparations enriched in lysosomes or in particles containing urate oxidase, D-amino acid oxidase, and catalase. J. Cell Biol. 26(1): 219-243.

Bauer, M. E. & Tejani-Butt, S. M. 1992. Effects of repeated administration of desipramine or electroconvulsive shock on norepinephrine uptake sites measured by [3H]nisoxetine autoradiography. Brain Res. 582(2): 208–214.

Beguinot, L., Lyall, R. M., Willingham, M. C. & Pastan, I. 1984. Down-regulation of the epidermal growth factor receptor in KB cells is due to receptor internalization and subsequent degradation in lysosomes. Proc. Natl. Acad. Sci. 81(8): 2384–2388.

Belnap, D. M., Filman, D. J., Trus, B. L., Cheng, N., Booy, F. B., Conway, J. F., Curry, S., Hiremath, C. N., Tsang, S. K., Steven, A. C. & Hogle, J. M. 2000. Molecular tectonic model of virus structural transitions: the putative cell entry states of poliovirus. J. Virol. 74(3): 1342–1354.

Berendsen, H. J. C., Postma, J. P. M., van Gunsteren, W. F. & Hermans, J. 1981. Interaction models for water in relation to protein hydration. Intermolecular Forces pp. 331-342 ed. B. Pullman. Reidel, Dordrecht.

Bergelson, J. M., Chan, M., Solomon, K., St John, N. F., Lin, H. & Finberg, R. W. 1994. Decay-accelerating factor (CD55), a glycosylphosphatidylinositol-anchored complement regulatory protein, is a receptor for several echoviruses. Proc. Natl. Acad. Sci. 91(13): 6245–6248.

Berger, O., Edholm, O. & Jähnig, F. 1997. Molecular dynamics simulations of a fluid bilayer of dipalmitoylphosphatidylcholine. Biophys J. 72(5): 2002–2013.

Bondeva, T., Pirola, L., Bulgarelli-Leva, G., Rubio, I., Wetzker, R., Wymann, M. P. 1998. Bifurcation of lipid and protein kinase signals of PI3K to the protein kinases PKB and MAPK. Science 282(5387): 293–296.

Bousarghin, L., Touzé, A., Sizaret, P. Y. & Coursaget, P. 2003. Human papillomavirus types 16, 31, and 58 use different endocytosis pathways to enter cells. J. Virol. 77(6): 3846–3850.

Brügger, B., Krautkrämer, E., Tibroni, N., Munte, C. E., Rauch, S., Leibrecht, I., Glass, B., Breuer, S., Geyer, M., Kräusslich, H. G., Kalbitzer, H. R., Wieland, F. T. & Fackler, O. T. 2007. Human Immunodeficiency Virus Type 1 Nef protein modulates the lipid composition of virions and host cell membrane microdomains. Retrovirology 4:70.

Brabec, M., Baravalle, G., Blaas, D., & Fuchs, R. 2003. Conformational changes, plasma membrane penetration, and infection by human rhinovirus type 2: role of receptors and low pH. J. Virol. 77(9):5370–5377.

Braell, W. A., Schlossman, D. M., Schmid, S. L. & Rothman, J. E. 1984. Dissociation of clathrin coats coupled to the hydrolysis of ATP: role of an uncoating ATPase. J. Cell Biol. 99: 734–741.

Bremer, C. M., Bung, C., Kott, N., Hardt, M. & Glebe, D. 2008. Hepatitis B virus infection is dependent on cholesterol in the viral envelope. Cell. Microbiol. 11(2): 249–260.

Breneman, C. M. & Wiberg, K. B. 1990. Determining atom-centered monopoles from molecular electrostatic potentials. The need for high sampling density in formamide conformational analysis. J. Comp. Chem. 11(3): 361–373.

Bright, N. A., Reaves, B. J., Mullock, B. M., & Luzio, J. P. 1997. Dense core lysosomes can fuse with late endosomes and are reformed from the resultant hybrid organelles. J. Cell Sci. 110(17): 2027–2040.

Bright, N., Gratian, M. & Luzio, J. 2005. Endocytic delivery to lysosomes mediated by concurrent fusion and kissing events in living cells. Curr. Biol. 15(4): 360–365.

Bron, R., Wahlberg, J. M., Garoff, H. & Wilschut, J. 1993. Membrane fusion of Semliki Forest virus in a model system: correlation between fusion kinetics and structural changes in the envelope glycoprotein. EMBO J. 12(2): 693–701.

Brotherus, J. & Renkonen, O. 1977. Subcellular distributions of lipids in cultured BHK cells: evidence for the enrichment of lysobisphosphatidic acid and neutral lipids in lysosomes. J. Lipid Res. 18(2): 191–202

Brown, D.A. & London, E. 1998. Functions of lipid rafts in biological membranes. Annu. Rev. Cell Dev. Biol. 14: 111–136.

Brown, D. A. & Rose, J. K. 1992. Sorting of GPI-anchored proteins to glycolipid-enriched membrane subdomains during transport to the apical cell surface. Cell 68(3): 533–544.

Brown, D. 1994. GPI-anchored proteins and detergent-resistant membrane domains. Braz. J. Med. Biol. Res. 27(2): 309–315.

Butler, J. D., Blanchette-Mackie, J., Goldin, E., O'Neill, R. R. Carstea, G., Roff, C. F., Patterson, M. C., Patel, S., Comly, M. E. & Cooney, A. 1992. Progesterone blocks cholesterol translocation from lysosomes. J. Biol. Chem. 267(33): 23797–23805.

Bär, S., Daeffler, L., Rommelaere, J., Nüesch, J. P. F. 2008. Vesicular egress of non-enveloped lytic parvoviruses depends on gelsolin functioning. PLoS Pathog. 4(8): e1000126.

Callaghan, P. T. 1977. The use of 13C spin relaxation to investigate molecular motion in liquid tristearin. 19(1): 56–73.

Canaan, S., Zádori, Z., Ghomashchi, F., Bollinger, J., Sadilek, M., Moreau, M. E., Tijssen, P. & Gelb, M. H., 2004. Interfacial enzymology of parvovirus phospholipases A2. J. Biol. Chem. 279(15): 14502–14508.

Canonico, P. G. & Bird, J. W. C. 1969. The use of acridine orange as a lysosomal marker in rat skeletal muscle cells. J. Cell Biol. 43(2): 367–371.

Chachaty, C., Rainteau, D., Tessier, C., Quinn, P. J. & Wolf, C. 2005. Building Up of the Liquid-Ordered Phase Formed by Sphingomyelin and Cholesterol. Biophys. J. 88(6): 4032–4044.

Chapman, M. S. & Rossmann, M. G. 1993. Structure, sequence and function correlations among parvoviruses. Virology 94(2): 491–508.

Chapman, M. S.Ê& Rossmann, M. G., 1993. Structure, sequence and function correlations among parvoviruses. Virology 194(2): 491–508.

Chatterjee, S. & Mayor, S. 2001. The GPI-anchor and protein sorting. Cell. Mol. Life Sci. 58(14):1969–1987.

Chemello, M. E., Aristimuño, O. C., Michelangeli, F. & Ruiz, M. C. 2002. Requirement for vacuolar H+-ATPase activity and Ca2+ gradient during entry of rotavirus into MA104 cells.

Chen, W., Feng, Y., Chen, D. & Wandinger-Ness, A. 1998. Rab11 is required for trans-Golgi networkÐtoÐplasma membrane transport and a preferential target for GDP dissociation inhibitor. Mol. Biol. Cell 9(11): 3241–3257.

Chiu, S.-W., Clark, M., Balaji, V., Subramaniam, S., Scott, H. L. & Jakobsson, E. 1995. Incorporation of surface tension into molecular dynamics simulation of an interface: a fluid phase lipid bilayer membrane. Biophys. J. 69(4): 1230–1245.

Christoforidis, S., McBride, H. M., Burgoyne, R. D. & Zerial, M. 1999. The Rab5 effector EEA1 is a core component of endosome docking. Nature 397(6720): 621–625.

Clemente, R., de Parseval, A., Perez, M., & de la Torre, J. C. 2009. Borna Disease Virus requires cholesterol in both cellular membrane and viral envelope for efficient cell entry. J. Virol. doi:10.1128/JVI.02206-08 (published electronically ahead of print)

Cohen, S. & Panté, N. 2005. Pushing the envelope: microinjection of Minute virus of mice into Xenopus oocytes causes damage to the nuclear envelope. J. Gen. Virol. 86(12): 3243–3252.

Conibear, E. 2002. An ESCRT into the endosome. Mol. Cell 10(2): 215–216.

Conner, S. D. & Schmid, S. L. 2003. Regulated portals of entry into the cell. Nature 422(6927): 37–44.

Cotmore, S. F. & Tattersall, P. 1987. The autonomously replicating parvoviruses of vertebrates. Adv. Virus Res. 33: 91–169.

Cotmore, S. F., Dábramo, A. M., Ticknor, C. M. & Tattersall, P. 1999. Controlled conformational transitions in the MVM virion expose the VP1 N-terminus and viral genome without particle disassembly. Virology 254(1): 169–181.

Cotten, M. & Weber, J. M. 1995. The adenovirus protease is required for virus entry into host cells. Virology 213(2): 494–502.

Cox, B. E., Griffin, E. E., Ullery, J. C. & Jerome, W. G. 2007. Effects of cellular cholesterol loading on macrophage foam cell lysosome acidification. J. Lipid Res.48(5): 1012-1021.

Cullis, P. R., Hope, M. J. & Tilcock, C. P. S. Lipid polymorphism and the roles of lipids in membranes. Chem. Phys. Lipids 40(2-4):127–144.

Daro, E., van der Sluijs, P., Galli, T. & Mellman, I. 1996. Rab4 and cellubrevin define different early endosome populations on the pathway of transferrin receptor recycling. Proc. Natl. Acad. Sci. 93(18): 9559–9564.

Daura, X., Oliva, B., Querol, E., Avilés, F. X. & Tapia, O. 1996. On the sensitivity of MD trajectories to Changes in Water-Protein Interaction Parameters: The Potato Carboxypeptidase Inhibitor in Water as a Test Case for the GROMOS force field. Proteins 25(1): 89–103.

de Duve, C., Pressman, B. C., Gianetto, R., Wattiaux, R. & Appelmans, F. 1955. Tissue fractionation studies. 6. Intracellular distribution patterns of enzymes in rat liver tissue. Biochem J. 60(4): 604–617.

de Meyer, F. & Smit, B. 2009. Effect of cholesterol on the structure of a phospholipid bilayer. Proc. Natl. Acad. Sci. 106(10): 3654–3658.

Delmas, O., Breton, M., Sapin, C., Le Bivic, A., Colard, O. & Trugnan, G. 2007. Heterogeneity of raft-type membrane microdomains associated with VP4, the rotavirus spike protein, in Caco-2 and MA 104 cells. J. Virol. 81(4): 1610–1618.

Delton-Vandenbroucke, I., Bouvier, J., Makino, A., Besson, N., Pageaux, J. P., Lagarde, M. & Kobayashi, T. 2007. Anti-bis(monoacylglycero)phosphate antibody accumulates acetylated LDL-derived cholesterol in cultured macrophages. J. Lipid Res. 48(3): 543–552.

Dietrich, C., Bagatolli, L. A., Volovyk, Z. N., Thompson, N.L., Levi, M., Jacobson, K. & Gratton, E. 2001. Lipid rafts reconstituted in model membranes. Biophys. J. 80(3): 1417–1428.

Dietrich, C., Yang, B., Fujiwara, T., Kusumi, A & Jacobson, K. 2002. Relationship of lipid rafts to transient confinement zones detected by single particle tracking. Biophys. J. 82(1) 274–284.

Doms, R. W., Helenius, A. & White, J. 1985. Membrane fusion activity of the influenza virus hemagglutinin. The low pH-induced conformational change. J. Biol. Chem. 260(5): 2973–2981.

Dufourc, E. J., Parish, E. J., Chitrakorn, S & Smith, I. C. P. 1984. Structural and dynamical details of cholesterol-lipid interaction as revealed by deuterium NMR. Biochemistry, 23(25): 6062–6071.

Duncan, R., Chen, Z., Walsh, S. & Wu, S. 1996. Avian reovirus-induced syncytium formation is independent of infectious progeny virus production and enhances the rate, but is not essential, for virus-induced cytopathology and virus egress. Virology 224(2): 453–464.

Dunn, K. W. & Maxfield, F. R. 1992. Delivery of ligands from sorting endosomes to late endosomes occurs by maturation of sorting endosomes. J. Cell Biol. 117(2): 301–310.

Duwe, H. P., Kaes, J. & Sackmann, E. 1990. Bending elastic moduli of lipid bilayers: modulation by solutes. J. Phys. France 51: 945–962.

Eisensamer, B., Uhr, M., Meyr, S., Gimpl, G., Deiml, T., Rammes, G., Lambert, J. J., Zieglgängsberger, W., Holsboer, F. & Rupprecht, R. 2005. Antidepressants and antipsychotic drugs colocalize with 5-HT3 receptors in raft-like domains. J. Neurosci. 25(44): 10198–10206

Endress, E., Bayerl, S., Prechtel, K., Maier, C., Merkel, R. & Bayerl, T. M. 2002. The effect of cholesterol, lanosterol, and ergosterol on lecithin bilayer mechanical properties at molecular and microscopic dimensions: a solid-state NMR and micropipet study. Langmuir 18(8): 3293–3299.

Engelman, D. M. 2005. Membranes are more mosaic than fluid. Nature 438: 578-580.

Eskelinen, E. L. 2006. Roles of LAMP-1 and LAMP-2 in lysosome biogenesis and autophagy. Mol. Aspects Med. 27(5-6): 95Ð502.

Eskelinen, E. L., Tanaka, Y. & Saftig, P. 2003. At the acidic edge: emerging functions for lysosomal membrane proteins. Trends Cell Biol. 13(3): 137–145.

Eskelinen, E. L., Schmidt, C. K., Neu, S., Willenborg, M., Fuertes, G., Salvador, N., Tanaka, Y., Lüllmann-Rauch, R., Hartmann, D., Heeren, J., von Figura, K., Knecht, E. & Saftig, P. 2004. Disturbed cholesterol traffic but normal proteolytic function in LAMP-1/LAMP-2 double-deficient fibroblasts. Mol. Biol. Cell 15(7): 3132–3145.

Essner, E. & Novikoff, A. B. 1961. Localization of acid phosphatase activity in hepatic lysosomes by means of electron microscopy. J. Biophys. Biochem. Cytol. 9(4): 773–784.

Fackler, O. T., Luo, W., Geyer, M., Alberts, A. S. & Peterlin, B. M. 1999. Activation of Vav by Nef induces cytoskeletal rearrangements and downstream effector functions. Mol. Cell 3(6): 729–739.

Fahy, E., Subramaniam, S., Brown, H.A., Glass, C.K., Merrill, A.H., Murphy, R.C., Raetz, C.R.H., Russell, D.W., Seyama, Y., Shaw, W., Shimizu, T., Spener, F., van Meer, G., VanNieuwenhze, M.S., White, S.H., Witztum, J.L. & Dennis, E.A. 2005. A comprehensive classification system for lipids. J. Lipid Res. 46(5): 839–861.

Falck, E., Patra, M., Karttunen, M., Hyvonen, M. T. & Vattulainen, I. 2004. Lessons of slicing membranes: interplay of packing, free area, and lateral diffusion in phospholipid / cholesterol bilayers. Biophys. J. 87(2): 1076–1091.

Farr, G. A., Cotmore, S. F. & Tattersall, P. 2006. VP2 cleavage and the leucine ring at the base of the fivefold cylinder control pH-dependent externalization of both the VP1 N-terminus and the genome of minute virus of mice. J. Virol. 80(1): 161–171.

Favoreel, H. W., Minnebruggen, G. W., Adriaensen, D. & Nauwynck, H. J. 2005. Cytoskeletal rearrangements and cell extensions induced by the US3 kinase of an alphaherpesvirus are associated with enhanced spread. Proc. Natl. Acad. Sci. 102(25): 8990–8995.

Feng, Y., Press, B. & Wandinger-Ness, A. 1995. Rab 7: an important regulator of late endocytic membrane traffic. J. Cell Biol. 131(6): 1435–1452.

Fili, N.,Calleja, V., Woscholski, R., Parker, P. J. & Larijani, B. 2006. Compartmental signal modulation: Endosomal phosphatidylinositol 3-phosphate controls endosome morphology and selective cargo sorting. Proc. Natl. Acad. Sci. 103(42): 15473–15478.

Finkelstein, A. 1976. Water and nonelectrolyte permeability of lipid bilayer membranes. J. Gen. Physiol. 68(2): 127–135.

Finnegan, C. M., Rawat, S. S., Puri, A., Wang, J. M., Ruscetti, F. W. & Blumenthal, R. 2004. Ceramide, a target for antiretroviral therapy. Proc. Natl. Acad. Sci. 101(43): 15452–15457.

Fleming, D. M. 2001. Managing influenza: amantadine, rimantadine and beyond. Int. J. Clin. Pract. 55(3): 189–195.

Fleming, E. H., Kolokoltsov, A. A., Davey, R. A., Nichols, J. E. & Roberts Jr., N. J. 2006. Respiratory syncytial virus F envelope protein associates with lipid rafts without a requirement for other virus proteins. J. Virol. 80(24): 12160–12170.

Forzan, M., Wirblich, C. & Roy, P. 2004. A capsid protein of nonenveloped Bluetongue virus exhibits membrane fusion activity. Proc. Natl. Acad. Sci. 101(7): 2100–2105.

Fra, A. M., Masserini, M., Palestini, P., Sonnino, S. & Simons, K. 1995. A photoreactive derivative of ganglioside GM1 specifically cross-links VIP21-caveolin on the cell surface. FEBS Lett. 375(1-2): 11-14.

Franks, N.P. 1976. Structural analysis of hydrated egg lecithin and cholesterol bilayers I. X-ray diffraction. J. Mol. Biol. 100(3): 345–358

Frisch, M. J., Trucks, G. W., Schlegel, H. B., Scuseria, G. E., Robb, M. A., Cheeseman, J. R. Montgomery, Jr., J. A., Vreven, T., Kudin, K. N., Burant, J. C., Millam, J. M., Iyengar, S. S., Tomasi, J., Barone, V., Mennucci, B., Cossi, M., Scalmani, G., Rega, N., Petersson, G. A., Nakatsuji, H., Hada, M., Ehara, M., Toyota, K., Fukuda, R., Hasegawa, J., Ishida, M., Nakajima, T., Honda, Y., Kitao, O., Nakai, H., Klene, M., Li, X., Knox, J. E., Hratchian, H. P., Cross, J. B., Bakken, V., Adamo, C., Jaramillo, J., Gomperts, R., Stratmann, R. E., Yazyev, O., Austin, A. J., Cammi, R., Pomelli, C., Ochterski, J. W., Ayala, P. Y., Morokuma, K., Voth, G. A., Salvador, P., Dannenberg, J. J., Zakrzewski, V. G., Dapprich, S., Daniels, A. D., Strain, M. C., Farkas, O., Malick, D. K., Rabuck, A. D., Raghavachari, K., Foresman, J. B., Ortiz, J. V., Cui, Q., Baboul, A. G., Clifford, S., Cioslowski, J.,

Stefanov, B. B., Liu, G., Liashenko, A., Piskorz, P., Komaromi, I., Martin, R. L., Fox, D. J., Keith, T., Al-Laham, M. A., Peng, C. Y., Nanayakkara, A., Challacombe, M., Gill, P. M. W., Johnson, B., Chen, W., Wong, M. W., Gonzalez, J., & Pople, J. A. 2004. Gaussian 03, Revision D.02. Gaussian, Inc., Wallingford, CT.

Futerman, A.H. & Hannun, Y.A. 2004. The complex life of simple sphingolipids. EMBO Reports 5(8): 777–782.

Futerman, A. F. & van Meer, G. 2004. The cell biology of lysosomal storage disorders. Nat. Rev. Mol. Cell Biol. 5(7):554–565.

Gagescu, R., Demaurex, N., Parton, R. G., Hunziker, W., Huber, L. A. & Gruenberg, J. 2000. The Recycling endosome of Madin-Darby Canine Kidney cells is a mildly acidic compartment rich in raft components. Mol. Biol. Cell 11(8): 2775–2791.

Gallo, S. A., Finnegan, C. M., Viard, M., Raviv, Y., Dimitrov, A., Rawat, S. S., Puri, A., Durell, S. & Blumenthal, R. 2003. The HIV Env-mediated fusion reaction. Biochim. Biophys. Acta 1614(1): 36–50.

Ganley, I. G. & Pfeffer, S. R. 2006. Cholesterol accumulation sequesters Rab9 and disrupts late endosome function in NPC1-deficient cells. J. Biol. Chem. 281(26): 17890–17899.

Garrett, W. S., Chen, L. M., Kroschewski, R., Ebersold, M., Turley, S., Trombetta, S., Galán, J. E. & Mellman, I. 2000. Developmental Control of Endocytosis in Dendritic Cells by Cdc42. Cell 102(3): 325–334.

Gennis, R.B. Biomembranes. Molecular Structure and Function. In: Cantor, C.R. (ed.) Springer Advanced Texts in Chemistry. Springer Verlag New York Inc. 1989.

Genz, A., Holzwarth, J. F. & Tsong, T. Y. 1986. The influence of cholesterol on the main phase transition of unilamellar dipalmytoylphosphatidylcholine vesicles. A differential scanning calorimetry and iodine laser T-jump study. Biophys. J. 50(6): 1043–1051.

Gidwani, A., Brown, H. A. Holowka, D. & Baird, B. 2003. Disruption of lipid order by short-chain ceramides correlates with inhibition of phospholipase D and downstream signaling by FcϵRI. J. Cell Sci. 116(15): 3177–3187.

Gilbert, J. & Benjamin, T. 2004. Uptake pathway of polyomavirus via ganglioside GD1a. J. Virol. 78(22): 12259–12267.

Gillooly, D. J., Morrow, I. C., Lindsay, M., Gould, R., Bryant, N. J., Gaullier, J. M., Parton, R. G. & Stenmark, H. 2000. Localization of phosphatidylinositol 3-phosphate in yeast and mammalian cells. EMBO J. 19(17): 4577–4588

Goetzl, E.J., Kong, Y. & Mei, B. 1999. Lysophosphatidic acid and sphingosine 1-phosphate protection of T cells from apoptosis in association with suppression of Bax1. J. Immunol. 162: 2049–2056.

Goren, M. B., Swendsen, C. L., Fiscus, J. & Miranti, C. 1984. Fluorescent markers for studying phagosome-lysosome fusion. J. Leuk. Biol. 36(3): 273–292.

Graham, D. R. M., Chertova, E., Hilburn, J. M., Arthur, L. O. & Hildreth, J. E. K. 2003. Cholesterol depletion of human immunodeficiency virus type 1 and simian immunodeficiency virus with β-cyclodextrin inactivates and permeabilizes the virions: evidence for virion-associated lipid rafts. J. Virol. 77(15): 8237–8248.

Gri, G., Molona, B., Manes, S., Pozzana, T. & Viola, A. 2004. The inner side of T cell lipid rafts. Immunol. Letters 94(3): 247–252.

Gruenberg, J. & Stenmark, H. 2004. The biogenesis of multivesicular endosomes. Nat. Rev. Mol. Cell Biol. 5(4): 317–323.

Gruenberg, J. 2001. The endocytic pathway: a mosaic of domains. Nat. Rev. Mol. Cell Biol. 2(10): 721–730.

Gruenberg, J. 2003. Lipids in endocytic membrane transport and sorting. Curr. Opin. Cell Biol. 15(4): 382–388.

Gruenberg, J., Griffiths, G. & Howell, K. E. 1989. Characterization of the early endosome and putative endocytic carrier vesicles in vivo and with an assay of vesicle fusion in vitro. J. Cell Biol. 108: 1301–1316.

Höltje, M., Förster, T., Brandt, B., Engels, T., von Rybinski, W. & Höltje, H.-D. 2001. Molecular dynamics simulations of stratum corneum lipid models: fatty acids and cholesterol. Biochim. Biophys. Acta 1511(1): 156–167.

Hall, A., Repakova, J., & Vattulainen, I. 2008. Modeling of the triglyceride-rich core in lipoprotein particles. J. Phys. Chem. B 112(44): 13772–13782.

Hamilton, J. A. & Small, D. M. 1981. Solubilization and localization of triolein in phosphatidylcholine bilayers: a 13C NMR study. Proc. Natl. Acad. Sci. 78(11): 6878–6882.

Hancock, J. F. 2006. Lipid rafts: contentious only from simplistic standpoints. Nat. Rev. Mol. Cell. Biol. 6(7): 456–462.

Harder, T., Kellner, R., Parton, R. G. & Gruenberg, J. 1997. Specific release of membrane-bound Annexin II and cortical cytoskeletal elements by sequestration of membrane cholesterol. Mol. Biol. Cell 8(3): 533–545.

Harder, T., Scheiffele, P., Verkade, P. & Simons, K. 1998. Lipid domain structure of the plasma membrane revealed by patching of membrane components. J. Cell Biol. 141(4): 929–942.

Hauser, H. & Poupart, G. 2005 In: Yeagle, P.L. (ed.) The Structure of Biological membranes. CRC Press Boca Raton, FL.

Heeren, J. & Beisiegel, U. 2001. Intracellular metabolism of triglyceride-rich lipoproteins. Curr. Opin. Lipidol. 12(3): 255–260.

Heeren, J., Weber, W. & Beisiegel, U. 1999. Intracellular processing of endocytosed triglyceride-rich lipoproteins comprises both recycling and degradation. J. Cell Sci. 112(3): 349–359.

Heerklotz, H. 2002. Triton promotes domain formation in lipid raft mixtures. Biophys. J. 83(5): 2693–2701.

Heimburg, T. 1998. Mechanical aspects of membrane thermodynamics. Estimation of the mechanical properties of lipid membranes close to the chain melting transition from calorimetry. Biochim. Biophys. Acta 1415(1): 147–162.

Heimburg, T. 2000. A Model for the Lipid Pretransition: Coupling of Ripple Formation with the Chain-Melting Transition. Biophys. J. 78(3): 1154–1165.

Helenius, A., Kartenbeck, J., Simons, K. & Fries, E. 1980. On the entry of semliki forest virus into BHK-21 cells. J. Cell Biol. 84(2): 404–420.

Helenius, A., Marsh, M. & White, J. 1982. Inhibition of semliki forest virus penetration by lysosomotropic weak bases. J. Gen. Virol. 58(1): 47–61.

Henriksen, J., Rowat, A. C. & Ipsen, J. H. 2004. Vesicle fluctuation analysis of the effects of sterols on membrane bending rigidity. Eur. Biophys J. 33(8): 732–741.

Henriksen, J., Rowat, A.C., Brief, E., Hsueh, Y.W., Thewalt, J.L., Zuckermann, M.J. & Ipsen, J.H. 2006. Universal Behavior of Membranes with Sterols. Biophys. J. 90(5): 1639Ð1649.

Hepbildikler, S. T., Sandhoff, R., Kölzer, M., Proia, R. L. & Sandhoff, K. 2002. Physiological substrates for human lysosomal β -hexosaminidase S. J. Biol. Chem. 277(4): 2562–2572.

Herbst, J. J., Opresko, L. K., Walsh, B. J., Lauffenburger, D. A. & Wiley, H. S. 1994. Regulation of postendocytic trafficking of the epidermal growth factor receptor through endosomal retention. J. Biol. Chem. 269(17): 12865–12873.

Hinshaw, J. E. & Schmid, S. L. 1995. Dynamin self-assembles into rings suggesting a mechanism for coated vesicle budding. Nature 374(6518): 190–192.

Hofsä, C., Lindahl, E. & Edholm, O. 2003. Molecular Dynamics Simulations of Phospholipid Bilayers with Cholesterol. Biophys. J. 84(4): 2192–2206.

Honegger, U. E., Roscher, A. A. & Wiesmann, U. N. 1983. Evidence for lysosomotropic action of desipramine in cultured human fibroblasts. J. Pharmacol. Exp. Ther. 225(2): 436–441.

Hoover, W. G. 1985. Canonical dynamics: equilibrium phase-space distributions. Phys. Rev. A 31(3): 1695–1697.

Hopkins, C. R., Gibson, A., Shipman, M. & Miller, K. 1990. Movement of internalized ligand-receptor complexes along a continuous endosomal reticulum. Nature 346(6282): 335–339.

Huang, H., Li, Y., Sadaoka, T., Tang, H., Yamamoto, T., Yamanishi, K. & Mori, Y. 2006. Human herpesvirus 6 envelope cholesterol is required for virus entry. J Gen. Virol. 87(2): 277–285.

Hunziker, W. & Peters, P. J. 1998. Rab17 Localizes to recycling endosomes and regulates receptor-mediated transcytosis in epithelial cells. J. Biol Chem. 273(25): 15734–15741.

Ikonen E. 2001. Roles of lipid rafts in membrane transport. Curr. Opin. Cell Biol. 13(4): 470–477.

Ikonomov, O. C., Sbrissa, D., Mlak, K., Kanzaki, M., Pessin, J. & Shisheva, A. 2002. Functional dissection of lipid and protein kinase signals of PIKfyve reveals the role of PtdIns 3,5-P2 production for endomembrane integrity. J. Biol. Chem. 277(11): 9206–9211.

Imhoff, H., von Messling, V., Herrler, G. & Haas, L. 2007. Canine Distemper virus infection requires cholesterol in the viral envelope. J. Virol. 81(8): 4158–4165.

Inoue, T. Kitahashi, T. & Nibu, Y. 1999. Phase behavior of hydrated bilayer of binary phospholipid mixtures composed of 1,2-distearoylphosphatidylcholine and 1-stearoyl-2-oleoylphosphatidylcholine or 1-oleoyl-2-stearoylphosphatidylcholine. Chem. Phys. Lipids 99(1):103–109.

Ipsen, J.H., Karlström, G., Mouritsen, O.G., Wennerström, H., & Zuckermann, M.J. 1987. Phase equilibria in the phosphatidylcholine-cholesterol system. Biochim. Biophys. Acta 905(1): 162–172.

Ipsen, J. H., Jørgensen, K. & Mouritsen, O. G. 1990. Density fluctuations in saturated phospholipid bilayers increase as the acyl-chain length decreases. Biophys. J. 58(5): 1099-1107.

lpsen, J. H., Mouritsen, O. G. & Bloom, M. 1990. Relationships between lipid membrane area, hydrophobic thickness and acyl-chain orientational order. The effects of cholesterol. Biophys. J. 57(3): 405–412.

Israelachvili, J. 1992. Intermolecular & Surface Forces. Academic Press, London.

Israelachvili, J.N., Mitchell, D.J. & Ninham, B.W. 1976. Theory of self-assembly of hydrocarbon amphiphiles into micelles and bilayers. J. Chem. Soc. Faraday Trans. 72: 1525–1568.

Ivanovic, T., Agosto, M. A., Zhang, L., Chandran, K., Harrison, S. E., & Nibert, M. L. 2008. Peptides released from reovirus outer capsid form membrane pores that recruit virus particles. EMBO J. 27(8) 1289–1298.

Izagirre, U., Angulo, E., Wade, S. C., ap Gwynn, I. & Marigómez, I. 2009. Beta-glucuronidase and hexosaminidase are marker enzymes for different compartments of the endo-lysosomal system in mussel digestive cells. Cell Tissue Res. 335(2): 441-454.

Jørgensen, K., Ipsen, J. H., Mouritsen, O. G., Bennett, D. & Zuckermann, M. J. 1991. A general model for the interaction of foreign molecules with lipid membranes: drugs and anaesthetics.

Jacobson, K., Mouritsen, O. G. & Anderson, R. G. W. 2007. Lipid rafts: at a crossroad between cell biology and physics. Nature Cell Biology 9(1): 7–14.

Janes, P. W., Ley, S. C., Magee, A. I. & Kabouridis, P. S. 2000. The role of lipid rafts in T cell antigen receptor (TCR) signalling. Semin. Immunol. 12(1): 23–34.

Janiak, M. J., Small, D. M. & Shipley, G. G. 1976. Nature of the thermal pretransition of synthetic phospholipids: dimyristoyl- and dipalmitoyllecithin. Biochemistry15(21): 4575–4580.

Janiak, M. J., Small, D. M. & Shipley, G. G. 1979. Temperature and compositional dependence of the structure of hydrated dimyristoyl lecithin. J. Biol. Chem. 254(13): 6068-6078.

Jayanthi, L. D., Samuvel, D. J. & Ramamoorthy, S. 2004. Regulated internalization and phosphorylation of the native norepinephrine transporter in response to phorbol esters. J. Biol. Chem. 279(18): 19315–19326.

Jerome, W. G., Casha, C., Webber, R., Horton, R. & Yancey, P. G. 1998. Lysosomal lipid accumulation from oxidized low density lipoprotein is correlated with hypertrophy of the Golgi apparatus and trans-Golgi network. J. Lipid Res. 39(7): 1362–1371.

Jerome, W. G., Cox, B. E., Griffin, E. E. & Ullery, J. C. 2008. Lysosomal cholesterol accumulation inhibits subsequent hydrolysis of lipoprotein cholesteryl ester. Microscopy Microanal.14(2): 138–149.

Jin, M., Sahagian , G. G. Jr. & Snider, M. D. 1989. Transport of surface mannose 6-phosphate receptor to the Golgi complex in cultured human cells. J. Biol. Chem. 264(13): 7675-7680.

Jin L., Millard, A. C., Wuskell, J. P., Dong, X., Wu, D., Clark, H. A. & Loew, L. M. 2006. Characterization and application of a new optical probe for membrane lipid domains. Biophys. J. 90(7): 2563-2575

Jost, M., Simpson, F., Kavran, J. M., Lemmon, M. A. & Schmid, S. L. 1998. Phosphatidylinositol-4,5-bisphosphate is required for endocytic coated vesicle formation. Curr. Biol. 8(25):1399–1402.

Kamata, K., Manno, S., Ozaki, M. & Takakuwa, Y. 2008. Functional evidence for presence of lipid rafts in erythrocyte membranes: Gsα in rafts is essential for signal transduction. Am. J. Hematol. 83(5):371–375.

Kartenbeck, J., Stukenbrok, H. & Helenius, A. 1989. Endocytosis of simian virus 40 into the endoplasmic reticulum. J. Cell Biol. 109(6): 2721–2729.

Kavalenka, A. A., Filipic, B., Hemminga, M. A. & Strancar, J. 2005. Speeding up a genetic algorithm for EPR-based spin label characterization of biosystem complexity. J. Chem. Inf. Model 45(6): 1628–1635

Kielian, M. & Rey, F. A. 2006. Virus membrane-fusion proteins: more than one way to make a hairpin. Nat. Rev. Microbiol. 4(1): 67–76.

Kielian M. 2006. Class II virus membrane fusion proteins. Virology 344(1): 38–47.

Kim, D. S., Jeong, S. K., Kim, H. R., Kim, D. S., Chae, S. W. & Chae, H. J. 2007. Effects of triglyceride on ER stress and insulin resistance. Biochem. Biophys. Res. Commun. 363(1): 140–145

Klingenstein, R., Löber, S., Kujala, P., Godsave, S., Leliveld, S. R., Gmeiner, P., Peters, P. J. & Korth, C. 2006. Tricyclic antidepressants, quinacrine and a novel, synthetic chimera thereof clear prions by destabilizing detergent-resistant membrane compartments. J. Neurochem. 98(3): 748–759.

Klumperman, J., Hille, A., Veenendaal, T., Oorschot, T., Stoorvogel, W., von Figura, K. & Geuze, H. J. 1993. Differences in the Endosomal Distributions of the Two Mannose 6-Phosphate Receptors. J. Cell Biol. 121(5): 997-1010.

Kobayashi, T., Stang, E., Fang, K. S., de Moerloose, P., Parton, R. G. & Gruenberg, J. 1998. A lipid associated with the antiphospholipid syndrome regulates endosome structure and function. Nature 392(6672): 193–197.

Kobayashi, T., Gu, F. & Gruenberg, J. 1998. Lipids, lipid domains and lipidÐprotein interactions in endocytic membrane traffic. Semin. Cell Dev. Biol. 9(5):517-26.

Kobayashi, T., Beuchat, H. M., Lindsay, M., Frias, S., Palmiter, R. D., Sakuraba, H., Parton, R. G. & Gruenberg, J. 1999. Late endosomal membranes rich in lysobisphosphatidic acid regulate cholesterol transport. Nat. Cell Biol. 1(2): 113–118.

Kobayashi, T., Beuchat, M. H., Chevallier, J., Makino, J., Mayran, N., Escola, J. M., Lebrand, C., Cosson, P., Kobayashi, T. & Gruenberg, J. 2002. Separation and characterization of late endosomal membrane domains. J. Biol. Chem. 277(35): 32157–32164.

Kolesnikova, L., Bohil, A. P., Cheney, R. E. & Becker, S. 2006. Budding of Marburgvirus is associated with filopodia. Cell. Microbiol. 9(4): 939–951.

Kornfeld, S.Ê& Mellman, I. 1989. The biogenesis of lysosomes. Annu. Rev. Cell Biol. 5: 483–525.

Koynova, R. & Caffrey, M. 1998. Phases and phase transitions of the phosphatidylcholines. Biochim. Biophys. Acta 1376(1): 91–145.

Krautkrämer, E. & Zeier, M. 2008. Hantavirus causing hemorrhagic fever with renal syndrome enters from the apical surface and requires decay-accelerating factor (DAF/CD55). J. Virol. 82(9): 4257–4264.

Kučerka, N., Perlmutter, J. D., Pan, J., Tristram-Nagle, S., Katsaras, J.& Sachs, J. N. 2008. The Effect of Cholesterol on Short- and Long-Chain Monounsaturated Lipid Bilayers as Determined by Molecular Dynamics Simulations and X-Ray Scattering. Biophys. J. 95(6): 2792–2805.

Kundra, R. & Kornfeld, S. 1999. Asparagine-linked oligosaccharides protect Lamp-1 and Lamp-2 from intracellular proteolysis. J Biol. Chem. 274(43): 31039–31046.

Löffler, B. M., Hesse, B. & Kunze, H. 1984. A combined assay of three lysosomal marker enzymes: Acid phosphatase, ?-glucuronidase, and ?-N-acetylhexosaminidase. Anal. Biochem. 142(2): 312–316.

Laakkonen, P., Auvinen, P., Kujala, P. & Kääriäinen, L. 1998. Alphavirus replicase protein NSP1 induces filopodia and rearrangement of actin filaments. J. Virol. 72(12): 10265–10269.

Lakowicz, J. R. 2006. Principles of Fluorescence Spectroscopy. Springer Science+Business Media, LLC. NY, USA.

Lalezari, J. P., Henry, K., OÕHearn, M., Montaner, J. S. G., Piliero, P. J., Trottier, B., Walmsley, S., Cohen, C., Kuritzkes, D. R., Eron, J. R. Jr., Chung, J., DeMasi, R., Donatacci, L. Drobnes, C., Delehanty, J., & Salgo, M. 2003. Enfuvirtide, an HIV-1 fusion inhibitor, for drug-resistant HIV infection in north and south america. N. Engl. J. Med. 348(22): 2175–2185.

Lande, M. B., Donovan, J. M. & Zeidel, M. L. 1995. The relationship between membrane fluidity and permeabilities to

Lange, Y., Swaisgood, M.H., Ramos, B.V. & Steck, T.L. 1989. Plasma membranes contain half the phospholipid and 90% of the cholesterol and sphingomyelin in cultured human fibroblasts. J. Biol. Chem. 264(7): 3786–3793.

Lange, Y., Ye, J. & Chin, J. 1997. The fate of cholesterol exiting lysosomes. J. Biol. Chem. 272(27): 17018–17022.

Lange, Y., Ye, J., Rigney, M. & Steck, T. 2000. Cholesterol movement in Niemann-Pick type C cells and in cells treated with amphiphiles. J. Biol. Chem. 275(23): 17468–17475.

Lange, Y., Ye, J., Rigney, M and Steck, T. L. 2002. Dynamics of lysosomal cholesterol in Niemann-Pick type C and normal human fibroblasts. J. Lipid Res. 43(2): 198–204.

Lavillette, D., Bartosch, B., Nourrisson, D. Verney, G., Cosset, F. L., Penin, F. & Pécheur, E. I. 2006. Hepatitis C virus glycoproteins mediate low pH-dependent membrane fusion with liposomes. J. Biol. Chem. 281(7): 3909.-3917.

Lebrand, C., Corti, M., Goodson, H., Cosson, P., Cavalli, V., Mayran, N., Fauré, J. & Gruenberg, J. 2002. Late endosome motility depends on lipids via the small GTPase Rab7. EMBO J. 21(6): 1289–1300.

Lee, Y. C., Zheng, Y. O., Taraschi, T. F. & Janes, N. 1996. Hydrophobic alkyl headgroups strongly promote membrane curvature and violate the headgroup volume correlation due to headgroup insertion. Biochemistry 35(12): 3677–3684.

Legler, D. L., Doucey, M. A., Schneider, P., Chapatte, P., Bender, F. C. & Bron, C. 2005. Differential insertion of GPI-anchored GFPs into lipid rafts of live cells. FASEB J. 19(1):73–75.

Lemieux, B., Percival, M. D. & Falgueyret, J. P. 2004. Quantitation of the lysosomotropic character of cationic amphiphilic drugs using the fluorescent basic amine Red DND-99. Anal. Biochem. 327(2): 247–251.

Leuzinger, H., Ziegler, U., Schraner, E. M., Fraefel, C., Glauser, D. L., Heid, I., Ackermann, M., Mueller, M. & Wild, P. 2005. Herpes Simplex Virus 1 envelopment follows two diverse pathways. J. Virol. 79(20): 13047–13059.

Leventis, R. & Silvius, J.R. 2001. Use of cyclodextrins to monitor transbilayer movement and differential lipid affinities of cholesterol. Biophys. J. 81(4): 2257 – 2267.

Lewis, R. N. A. H., Mak, N. & McElhaney, R. N. 1987. A differential scanning calorimetric study of the thermotropic phase behavior of model membranes composed of phosphatidylcholines containing linear saturated fatty acyl chains. Biochemistry26(19): 6118–6126.

Lewis, R. N. A. H., Sykes, B. D. & McElhaney, R. N. 1988. Thermotropic phase behavior of model membranes composed of phosphatidylcholines containing cis-monounsaturated acyl chain homologs of oleic acid: differential scanning calorimetric and phosphorus-31 NMR spectroscopic studies. Biochemistry 27(3): 880-887.

Li, S., Couet, J. & Lisanti, M. P. Src tyrosine kinases, G subunits, and H-Ras share a common membrane-anchored scaffolding protein, caveolin. Caveolin binding

negatively regulates the autoactivation of Src tyrosine kinases. J. Biol. Chem. 271(46): 29182–29190.

Liao, G., Yao, Y., Liu, J., Yu, Z., Cheung, S., Xie, A., Liang, X. & Bi, X. 2007. Cholesterol accumulation is associated with lysosomal dysfunction and autophagic stress in Npc1-/- mouse brain. Am. J. Pathol. 171(3): 962–975.

Lichtenberg, D., Goñi, F. & Heerklotz, H. 2005. Detergent-resistant membranes should not be identified with membrane rafts. Trends Biochem. Sci. 30(8): 430–436.

Lindahl, E., Hess, B., & van der Spoel, D. 2001. GROMACS 3.0: A package for molecular simulation and trajectory analysis. J. Mol. Mod. 7(8): 306–317.

Lindblom, G., Johansson, L. B. A & Arvidson, G. 1981. Effect of cholesterol in membranes. Pulsed nuclear magnetic resonance measurements of lipid lateral diffusion. Biochemistry 20(8): 2204–2207.

Lindblom, G., Orädd, G. & Filippov, A. 2006. Lipid lateral diffusion in bilayers with phosphatidylcholine, sphingomyelin and cholesterol: An NMR study of dynamics and lateral phase separation. Chem. Phys. Lipids 141(1-2): 179–184.

Liscum, L. & Faust, J. R. 1989. The Intracellular transport of low density lipoprotein-derived cholesterol is inhibited in chinese hamster ovary cells cultured with 3-β-[2-(Diethylamino)ethoxy]androst-5-en-17-one. J. Biol. Chem. 264(20): 11796–11806.

Liscum, L. 2000. NiemannÐPick type C mutations cause lipid traffic jam. Traffic 1(3):218–225.

Lombardi, D., Soldatil, D., Riederer, M. A., Goda, Y., Zerial, M. & Pfeffer, S. R. 1993. Rab9 functions in transport between late endosomes and the trans Golgi network. EMBO J. 12(2): 677–682.

London, E. & Brown, D. A. 2000. Insolubility of lipids in triton X-100: physical origin and relationship to sphingolipid/cholesterol membrane domains (rafts). Biochim. Biophys. Acta. 1508(1-2): 182–195.

London, E. 2005. Sphingolipid organization in biomembranes: What physical studies of model membranes reveal. Biochim. Biophys. Acta 1746(3): 203–220.

Low, M. G. 1989. Glycosyl-phosphatidylinositol: a versatile anchor for cell surface proteins. FASEB J. 3(5): 1600–1608.

Lund-Katz, S. Laboda, H. M., McLean, L. R. & Phillips, M. C. 1988. Influence of molecular packing and phospholipid type on rates of cholesterol exchange. Biochemistry 27(9): 3416–3423.

Lusa, S., Blom, T. S., Eskelinen, E. L., Kuismanen, E., Månsson, J. E., Simons, K. & Ikonen, E. Depletion of rafts in late endocytic membranes is controlled by NPC1-dependent recycling of cholesterol to the plasma membrane. J. Cell Sci. 114(Pt 10): 1893–1900.

Luykx, D. M. A. M., Casteleijn, M. G., Jiskoot, W., Westdijk, J. & Jongen, P. M. J. M. 2004. Physicochemical studies on the stability of influenza haemagglutinin in vaccine bulk material. Eur. J. Pharm. Sci. 23(1): 65–75.

Luzio, J. P., Rous, B. A., Bright, N. A., Pryor, P. R., Mullock, B. M. & Piper, R. C. Lysosome-endosome fusion and lysosome biogenesis. J. Cell Sci. 113(9): 1515–1524.

Luzio, J. P., Pryor, P. R. & Bright, N. A. 2007. Lysosomes: fusion and function. Nat. Rev. Mol. Cell Biol. 8(8): 622–632.

Lynch, D.V. & Steponkus, P.L. 1987 Plasma Membrane Lipid Alterations Associated with Cold Acclimation of Winter Rye Seedlings (Secale cereale L. cv Puma). Plant Physiol. 83(4): 761-767.

Möbius, W., Ohno-Iwashita, Y.,van Donselaar, E. G., Oorschot, V. M. J., Shimada, Y., Fujimoto, T., Heijnen, H. F. G., Geuze, H. J. & Slot, J. W. 2002. Immunoelectron microscopic localization of cholesterol using biotinylated and non-cytolytic perfringolysin O. J. Histochem. Cytochem. 50(1): 43–55.

Möbius, W., van Donselaar, E., Ohno-Iwashita, Y., Shimada, Y., Heijnen, H. F., Slot, J. W. & Geuze, H. J. Recycling compartments and the internal vesicles of multivesicular bodies harbor most of the cholesterol found in the endocytic pathway. Traffic. 4(4):222–231.

Mabrey, S. & Sturtevant, J. M. 1976. Investigation of phase transitions of lipids and lipid mixtures by high sensitivity differential scanning calorimetry. Proc. Natl. Acad. Sci. 73(11): 3862–3866.

Maceyka, M., Payne, S.G., Milstien, S. & Spiegela, S. 2002. Sphingosine kinase, sphingosine-1-phosphate, and apoptosis. Biochim. Biophys. Acta 1585(3): 193–201.

Madsen, H., Rasmussen, B. B., Brøsen, K. 1997. Imipramine demethylation in vivo: impact of CYP1A2, CYP2C19, and CYP3A4. Clin. Pharmacol. Ther. 61(3): 319–324.

Magnuson, B., Rainey, E. K., Benjamin, T., Baryshev, M., Mkrtchian, S. & Tsa, B. 2005. ERp29 triggers a conformational change in polyomavirus to stimulate membrane binding. Mol. Cell 20(2): 289–300.

Mahlberg, F. H., Glick, J. M., Jerome, W. G., Rothblat, G. H. 1990. Metabolism of cholesteryl ester lipid droplets in a J774 macrophage foam cell model. Biochem. Biophys. Acta 1045(3): 291–298.

Mallet, W. G. & Maxfield, F. R. 1999. Chimeric forms of furin and TGN38 are transported from the plasma membrane to the trans-Golgi network via distinct endosomal pathways. J. Cell Biol. 146(2): 345–360.

Mani, B., Baltzer, C., Valle, N., Almendral, J. M., Kempf, C., & Ros, C. 2006. Low pH-dependent endosomal processing of the incoming parvovirus minute virus of mice virion leads to externalization of the VP1 N-terminal sequence (N-VP1), N-VP2 cleavage, and uncoating of the full-length genome. J. Virol. 80(2): 1015-1024

Marjomäki, V., Pietiäinen, V., Matilainen, H., Upla, P., Ivaska, J., Nissinen, L., Reunanen, H., Huttunen, P., Hyypiä, T. & Heino, J. 2002. Internalization of echovirus 1 in caveolae. J. Virol. 76(4): 1856–1865.

Marsh, M. & Helenius, A. 2006. Virus entry: open sesame. Cell 124(4): 729–740.

Marsh, D. 2001. Polarity and permeation profiles in lipid membranes. Proc. Natl. Acad. Sci. 98(14): 7777–7782.

Marsh, M., Griffiths, G., Dean, G. E., Mellman, I. & Helenius, A. 1986. Three-dimensional structure of endosomes in BHK-21 cells. Proc. Natl. Acad. Sci. 83(9): 2899–2903.

Marsh, M., Schmid, S., Kern, H., Harms, E., Male, P., Mellman, I. & Helenius, A. 1987. Rapid analytical and preparative isolation of functional endosomes by free flow electrophoresis. J. Cell Biol. 104(4): 875–886.

Matsuo, H., Chevallier, J., Mayran, N., Le Blanc, I., Ferguson, C., Fauré, J., Sartori Blanc, N., Matile, S., Dubochet, J., Sadoul, R., Parton, R. G., Vilbois, F. & Gruenberg, J. 2004. Role of LBPA and Alix in multivesicular liposome formation and endosome organization. Science 303(5657): 531–534.

Mayor, S. & Pagano, R. E. 2007. Pathways of clathrin-independent endocytosis. Nat. Rev. Mol. Cell Biol. 8(8): 603–612.

Mayor, S., Presley, J. F. & Maxfield, F. R. 1993. Sorting of membrane components from endosomes and subsequent recycling to the cell surface occurs by a bulk flow process. J. Cell Biol. 121: 1257–1269.

Mayor, S., Sabharanjak, S. & Maxfield, F. R. 1998. Cholesterol-dependent retention of GPI-anchored proteins in endosomes. EMBO J. 17(16): 4626–4638.

McLauchlan, H., Newell. J., Morrice, N., Osborne, A., West, M., Smythe, E. 1998. A novel role for Rab5-GDI in ligand sequestration into clathrin-coated pits. Curr. Biol. 8(1): 34–45.

McMullen, T. P. W. & McElhaney, R. N. 1997. Differential scanning calorimetric studies of the interaction of cholesterol with distearoyl and dielaidoyl molecular species of phosphatidylcholine, phosphatidylethanolamine, and phosphatidylserine. Biochemistry 36(16): 4979–4986.

Meder, D. & Simons, K. 2006. Lipid rafts, caveolae, and membrane traffic. In: Fielding, C. J. (ed.) Lipid Rafts and Caveolae. Wiley GmbH & Co. KGaA, Weinheim, Germany.

Meleard, P., Gerbeaud, C., Pott, T., Fernandez-Puente, L., Bivas, I., Mitov, M. D., Dufourcq, J. & Bothorel, P. 1997. Bending elasticities of model membranes: influences of temperature and sterol content. Biophys. J. 72(6): 2616–2629.

Melikyana, G. B., Markosyana, R. M., Hemmatia, H., Delmedicob, M. K., Lambertb, D. M. & Cohen, F. S. 2000. Evidence that the transition of HIV-1 gp41 into a six-helix bundle, not the bundle configuration, induces membrane fusion. J. Cell Biol. 151(2): 413–424.

Melkonian, K. A., Ostermeyer, A. G., Chen, J. Z., Roth, M. G. & Brown, D. A. 1999. Role of lipid modifications in targeting proteins to detergent-resistant membrane rafts. Many raft proteins are acylated, while few are prenylated. J. Biol. Chem. 274(6): 3910–3917.

Mellman I. 1996. Endocytosis and molecular sorting. Annu. Rev. Cell Dev. Biol. 12: 575–625.

Miller, A. L., Kress, B. C., Stein, R., Kinnon, C., Kern, H., Schneider, J. A. & Harms, E. 1981. Properties of N-Acetyl-P-D-hexosaminidase from isolated normal and I-cell lysosomes. J. Biol. Chem. 256(17): 9352–9362.

Moffitt, J. H., Fielding, B. A., Evershed, R., Berstan, R., Currie, J. M. & Clark, A. 2005. Adverse physicochemical properties of tripalmitin in beta cells lead to morphological changes and lipotoxicity in vitro. Diabetol. 48(9): 1819–1829.

Mohrmann, K. & Van Der Sluijs, P. 1999. Regulation of membrane transport through the endocytic pathway by rabGTPases. Mol. Membr. Biol. 16(1): 81–87.

Monier, S., Parton, R. G., Vogel, F., Behlke, J., Henske, A. & Kurzchalia, T. V. 1995. VIP21-caveolin, a membrane protein constituent of the caveolar coat, oligomerizes in vivo and in vitro. Mol. Biol. Cell 6(7): 911–927.

Morrow, M. R., Singh, D., Lu, D. & Grantt, C. W. M. 1995. Glycosphingolipid Fatty Acid Arrangement in Phospholipid Bilayers: Cholesterol Effects Biophys. J. 68(1): 179–186.

Mouritsen, O. G. & Jørgensen, K. 1994. Dynamical order and disorder in lipid bilayers. Chem. Phys. Lipids 73(1-2): 3–25.

Mu, F. T., Callaghan, J. M., Steele-Mortimer, O., Stenmark, H., Parton, R. G., Campbell, P. L., McCluskey, J., Yeo, J. P., Tock, E. P. C. & Toh, B. H. EEA1, an Early Endosome-Associated Protein. J. Biol. Chem. 270(22): 13503–13511.

Mukherjee, S. & Maxfield, F. R. 2000. Role of membrane organization and membrane domains in endocytic lipid trafficking. Traffic 1(3): 203–211.

Mukherjee, S., Ghosh, R. N. & Maxfield, F. R. 1997. Endocytosis. Physiol. Rev. 77: 759–803.

Mullock, B. M., Bright, N. A., Fearon, C. W., Gray, S. R. & Luzio, J. 1998. Fusion of lysosomes with late endosomes produces a hybrid organelle of intermediate density and is NSF dependent. J. Cell Biol.140(3): 591–601.

Munro, S. 2003 Lipid rafts: elusive or illusive? Cell 115(4): 377–388.

Murata, M., Peränen, J., Schreiner, R., Wieland, F., Kurzchalia, T. V. & Simons, K. 1995. VIP21/caveolin is a cholesterol-binding protein. Proc. Natl. Acad. Sci. 92(22): 10339–10343.

Murphy, R. F. 1991. Maturation models for endosome and lysosome biogenesis. Trends Cell Biol. 1(4): 77–82.

Murray, J. W., Bananis, E. & Wolkoff, A. W. 2000. Reconstitution of ATP-dependent movement of endocytic vesicles along microtubules in vitro: an oscillatory bidirectional process. Mol. Biol. Cell 11(2): 419–433.

Nada, S., Hondo, A., Kasai, A., Koike, M., Saito, K., Uchiyama, Y. & Okada, M. 2009. The novel lipid raft adaptor p18 controls endosome dynamics by anchoring the MEKĐERK pathway to late endosomes. EMBO J. 28(5): 477 – 489.

Nagle J. F. & Wilkinson, D. A. 1978. Lecithin bilayers. Density measurements and molecular interactions. Biophys. J. 23(2): 159–175.

Nagle, J. F., Zhang, R., Tristram-Nagle, S., Sun, W., Petrache, H. I. & Suter, R. M. 1996. X-Ray structure determination of fully hydrated Lα phase dipalmitoylphosphatidylcholine bilayers. Biophys. J. 70(3): 1419–1431.

Nakanishi, A., Clever, J., Yamada, J., Li, P. P. & Kasamatsu, H. 1996. Association with capsid proteins promotes nuclear targeting of simian virus 40 DNA. Proc. Natl. Acad. Sci. 93(1): 96–100.

Needham, D. & Evans, E. 1988. Structure and mechanical properties of giant lipid (DMPC) vesicle bilayers from 20°C below to 10°C above the liquid crystal-crystalline phase transition at 24°C . Biochemistry 27(21): 8261–8269.

Needham, D., McIntosh, T. J. & Evans, E. 1988. Thermomechanical and transition properties of dimyristoylphosphatidylcholine/cholesterol bilayers. Biochemistry 27(13): 4668–4673.

Needham, D. & Nunn, R. S. 1990. Elastic deformation and failure of lipid bilayer membranes containing cholesterol. Biophys. J. 58(4): 997–1009.

Neiss, W. F. 1984. A coat of glycoconjugates on the inner surface of the lysosomal membrane in the rat kidney. Histochemistry 80(6): 603–608.

Newcombe, N. G., Beagley, L. G., Christiansen, D., Loveland, B. E., Johansson, E. S., Beagley, K. W., Barry, R. D. & Shafren, D. R. 2004. Novel role for decay-accelerating factor in coxsackievirus A21-mediated cell infectivity. J. Virol. 78(22): 12677–12682.

Nielsen, E., Severin, F., Backer, J. M., Hyman, A. A. & Zerial, M. 1999. Rab5 regulates motility of early endosomes on microtubules. Nat. Cell Biol. 1(6): 376–382.

Niemela, P., Ollila, S., Hyvonen, M. T., Karttunen, M. & Vattulainen, I. 2007. Assessing the nature of lipid rafts. PLoS Comp. Biol. 3(2): 304–312.

Nieva, J. L., Bron, R., Corver, J. & Wilschut, J. 1994. Membrane fusion of Semliki Forest virus requires sphingolipids in the target membrane. EMBO J. 13(12): 2797–2804.

Niu, S-L. & Litman, B. J. 2002. Determination of membrane cholesterol partition coefficient using a lipid vesicle-cyclodextrin binary system: effect of phospholipid acyl chain unsaturation and headgroup composition. Biophys. J. 83(6): 3408–3415.

Nosè, S. 1984. A molecular dynamics method for simulations in the canonical ensemble. Mol. Phys. 52(2): 255–268.

Novikoff, A. B., Beaufay, H. & de Duve, C. 1956. Electron microscopy of lysosome-rich fractions from rat liver. J. Biophys. and Biochem. Cytol., 2(4):179–184.

Ohvo-Rekilä, H., Ramstedt, B., Leppimäki, P. & Slotte, J. P. 2002. Cholesterol interactions with phospholipids in membranes. Prog. Lipid Res. 41(1): 66Ð97.

Okamoto, T., Schlegel, A., Scherer, P. E. & Lisanti, M. P. 1998. Caveolins, a family of scaffolding proteins for organizing "preassembled signaling complexes" at the plasma membrane. J. Biol. Chem. 273(10): 5419–5422.

Oliver, C., Dromy, R. & Hart, T. K. 1989. Density gradient separation of two populations of lysosomes from rat parotid acinar cells. J. Histochem. Cytochem. 37(11): 1645–1652.

Olkkonen, V. M., Dupree, P., Killisch, I., Lutcke, A., Zerial, M. & Simons, K. 1993. J. Cell Sci, 106(4): 1249–1261.

Ollila, S., Hyvönen, M. T. & Vattulainen, I. 2007. Polyunsaturation in lipid membranes: dynamic properties and lateral pressure profiles. J. Phys. Chem. B 111(12): 3139–3150

Orädd, G., Lindblom, G. & Westerman, P. W. 2003. Lateral Diffusion of Cholesterol and Dimyristoylphosphatidylcholine in a Lipid Bilayer Measured by Pulsed Field Gradient NMR Spectroscopy. Biophys J. 83(5): 2702–2704.

Orlandi, P. & Fishman, P. H. 1998. Filipin-dependent inhibition of cholera toxin: evidence for toxin internalization and activation through caveolae-like domains. J. Cell Biol. 141(4): 905–915.

Pèrez, L. & Carrasco, L. 1993. Entry of poliovirus into cells does not require a low-pH step.J Virol. 67(8): 4543–4548.

Pakkanen, K., Kirjavainen, S., Mäkelä, A. R., Rintanen, R., Oker-Blom, C., Jalonen, T. O. & Vuento, M. 2009. Parvovirus capsid disorders cholesterol-rich membranes. Biochem. Biophys. Res. Comm. 379(2): 562–566.

Paladino, S., Sarnataro, D., Pillich, R., Tivodar, S., Nitsch, L. & Zurzolo, C. 2004. Protein oligomerization modulates raft partitioning and apical sorting of GPI-anchored proteins. J. Cell. Biol. J. Cell Biol. 167(4): 699–709.

Paradiso, P. R., Rhode, S. L. III & Singer, I., 1982. Canine parvovirus: a biochemical and ultrastructural study. J. Gen. Virol. 62: 113–125.

Parasassi, T., De Stasio, G.,d'Ubaldo, A. & Gratton, E. 1990. Phase fluctuation in phospholipid membranes revealed by Laurdan fluorescence. Biophys. J. 57(6): 1179–1186.

Parasassi, T., Krasnowska, E. K., Bagatolli L. & Gratton E. Laurdan and Prodan as Polarity-Sensitive Fluorescent Membrane Probes. J. Fluor. 8(4): 365–373.

Parker, J.S. & Parrish, C.R. 2000. Cellular uptake and infection by canine parvovirus involves rapid dynamin-regulated clathrin-mediated endocytosis, followed by slower intracellular trafficking. J. Virol. 74(4): 1919–1930.

Parker, J. S., Murphy, W. J., Wang, D., O'Brien, S. J. & Parrish, C. R. 2001. Canine and feline parvoviruses can use human or feline transferrin receptors to bind, enter, and infect cells. J. Virol. 75(8): 3896–3902.

Parrinello, M. & Rahman, A. 1981. Polymorphic transitions in single crystals: a new molecular dynamics method. J. Appl. Phys. 52(12): 7182–7190.

Parrish, C. R. 1991. Mapping specific functions in the capsid structure of canine parvovirus and feline panleukopenia virus using infectious plasmid clones. Virology 183(1): 195–205.

Parton, R. G., Joggerst, B. & Simons, K. 1994. Regulated internalization of caveolae. J. Cell Biol. 127(5): 1199–1215.

Pelkmans, L. & Zerial, M. 2005. Kinase-regulated quantal assemblies and kiss-and-run recycling of caveolae. Nature 436(7047): 128–133.

Pelkmans, L., Kartenbeck, J. & Helenius, A. 2001. Caveolar endocytosis of simian virus 40 reveals a new two-step vesicular-transport pathway to the ER. Nat. Cell Biol. 3(5): 473–483.

Pelkmans, L., Bürli, T., Zerial, M. & Helenius, A. 2004. Caveolin-stabilized membrane domains as multifunctional transport and sorting devices in endocytic membrane traffic. Cell 118(6): 767–780.

Perret, E., Lakkaraju, A., Deborde, S., Schreiner, R. & Rodriguez-Boulan, E. 2005. Evolving endosomes: how many varieties and why? Curr. Opin. Cell Biol. 17(4): 423–434.

Peters, K. R., Carley, W. W. & Palade, G. E. 1985. Endothelial plasmalemmal vesicles have a characteristic striped bipolar surface structure. J. Cell Biol. 101: 2233–2238.

Phalen, T. & Kielian, M. 1991. Cholesterol is required for infection by semliki forest virus. J. Cell Biol. 112(4): 615–623.

Pierce, S. K. 2002. Lipid rafts and B-cell activation. Nat. Rev. Immunol. 2(2): 96–105.

Pietiäinen, V., Marjomäki, V., Upla, P., Pelkmans, L., Helenius, A. & Hyypiä, T. 2004. Echovirus 1 endocytosis into caveosomes requires lipid rafts, dynamin II, and signaling events. Mol. Biol. Cell 15(11): 4911–4925.

Piironen, V., Lindsay, D.G., Miettinen, T.A., Toivo, J., & Lampi, A-M. 2000. Plant sterols: biosynthesis, biological function and their importance to human nutrition. J. Sci. Food Agric. 80(7): 939–966.

Piper, R. C. & Luzio, J. P. 2001. Late endosomes: sorting and partitioning in multivesicular bodies. Traffic 2(9): 612–621.

Poole, B. & Ohkuma, S. 1981. Effect of weak bases on the intralysosomal pH in mouse peritoneal macrophages. J. Cell Biol. 90(3): 665–669.

Powell, K. & Leslie, M. 2006. From the Archive. Lipid raft idea is floated. J. Cell Biol. 172(2): 166–167.

Prades, J., Funari, S. S., Escriba, P. V. & Barcelo, F. 2003. Effects of unsaturated fatty acids and triacylglycerols on phosphatidylethanolamine membrane structure. J.Lip. Res. 44(9): 1720–1727.

Prallea, A., Kellera, P., Florina, E.-L., Simons, K. & Hörber, J. K. H. 2000. SphingolipidÐcholesterol rafts diffuse as small entities in the plasma membrane of mammalian cells. J. Cell Biol. 148(5): 997–1008.

Pryor, P. R., Mullock, B. M., Bright, N. A., Gray, S. R., & Luzio, J. P. 2000. The role of intraorganellar Ca2+ in late endosome-lysosome heterotypic fusion and in the reformation of lysosomes from hybrid organelles. J. Cell Biol. 149(5): 1053–1062.

Rainey-Barger, E. K., Magnuson, B. & Tsai, B. 2007. A chaperone-activated nonenveloped virus perforates the physiologically relevant endoplasmic reticulum membrane. J. Virol. 81(23): 12996–13004.

Rajendran, L.& Simons, K. 2005. Lipid rafts and membrane dynamics. J. Cell Sci. 118: 1099–1102.

Rajendran, L., Masilamani, M., Solomon, S., Tikkanen, R., Stuermer, C. A., Plattner, H. & Illges, H. 2003. Asymmetric localization of flotillins/reggies in preassembled platforms confers inherent polarity to hematopoietic cells. Proc. Natl. Acad. Sci. 100(14): 8241–8246.

Ramstedt, B. & Slotte, J.P. 2003 Sphingolipids and the formation of sterol-enriched ordered membrane domains. Biochim. Biophys. Acta 1758(12): 1945–1956.

Rand, R.P., Chapman, D. & Larsson, K. 1975. Tilted hydrocarbon chains of dipalmitoyl lecithin become perpendicular to the bilayer before melting. Biophys. J. 15(11): 1117–1124.

Rappolt, M., Vidal, M. F., Kriechbaum, M., Steinhart, M., Amenitsch, H., Bernstorff, S. & Laggner P. 2003. Structural, dynamic and mechanical properties of POPC at low cholesterol concentration studied in pressure/temperature space. Eur. Biophys. J. 31(8): 575–585.

Ray, T.K., Skipski, V.P., Barclay, M., Essner, E., & Archibald, F.M. 1969. Lipid composition of rat liver plasma membranes. J. Biol. Chem. 244(20): 5528–5536.

Reczek, D., Schwake, M, Schröder, J., Hughes, H., Blanz, J., Jin, X., Brondyk, W., Van Patten, S., Edmunds, T. & Saftig, P. 2007. LIMP-2 Is a receptor for lysosomal mannose-6-phosphate-independent targeting of β-glucocerebrosidase. Cell 131(4): 770–783.

Ren, M., Xu, G., Zeng, J., De Lemos-Chiarandini, C., Adesnik, M. & Sabatini, D. D. 1998. Hydrolysis of GTP on rab11 is required for the direct delivery of transferrin from the pericentriolar recycling compartment to the cell surface but not from sorting endosomes. Proc. Natl. Acad. Sci.95(11): 6187–6192.

Repáková, J., Čapková, P., Holopainen, J. M. & Vattulainen, I. 2004. Distribution, orientation, and dynamics of DPH probes in DPPC bilayer. J. Phys. Chem. B 108(35): 13438 – 13448.

Richterová, Z., Liebl, D., Horák, M., Palková, Z., Štokrová, J., Hozák, P., Korb, J. & Forstová, J. 2001. Caveolae are involved in the trafficking of mouse polyomavirus virions and artificial VP1 pseudocapsids toward cell nuclei. J. Virol. 75(22): 10880–10891.

Ridley, A. J. Paterson, H. F., Johnston, C. L., Diekmann, D. & Hall, A. 1992. The small GTP-binding protein rac regulates growth factor-induced membrane ruffling. Cell 70(3): 401–410.

Roederer, M., Bowser, R. & Murphy, R. F. 1987. Kinetics and temperature dependence of exposure of endocytosed material to proteolytic enzymes and low pH: Evidence for a maturation model for the formation of lysosomes. J. Cell. Physiol. 131(2): 200–209.

Ros, C., Gerber, M. & Kempf, C. 2006. Conformational changes in the VP1-unique region of native human parvovirus B19 lead to exposure of internal sequences that play a role in virus neutralization and infectivity. J. Virol. 80(24): 12017-12024

Rothberg, K. G., Heuser, J. E., Donzell, W. C., Ying, Y. S., Glenney, J. R. & Anderson, R. G. 1992. Caveolin, a protein component of caveolae membrane coats. Cell 68(4): 673–682.

Ruggiero, A. & Hudson, B. 1989. Critical density fluctuations in lipid bilayers detected by fluorescence lifetime heterogeneity. Biophys. J. 55(6): 1111–1124.

Ruiz, J. I. & Ochoa, B. 1997. Quantification in the subnanomolar range of phospholipids and neutral lipids by monodimensional thin-layer chromatography and image analysis. J. Lipid Res. 38(7): 1482–1489.

Ruiz, M. C., Abad, M. J., Charpilienne, A., Cohen, J. & Michelangeli, F. 1997. Cell lines susceptible to infection are permeabilized by cleaved and solubilized outer layer proteins of rotavirus. J. Gen. Virol. 78(11): 2883–2893.

Salome, N., van Hille, B., Geuskens, M. & Rommelaere, J. 1989. Partial reversion of conditional transformation correlates with a decrease in the sensitivity of rat cells to killing by the parvovirus minute virus of mice but not in their capacity for virus production: effect of a temperature-sensitive v-src oncogene. J Virol. 63(11): 4797–4807.

Sankaram, M. B. & Thompson, T. E. 1990. Interaction of Cholesterol with Various Glycerophospholipids and Sphingomyelin. Biochemistry 29(47): 10670–10675.

Sankaram, M. & Thompson, T. E. 1991. Cholesterol-induced fluid-phase immiscibility in membranes. Proc. Natl. Acad. Sci. 88(19): 8686–8690.

Sankaram, M.B., Marsh, D. & Thompson, T.E. 1992. Determination of fluid and gel domain sizes in two-component, two-phase lipid bilayers. An electron spin resonance spin label study. Biophys. J. 63(2): 340–349.

Sapin, C., Colard, O., Delmas, O., Tessier, C., Breton, M., Enouf, V., Chwetzoff, S., Ouanich, J., Cohen, J., Wolf, C. & Trugnan, G. 2002. Rafts promote assembly and atypical targeting of a nonenveloped virus, rotavirus, in Caco-2 cells. J. Virol. 76(9): 4591–4602.

Sargiacomo, M. Scherer, P. E., Tang, Z., Kübler, E, Song, K. S., Sanders, M. C. & Lisanti, M. P. 1995. Oligomeric structure of caveolin: implications for caveolae membrane organization. Proc. Natl. Acad. Sci. 92(20): 9407–9411.

Sbrissa, D., Ikonomov, O. C. & Shisheva, A. 2002. Phosphatidylinositol 3-Phosphate-interacting Domains in PIKfyve. Binding specificity and role in PIKfyve endomembrane localization. J. Biol. Chem. 277(8): 6073–6079.

Scaife, R.M., Job, D. & Langdon, W.Y. 2003. Rapid microtubule-dependent induction of neurite-like extensions

Scheiffele, P., Roth, M. G. & Simons, K. 1997. Interaction of influenza virus haemagglutinin with sphingolipid-cholesterol membrane domains via its transmembrane domain. EMBO J. 16(18): 5501–5508.

Scheiffele, P., Rietveld, A., Wilk, T. & Simons, K. 1999. Influenza viruses select ordered lipid domains during budding from the plasma membrane. J. Biol. Chem. 274(4): 2038–2044.

Schmid, S. L., Fuchs, R., Male, P. & Mellman, I. 1988. Two distinct subpopulations of endosomes involved in membrane recycling and transport to lysosome. Cell 52(1): 73-83.

Schoonderwoerd, K., Broekhoven-Schokker, S., Hülsmann, W. C. & Stam, H. 1990. Involvement of lysosome-like particles in the metabolism of endogenous myocardial triglycerides during ischemia/reperfusion. Uptake and degradation of triglycerides by lysosomes isolated from rat heart. Basic Res. Cardiol. 85(2): 153–163.

Schroeder, R., London, E. & Brown, D. 1994. Interactions between saturated acyl chains confer detergent resistance on lipids and glycosylphosphatidylinositol (GPI)-anchored proteins: GPI-anchored proteins in liposomes and cells show similar behavior. Proc Natl Acad Sci U S A 91(25): 12130–12134.

Schoer, J. K., Gallegos, A. M., McIntosh, A. L., Starodub, O., Kier, A. B., Billheimer, J. T. & Schroeder, F. 2000. Lysosomal membrane cholesterol dynamics. Biochemistry 39(26): 7662–7677.

Seth, P., Pastan, I. & Willingham, M. C. 1985. Adenovirus-dependent increase in cell membrane permeability. J. Biol. Chem. 260(17): 9598–9602.

Shafren, D. R., Bates, R. C., Agrez, M. V., Herd, R. L., Burns, G. F. & Barry, R. D. 1995. Coxsackieviruses B1, B3, and B5 use decay accelerating factor as a receptor for cell attachment. J. Virol. 69(6): 3873–3877.

Sherbet, G.V. 1989. Membrane fluidity and cancer metastasis. Expl. Cell Biol. 57(4): 198–205.

Sherer, N.M., Lehmann, M.J., Jimenez-Soto, L.F., Horensavitz, C., Pypaert, M. & Mothes, W. 2007. Retroviruses can establish filopodial bridges for efficient cell-to-cell transmission. Nat. Cell Biol. 9(3): 310–315

Shmulevitz, M. & Duncan, R. 2000. A new class of fusion-associated small transmembrane (FAST) proteins encoded by the non-enveloped fusogenic reoviruses. EMBO J. 19(5): 902–912.

Shmulevitz, M., Epand, R. F., Epand, R. M. & Duncan, R. 2004. Structural and functional properties of an unusual internal fusion peptide in a nonenveloped virus membrane fusion protein. Journal of Virology 78(6): 2808–2818.

Sieczkarski, S. B. & Whittaker, G. R. 2002. Dissecting virus entry via endocytosis. J. Gen. Virol. 83(7): 1535–1545.

Silverstein, S. C., Schonberg, M., Levin, D. H. & Acs, G. 1970. The Reovirus replicative cycle: conservation of parental RNA and protein. Prog. Natl. Acad. Sci. 67(1): 275–281.

Silvius, J. Role of cholesterol in lipid raft formation: lessons from lipid model systems. Biochim. Biophys. Acta 1610(2): 174Ð 183.

Simons, K. & Ehehalt, R. 2002. Cholesterol, lipid rafts, and disease. J. Clin. Invest. 110(5): 597–603.

Simons, K. & Ikonen, E. 1997. Functional rafts in cell membranes. Nature 387: 569–572.

Simons, K. & Toomre, D. 2000. Lipid rafts and signal transduction. Nat. Rev. Mol. Cell Biol. 1(1): 31–39.

Simons, K. & Vaz, W. L. 2004. Model systems, lipid rafts, and cell membranes. Annu. Rev. Biophys. Biomol. Struct. 33: 269–295.

Simonsen, A., Lippé, R., Christoforidis. S., Gaullier, J. M., Brech, A., Callaghan, J., Toh, B. H., Murphy, C., Zerial, M. & Stenmark, H. 1998. EEA1 links PI(3)K function to Rab5 regulation of endosome fusion. Nature. 394(6692): 494–498.

Simpson, A. A., Chandrasekar, V., Hébert, B., Sullivan, G. M., Rossmann, M. G. & Parrish, C. R. 2000. Host range and variability of calcium binding by surface loops in the capsids of canine and feline parvoviruses. J. Mol. Biol. 300(3): 597–610.

Singer, S. J. & Nicolson, G. L. 1972. The Fluid Mosaic Model of the Structure of Cell Membranes. 175(23): 720 – 731.

Singer, S. J. Some early history of membrane molecular biology. Annu. Rev. Physiol. 66:1–27.

Singh, D. K., Gesquiere, L. R. & Subbaiah, P. V. 2007. Role of sphingomyelin and ceramide in the regulation of the activity and fatty acid specificity of group V secretory phospholipase A_2. Arch. Biochem. Biophys. 459(2): 280–287.

Skehel, J. J. & Wiley, D. C. 1998. Coiled coils in both intracellular vesicle and viral membrane fusion. Cell 95(7): 871–874.

Smaby, J., Momsen, M. M., Brockman, H. L. & Brown, R. E. 1997. Phosphatidylcholine Acyl Unsaturation Modulates the Decrease in Interfacial Elasticity Induced by Cholesterol. Biophys. J. 73(3): 1492–1505.

Smith, A. E. & Helenius, A. 2004. How viruses enter animal cells. Science 304(5668): 237–242.

Sobo, K., Chevallier, J., Parton, R. G., Gruenberg, J. & van der Goot, F. G. 2007. Diversity of Raft-Like Domains in Late Endosomes. PLoS ONE 2(4): e391.

Somsel Rodman, J. & Wandinger-Ness, A. 2000. Rab GTPases coordinate endocytosis J. Cell Sci. 113(2): 183-192.

Song, K. S., Li, S., Okamoto, T., Quilliam, L. A., Sargiacomo, M. & Lisanti, M. P. 1996. Co-purification and direct interaction of Ras with caveolin, an integral membrane protein of caveolae microdomains. 271(16): 9690–9697.

Spooner, P. J. R. & Small, D. M.1987. Effect of free cholesterol on incorporation of triolein in phospholipid bilayers. Biochemistry 26(18): 5820–5825.

Staneva, G., Seigneuret, M., Koumanov, K., Trugnan, G. & Angelova, M. I. 2005. Detergents induce raft-like domains budding and fission from giant unilamellar heterogeneous vesicles: a direct microscopy observation. Chem. Phys. Lipids. 136(1):55–66.

Stewart, P. L., Dermody, T. S. & Nemerow, G. R. 2003. Structural basis of nonenveloped virus cell entry. Adv. Prot. Chem. 64: 455-491.

Stockton, G. W. & Smith, I. C. P. 1976. A deuterium nuclear magnetic resonance study of the condensing effect of cholesterol on egg phosphatidylcholine bilayer membranes. I. Perdeuterated fatty acid probes. Chem. Phys. Lipids 17(2-3): 251–263.

Stockton, G. W. & Smith, I. C. P. 1976. A deuterium nuclear magnetic resonance study of the condensing effect of cholesterol on egg phosphatidylcholine bilayer membranes. I. Perdeuterated fatty acid probes. Chem. Phys. Lipids 17(2-3): 251–263.

Stoffel, P., Burkart, T., Honegger, U. E. & Wiesmann, U. N. 1987. Subcellular distribution of the antidepressant drug desipramine in cultured human fibroblasts after chronic administration. Drug-effect on the subcellular distribution of accumulated phospholipids. Biochem Pharmacol. 36(5): 655–662.

Stoorvogel, W., Strous, G. J., Geuze, H. J., Oorschot, V. & Schwartzt, A. L. 1991. Late endosomes derive from early endosomes by maturation. Cell 65(3): 417–427.

Storrie, B. & Desjardins, M. 1996. The biogenesis of lysosomes: is it a kiss and run, continuous fusion and fission process? Bioessays 18(11): 895–903.

Stowell, M. H. B., Marks, B., Wigge, P. & McMahon, H. T. 1999. Nucleotide-dependent conformational changes in dynamin: evidence for a mechanochemical molecular spring. Nat. Cell Biol. 1(1): 27–32.

Štrancar, J., Šentjurc, M. & Schara, M. 2000. Fast and Accurate Characterization of Biological Membranes by EPR Spectral Simulations of Nitroxides. J. Magn. Reson. 142(2): 254–265.

Strassheim, M.L., Gruenberg, A., Veijalainen, P., Sgro, J.Y., Parrish, C.R., 1994. Two dominant neutralizing antigenic determinants of canine parvovirus are found on the threefold spike of the virus capsid. Virology 198(1): 175–184.

Stuart, L. M. & Ezekowitz, R. A. B. 2005. Phagocytosis: elegant complexity. Immunity 22(5): 539–550.

Stuart, A. D., Eustace, H. E., McKee, T. A. & Brown, T. D. K. 2002. A novel cell entry pathway for a DAF-using human enterovirus is dependent on lipid rafts. J. Virol. 76(18): 9307–9322.

Sturzenbecker, L. J., Nibert, M., Furlong, D. & Fields, B. N. 1987. Intracellular digestion of reovirus particles requires a low pH and is an essential step in the viral infectious cycle. J. Virol. 61(8): 2351–2361.

Subtil, A., Gaidarov, I., Kobylarz, K., Lampson, M. A., Keen, J. H. & McGraw, T. E. 1999. Acute cholesterol depletion inhibits clathrin-coated pit budding. Proc. Natl. Acad. Sci. 96(12): 6775–6780.

Suikkanen, S., Sääjärvi, K., Hirsimäki, J., Välilehto, O., Reunanen, H., Vihinen-Ranta, M. & Vuento, M. 2002. Role of recycling endosomes and lysosomes in dynein-dependent entry of canine parvovirus. J. Virol. 76(9): 4401–4411.

Suikkanen, S., Aaltonen, T., Nevalainen, M., Välilehto, O., Lindholm, O., Vuento, M. & Vihinen-Ranta, M. 2003. Exploitation of microtubule cytoskeleton and dynein during parvoviral traffic toward the nucleus. J. Virol.77(19): 10270–10279.

Suikkanen, S., Antila, M., Jaatinen, A., Vihinen-Ranta, M. & Vuento, M., 2003. Release of canine parvovirus from endocytic vesicles. Virology 316(2): 267–280.

Sun, X. & Whittaker, G. R. 2003. Role for influenza virus envelope cholesterol in virus entry and infection. J. Virol. 77(23): 12543–12551.

Swanson, J. A. & Watts, C. 1995. Macropinocytosis. Trends Cell Biol. 5(11): 424–428.

Swanson, J. A. 2008. Shaping cups into phagosomes and macropinosomes. Nat. Rev. Mol. Cell Biol. 9(8): 639–649.

Swanson, J., Bushnell, A. & Silverstein, S. C. 1987. Tubular lysosome morphology and distribution within macrophages depend on the integrity of cytoplasmic microtubules. Proc. Natl. Acad. Sci. 84(7): 1921–1925.

Sweitzer, S. M. & Hinshaw, J. E. 1998. Dynamin undergoes a GTP-dependent conformational change causing vesiculation. Cell 93(6):1021–1029.

Tanaka, Y., Guhde, G., Suter, A., Eskelinen, E. L., Hartmann, D., Lüllmann-Rauch, R., Janssen, P. M. L., Blanz, J., von Figura, K. & Saftig, P. 2000. Accumulation of autophagic vacuoles and cardiomyopathy in LAMP-2-deficient mice. Nature 406(6798): 902–906.

Tanford, C. 1980. The Hydrophobic Effect: Formation of Micelles and Biological Membranes. Wiley, New York.

Tangirala, R. K., Mahlberg, F. H., Glick, J. M., Jerome, W. G. & Rothblat, G. H. 1993. Lysosomal accumulation of unesterified cholesterol in model macrophage foam cells. J. Biol. Chem. 268(13): 9653–9660.

Tattersall, P. & Cotmore, S. F. 1988. The nature of parvoviruses. In: Parvoviruses and Human Disease. CRC Press, Boca Raton, FL.

Tauchi-Sato, K., Ozeki, S., Houjou, T., Taguchi, R. & Fujimoto, T. 2002. The surface of lipid droplets is a phospholipid monolayer with a unique fatty acid composition. J. Biol. Chem. 277(46): 44507–44512.

te Vruchte, D., Lloyd-Evans, E., Veldman, R. J., Neville, D. C. A., Dwek, R. A., Platt, F. M., van Blitterswijk, W. J. & Sillence, D. J. 2004. Accumulation of glycosphingolipids in Niemann-Pick C disease disrupts endosomal transport. J. Biol. Chem. 279(25): 26167–26175.

Teixeira, A. C. T, Brogueira, P., Fernandes, A. C. & Gonçalves da Silva, A. M. P. S. 2008. Phase behaviour of binary mixtures involving tristearin, stearyl stearate and stearic acid: thermodynamic study and BAM observation at the air-water interface and AFM analysis of LB films. Chem. Phys. Lipids 153(2): 98–108.

Thewalt, J. L. & Bloom, M. 1992. Phosphatidylcholine: cholesterol phase diagrams. Biophys. J. 63(4): 1176–1181.

Tien, Ti. H. & Ottova, A.L. 2001. The lipid bilayer concept and its experimental realization: from soap bubbles, kitchen sink, to bilayer lipid membranes. J. Membr. Sci. 189(1): 83 - 117.

Tooze, J.& Hollinshead, M. 1991. Tubular early endosomal networks in AtT20 and other cells. J. Cell Biol. 115(3).: 635–653

Tosteson, M. T., Nibert, M. L. & Fields, B. N. 1993. Ion channels induced in lipid bilayers by subvirion particles of the nonenveloped mammalian reoviruses. Proc. Natl. Acad. Sci. 90(22): 10549–10552.

Tsai, B., Gilbert, J. M., Stehle, T., Lencer, W., Benjamin, T. L. & Rapoport, T. A. 2003. Gangliosides are receptors for murine polyoma virus and SV40. EMBO J. 22(17): 4346–4355.

Tsamaloukas, A., Szadkowska, H. & Heerklotz, H. 2006. Thermodynamic Comparison of the Interactions of Cholesterol with Unsaturated Phospholipid and Sphingomyelins. Biophys. J. 90(12): 4479–4487.

Tsao, J., Chapman, M.S., Agbandje, M., Keller, W., Smith, K., Wu, H., Luo, M., Smith, T.J., Rossmann, M.G., Compans, R.W. & Parrish, C.R. 1991. The three-dimensional structure of canine parvovirus and its functional implications. Science 251(5000): 1456–1464.

Ullrich, O., Reinsch, S., Urbe, S., Zerial, M. & Parton, R. G. 1996. Rab11 regulates recycling through the pericentriolar recycling endosome. J. Cell Biol. 135: 913–924.

Valderrama, F., Cordeiro, J. V., Schleich, S., Frischknecht, F. & Way, M. 2006. Vaccinia virus-induced cell motility requires F11L-mediated inhibition of RhoA signaling. Science 311(5759): 377–381.

van Buuren, A. R., Marrink, S. J. & Berendsen, H. J. C. 1993. A molecular dynamics study of the decane/water interface. J. Phys. Chem. 97(36): 9206–9212.

Van den Broeke, C., Deruelle, M., Nauwynck, H. J., Coller, K. E., Smith, G. A., Van Doorsselaere, J. & Favoreel, H. W. 2009. The kinase activity of pseudorabies virus US3 is required for modulation of the actin cytoskeleton. Virology 385(1): 155–160

van der Spoel, D., Lindahl, E., Hess, B., Groenhof, G., Mark, A. E. & Berendsen, H. J. C. 2005. GROMACS: Fast, Flexible and Free. J. Comp. Chem. 26(16): 1701–1718.

van Gunsteren, W. F. & Berendsen, H. J. C. 1987. Gromos-87 manual. Biomos BV. Nijenborgh 4, 9747 AG Groningen, The Netherlands.

Van Minnebruggen, G., Favoreel, H. W., Jacobs, L. & Nauwynck, H. J. 2003. Pseudorabies virus US3 protein kinase mediates actin stress fiber breakdown. J. Virology 77(16): 9074–9080.

Vandenbroucke-Grauls, C. M., Thijssen, R. M., Marcelis, J. H., Sharma, S. D. & Verhoef, J. 1984. Effects of lysosomotropic amines on human polymorphonuclear leucocyte function. Immunol. 51(2): 319–326.

Varma, R & Mayor, S. 1998. GPI-anchored proteins are organized in submicron domains at the cell surface. Nature 394(6695): 798–801.

Veatch, S. L. & Keller, S. L. 2003. Separation of Liquid Phases in Giant Vesicles of Ternary Mixtures of Phospholipids and Cholesterol. Biophys. J. 85(5): 3074–3083.

Vereb, G., Szöllosi, J., Matkó, J., Nagy, P., Farkas, T., Vigh, L., Mátyus, L., Waldmann, T.A. & Damjanovich, S. 2003. Dynamic, yet structured: The cell membrane three decades after the Singer-Nicolson model. Proc Natl Acad Sci 100(14): 8053–8058.

Vida, T. & Gerhardt, B. 1999. A cell-free assay allows reconstitution of Vps33p-dependent transport to the yeast vacuole/lysosome. J. Cell Biol. 146(1): 85–98.

Vihinen-Ranta, M., Kakkola, L., Kalela, A., Vilja, P. & Vuento, M. 1997. Characterization of a nuclear localization signal of canine parvovirus proteins. Eur. J. Biochem. 250(2): 389–394.

Vihinen-Ranta, M., Yuan, W. & Parrish, C. R. 2000. Cytoplasmic trafficking of the canine parvovirus capsid and its role in infection and nuclear transport. J. Virol. 74(10): 4853–4859.

Vihinen-Ranta, M.,Wang, D.,Weichert,W. S. & Parrish, C. R. 2002. The VP1 N-terminal sequence of canine parvovirus affects nuclear transport of capsids and efficient cell infection. J. Virol. 76(4): 1884–1891.

Vist, M.R. & Davis, J.H. 1990. Phase equilibria of cholesterol/dipalmitoylphosphatidylcholine mixtures: 2H nuclear magnetic resonance and differential scanning calorimetry. Biochemistry 29(2): 451–464.

Vitelli, R., Santillo, M., Lattero, D., Chiariello, M., Bifulco, M., Bruni, C. B. & Bucci, C. 1997. Role of the small GTPase RAB7 in the late endocytic pathway. J. Biol. Chem. 272(7): 4391–4397.

Wang, T.Y. & Silvius, J.R. 2003. Sphingolipid partitioning into ordered domains in cholesterol-free and cholesterol-containing lipid bilayers. Biophys. J. 84(1): 367-378.

Wang, C., Takeuchi, K., Pinto, L. H. & Lamb, R. A. 1993. Ion channel activity of influenza A virus M2 protein: characterization of the amantadine block. J. Virol. 67(9): 5585–5594.

Wassall, S. R. & Stillwell W. 2008. Docosahexaenoic acid domains: the ultimate non-raft membrane domain. Chem. Phys. Lipids. 153(1): 57–63.

Wattiaux, R., Baudhuin, P., Berleur, A. M. & De Duve, C. 1956. Tissue fractionation studies. 8. Cellular localization of bound enzymes. Biochem J. 63(4): 608–612.

Watts, C. 1982. Rapid endocytosis of the transferrin receptor in the absence of bound transferrin. J. Cell Biol. 100: 633–663.

Weichert, W. S., Parker, J. S., Wahid, A. T. M., Chang, S. F., Meier, E. & Parrish, C. R. 1998. Assaying for structural variation in the parvovirus capsid and its role in infection. Virology 250(1): 106–117.

Wherrett, J. R. & Huterer, S. 1972. Enrichment of Bis-(monoacylglyceryl) phosphate in lysosomes from rat liver. J. Biol. Chem. 247(13): 4114–4120.

Wickham, T. J., Filardo, E. J., Cheresh, D. A. & Nemerow, G. R. 1994. Integrin alpha v beta 5 selectively promotes adenovirus mediated cell membrane permeabilization. J. Cell Biol. 127(1): 257–264.

Wiethoff, C. M., Wodrich, H., Gerace, L. & Nemerow, G. L. 2005. Adenovirus protein VI mediates membrane disruption following capsid disassembly. J. Virol. 79(4): 1992-2000.

Wong, T. K., Decker, G. L. & Lennarz, W. J. 1982. Localization of dolichol in the lysosomal fraction of rat live. J. Biol. Chem. 25(11): 6614–6618.

Woodman, P. G. & Futter, C. E.. 2008 Multivesicular bodies: co-ordinated progression to maturity. Curr. Opin. Cell Biol. 20(4-24): 408–414.

Worcester, D. L. & Franks, N.P. 1976. Structural analysis of hydrated egg lecithin and cholesterol bilayers II. Neutron diffraction. J. Mol. Biol. 100(3): 359–378

Xie, Q. & Chapman, M. S. 1996. Canine parvovirus capsid structure, analyzed at 2.9 Åresolution. J. Mol. Biol. 264(3): 497–520.

Yamashiro, D. J., Tycko, B., Fluss, S. R. & Maxfield, F. R. 1984. Segregation of transferrin to a mildly acidic (pH 6.5) para-Golgi compartment in the recycling pathway. Cell 37(3): 789–800.

Yao, J. K. & Rastetter, G. M. 1985. Microanalysis of Complex Tissue Lipids By High-Performance Thin-Layer Chromatography. Anal. Biochem. 150(): 111–116.

Yeo, D. S. Y., Chan, R., Brown, G., Ying, L., Sutejo, R., Aitken, J., Tand, B. H., Wenk, M. R. & Sugrue, R. J. 2007. Evidence that selective changes in the lipid composition of raft-membranes occur during respiratory syncytial virus infection. Virology 386(1): 168–182.

Yethiraj, A. & Weisshaar, J. C. 2007. Why are lipid rafts not observed in vivo? Biophys. J. 93(9): 3113–3119.

Zádori, Z., Szelei, J., Lacoste, M.-C., Li, Y., Gariepy, S., Raymond, P., Allaire, M., Nabi, I. R. & Tijssen, P. 2001. A viral phospholipase A2 is required for parvovirus infectivity. Dev. Cell 1(2): 291–302.

Zerial, M. & McBride, H. 2001. Rab proteins as membrane organizers. Nat. Rev. Mol. Cell Biol.2(2):107–117.

Zhou, F., Pu, Y., Wei, T., Liu, H., Deng, W., Wei, C., Ding, B., Omura, T. & Li, Y. 2007. The P2 capsid protein of the nonenveloped rice dwarf phytoreovirus induces membrane fusion in insect host cells. Proc. Natl. Acad. Sci. 104(49): 19547–19552.

Zhu, M-Y., Kyle, P. B., Hume, A. S. & Ordway, G. A. 2004. The persistent membrane retention of desipramine causes lasting inhibition of norepinephrine transporter function. Neurochem Res. 29(2): 419–427.

Zweytick, D., Athenstaedt, K. & Daum, G. 2000. Intracellular lipid particles of eukaryotic cells. Biochim. Biophys. Acta 1469(2): 101–120.